Studies on catalytic property of reduced V and Mo oxides for conversion of oxygenated compounds

(含酸素化合物転換反応における還元 V, Mo 酸化物の触媒作用に関する研究**)**

by

YOICHI NAKAMURA

Thesis submitted in partial fulfillment of the requirements for the degree of Doctor of Engineering

2015

Graduated School of Chemical Science and Engineering

Hokkaido University

TABLE OF CONTENTS

Chapter 1
General Introduction

1.1 Crystal structures and catalytic properties of VO_x and MoO_x

Vanadium and molybdenum oxides have been widely investigated in many fields and used in the technological application. The nature of these oxides is strongly dependent on that oxidation states. Among the vanadium oxides systems, the oxidation state varying from 5+ to 2+, V_2O_5 (V^{5+}), VO_2 (V^{4+}) and V_2O_3 (V^{3+}) have been well studied. On the other hand, MoO_3 and MoO_2 are widely known as molybdenum oxides. Moreover, Mo_4O_{11}, Mo_5O_{14}, $Mo_{17}O_{47}$ are also known as intermediates composition between MoO_3 and MoO_2. To the best of our knowledge, there are no reports for the synthesis of Mo_2O_5.

Crystal structure of V_2O_5 is orthorhombic (space group *Pmmn*, a = 11.48 Å, b = 3.55 Å, c=4.36 Å) and composed of zigzag ribbons of square pyramidal of VO_5 units, which share edges thus from double chains along the b direction. The chains are connected by their corners and the resulting layers are stacked along the c directions (110) as shown in Fig. 1-1(a) [1, 2]. VO_2 has tetragonal rutile structure (space group $P4_2/mnm$) and monoclinic structure (space group $P2_1/c$, a = 5.75 Å, b = 4.52 Å, c = 5.38 Å and β = 122.60°) [2-4] as shown in Fig. 1-1(b). In tetragonal rutile structure, VO_6 octahedra are elongated slightly along the fourfold axis, whereas in the monoclinic lattice the octahedra are more severely distorted yielding three V-O distances in the range 1.76-1.87 and 2.01-2.05 Å. The adjacent VO_6 units are connected by edge or corners in both structures. V_2O_3 has thermodynamically stable corundum structure (space group $R\bar{3}c$, a = 4.9492 Å, b = 4.9492 Å, c = 13.998 Å) at room temperature, with hexagonal close-packing of the oxygens and the cations occupying 2/3 of the octahedral sites as shown in Fig. 1-1(c) [1, 5]. The vanadium atoms form V-V pairs along the crystal *c*-axis and honeycomb lattices in the ab-plane. Corundum structure of V_2O_3 is changed to monoclinic structure above 168 K.

Fig. 1-2 shows the crystal structures of MoO_3 and MoO_2 [6, 7]. The crystal structure of MoO_3 is orthorhombic structure (space group *Pbcm*, a = 5.6109 Å, b = 4.8562 Å, c = 5.6285 Å) as shown

in Fig.2-1 (a). On the other hand, MoO_2 has monoclinic structure (space group $P2_1/c$ a = 3.962 Å, b = 13.855 Å, c = 3.699 Å and β = 120.95°) as shown in Fig.2-1 (b). The Mo metal of orthorhombic MoO_3 layered structure and monoclinic MoO_2 deformed rutile–like structure coordinated six oxygen atom and are described with distorted edge and corner sharing MoO_6 octahedra, however, the kinds of oxygen connected to molybdenum metal are different between MoO_3 and MoO_2. MoO_3 possesses three types of oxygen. The first is singly coordinated oxygen (terminal oxygen) with very short distance (Mo-O bond length 1.67 Å). The second is two coordinated oxygen and located asymmetrically between two Mo centers with bond length of 1.73 Å and 2.25 Å. The third is three coordinated oxygen and symmetrically placed between two Mo centers in a sub layer with a bond distance of 1.94 Å and also connected to another Mo center in the other sub layer with a bond length of 2.33 Å. On the other hand, MoO_2 possesses two kind of oxygen, thus there are two bond length of Mo-O.

On the surface of high oxidation state of V and Mo oxides (V_2O_5 (V^{5+}) and MoO_3 (Mo^{6+})) possesses terminal oxygen bonds (V=O or Mo=O), which are active for the oxidation of alkanes and alcohols as show in Fig. 1-1(a) and 1-2(a). Surface of oxygen on V_2O_5 and MoO_3 are removed with the extent of the reduction, and form coordinatively unsaturated sites as shown in Fig. 1-3. Therefore, the catalytic properties of V and Mo oxides are different between high and low oxidation states of V and Mo oxides. Catalytic reactions over V and Mo oxides with different oxidations states are listed in Table 1-1. High oxidation states of V and Mo oxide (V_2O_5 (V^{5+}), VO_2 (V^{4+}) and MoO_3 (Mo^{6+})) based catalysts have been widely used as selective oxidation of alcohols and light alkanes [8-12]. Moreover, MoO_3 based catalysts are also used as solid acid catalysts, such as dehydration of alcohols [13], reforming [14], isomerization [15] and cracking of light alkane [16].

The reduced V oxides (V_2O_3 (V^{3+})) was reported to be active for methanation of CO_2 [17]. To the best of our knowledge, there are no reports in which non-supported VO_2 and V_2O_3 oxides are used as

catalysts, though preparations of VO_2 and V_2O_3 oxides are reported by many authors [18, 19]. On the other hand, the catalytic activity of VO_x supported compounds have been widely studied which are mainly used for oxidative dehydrogenation of alkanes or alcohols. For reduced vanadium oxides, VO_2 and V_2O_3 oxides have attracted much attention for the electronic structure and the nature of magnetic properties. Monoclinic VO_2 oxide is attractive for the temperature sensors due to reversible change of its crystal structure from rutile phase to monoclinic phase at 340 K. In particular, VO_2 with monoclinic phase has attracted much attention for its layered structure owing high energy capacity to use in the field of energy technologies. As V_2O_3 showed metal-transition insulator at 160-170 K. The V_2O_3 has been also widely investigated as insulating material, electrode and battery [20-22]. V_2O_3 was also studied as an anode catalyst for SOFC (Solid Oxide Fuel Cell) due to its high melting point (1970 ℃) [23]. Moreover, reduced Mo oxides based catalysts, such as MoO_2, have been widely investigated for metathesis [24-29] and hydrodesulfurization [30-34].

In contrast to V and Mo oxide catalysts with high oxidation states (V^{5+}, V^{4+} and Mo^{6+}), there are few kind of catalytic reaction systems and reports for the reduced V and Mo oxides (V^{3+} and Mo^{4+}) used as catalysts. The catalytic systems using reduced V and Mo based catalysts are described below.

1.2 Catalytic reactions over reduced V and Mo oxide catalysts

1.2.1 Catalytic systems for reduced vanadium based oxides

For reduced vanadium oxide (VO_x) acted as a catalyst, there are many reports of VO_x supported oxides. The relation between the catalytic activity of VO_x species on the surface and supporting material was reported [35-40]. For these catalysts, there are V=O terminal bond, V-O-V bridging bond and V-O-support bond. Moreover, the degree of the dispersion of metal on the surface, and redox property between MO_x species and support compounds also affect the catalytic activity. Therefore, the elucidation of the active sites is difficult using metal supported catalysts. Li reported

that much amount of V^{4+} species on the surface of V/γ-Al_2O_3-TiO_2 exhibited high catalytic activity in oxidation of ethanol [36]. For vanadium supported on Al_2O_3-ZrO_2 [37] and TiO_2 [38], the observation of the relatively high amount of V^{4+} species on the surface of catalysts were also reported, however, these reports did not discuss the role of V^{4+} species in the catalytic activity.

VO_2 supported on multi-walled carbon nanotubes (VO_2-defect/MWCNTs) were reported as the catalyst for hydroxylation of benzene to produce phenol [39]. Ni-V_2O_3/Al_2O_3 catalyst exhibited good catalytic activity in methanation of CO, and reported that oxidation-reduction cycle of V_2O_3 enhanced the CO and CO_2 dissociation [40].

Xue et al. showed the preparation of high surface area and thermal stability of mesoporous VO_2, which exhibited high catalytic activity for the conversion of 2-propanol and selective oxidation of toluene compared with V_2O_5 catalyst due to strong acid property and redox ability on the surface of catalyst [41].

Among the catalytic reactions carried out over reduced vanadium oxide catalysts mentioned above, the selective oxidation of H_2S over vanadia supported on mesoporous zirconium phosphate was discussed by Soriano et al. [42]. They showed that V_2O_5 was partially reduced to V_4O_9, and V^{5+}-O-V^{4+} pairs on the surface of V_4O_9 played an important role for catalytic activity and selectivity to products for partial oxidation of H_2S. The redox nature of V^{5+}-O-V^{4+} linkage was discussed in this report, even though the Lewis acid-base property also possess in reduced vanadium oxide species.

1.2.2 Reduced molybdenum oxide (MoO_xH_y) acting as Brönsted acid catalyst

Non-supported and reduced Mo oxides have been widely studied as solid acid catalysts, and there are many reports that in which the MoO_2 oxide with high surface area was synthesized by reduction of MoO_3 with H_2 [43-51]. Matsuda's group reported the effect of H_2 reduction on the surface area of MoO_x and catalytic activities. They reported that the highest surface area (170-180 m^2 g^{-1}) was

obtained by reduction of MoO_3 at 573 K [43]. Katrib also showed the surface property of H_2-reduced MoO_3 catalysts [44]. MoO_xH_y phase was observed by reduction of MoO_3 with H_2 at 573 K. Mo-O-H and Mo-H bond are formed on the sample surface. Mo-O-H and Mo-H sites acted as Brönsted acid sites and were active for the dehydration of alcohols [43-46], isomerization [47], reforming [48] and cracking [49] reaction of C5-C8 alkanes [49]. Ha's group reported that MoO_2 catalysts showed high catalytic activity for oxidation of n-alkanes, and good tolerance to the sulfur compounds compared to Ni based catalyst due to high oxygen mobility [50].

1.2.3 Reduced molybdenum oxide (MoO_x species) for olefin metathesis

Reduced MoO_x species have been studied as catalysts for olefin metathesis reaction. Among the catalysts reported, supported molybdenum catalysts such as MoO_x/SiO_2 and MoO_x/Al_2O_3 have been widely investigated. They were prepared by impregnation methods using ammonium salt [24-29]. The reaction scheme for olefin (propylene) metathesis is shown in Fig.1-4. There are many reports discussing the effect of the surface MoO_x species on the catalytic activity because the catalytic activity is strongly dependent on the degree of the polymerization of surface MoO_x species. Many reports showed that lower loading amount of MoO_x led to the formation of isolated MoO_4 species which exhibited high catalytic activity, while crystalline MoO_3 was inactive for the olefine metathesis reaction. Amekawa et al. proposed that Brönsted acidity played important role for catalytic activity in olefin metathesis reaction. In this report, Mo^{6+}-isopropoxide species was generated by adsorption of propylene on Brönsted acid sites, subsequently this species was oxidized by lattice oxygen of MoO_x species to produce acetone. When acetone was formed by oxidation of isopropoxide species, Mo^{6+} anchored on basic sites could not be reduced while anchored on no-basic surface was reduced to Mo^{4+} [26]. Mo^{4+} sites react with propylene to form Mo^{6+}-alkyl diene as metathesis active intermediates. All of these reports mentioned above elucidated the active sites on

reduced MoO_x species. However, the correlation between Lewis acidity or oxygen vacancy on reduced MoOx species (Mo^{4+} sites) and catalytic activity was not demonstrated.

1.2.4 Reduced molybdenum oxide (MoO_x species) for hydrodesulfurization

From the view point of environment protection, the removal of organic sulfur compounds from liquid fuels, particularly from gasoline and diesel are still very important. There are many reports of the synthesis of molybdenum based catalysts with various methods, which discussed about the catalytic activity for the hydrodesulfurization of organic sulfur compounds [30-35]. MoO_3-CoO supported on Al_2O_3 showed a significant high activity for hydrodesulfurizaton due to the synergetic effect of sulfided Mo and Co, and the effects of preparation methods on the catalytic activity and molybdenum species on the surface of catalysts have been widely investigated [30-32]. MoO_3 supported on SiO_2 and Al_2O_3 oxides have been also used for hydrodesulfurization, and the reduced molybdenum species plays an important role in the catalytic activity [33]. MoS_2 is produced by reduction and sulfidation of supported molybdenum. Mo species on the surface of support material was reduced from Mo^{6+} to Mo^{5+} and Mo^{4+} in the sulfidation with H_2S/H_2 [34]. Damyanova et al. showed that the degree of the interaction between MoO_x and modified support material (ZrO_2-Al_2O_3) influenced on the reducibility of MoO_x species on the surface of ZrO_2-Al_2O_3 and catalytic activity [35]. Weak interaction of molybdenum species with ZrO_2-Al_2O_3 led to the significant high dispersion of molybdenum species on the surface of ZrO_2-Al_2O_3, and the formation of Lewis acid sites was attributed to Mo^{5+} sites formed by reduction of MoO_x species. As a result, molybdenumsulfide that is active for the hydrodesulfurization was formed. It was reported that the correlation between the catalytic activity and the degree of reduction of Mo oxide species.

1.3 V and Mo oxides as Lewis acid catalysts

Corma et al. discussed the role of Lewis acid sites of vanadium based catalyst for the oxidative dehydrogenation of alkanes [51]. In this report, the Lewis acid sites of vanadyl phosphate are attributed to oxygen defect vacancies formed during the reaction, and play a role in activation of alkanes for the oxidative dehydrogenation. Lewis acid sites and their ionic strength enhanced the catalytic activity in the oxidative dehydrogenation of ethane to produce ethylene. However, there are few reports discussing about Lewis acid property of reduced vanadium and molybdenum oxides.

Germain et al. reported the Lewis acid sites on MoO_3 oxide and its activity [52]. MoO_3 oxide possess the three type of crystal faces in orthorhombic phase, basal (010), side (100) and apical (001)+(101). Among the crystal phase of MoO_3 oxide, (100) phase acts as Lewis acids sites as well as vanadyl phosphates, and is active for the dehydration of ethanol. On the other hand, Tang et al. reported that Lewis acidity of MoO_3 cluster (Mo^{6+}) was very low, which showed non or quite low catalytic activity in dehydration of 2-propanol. The nature and strength of Mo^{5+} and Mo^{4+} in molybdenum oxide-alumina catalyst were studied by pyridine adsorbed IR measurements [53]. In the hydrogenation of pyridine to produce piperidine, the active sites with higher valence (Mo^{5+}) played an important role in the adsorption of substrates and the active site with lower valence (Mo^{4+}) played a role in the adsorption hydrogen. Therefore, metal cation with lower valence would be show the high hydrogen capability. Quincy et al. also reported that catalytic activity for the hydrogenation of benzene over Mo/TiO_2 catalysts was strongly dependent on the degree of reduction of Mo phase, and low oxidation states of Mo species (Mo^{2+}) showed high catalytic activity [54].

Lietti et al. reported that Mo^{5+} species were observed on TiO_2 supported MoO_3 catalysts [55]. Moreover, the loading of V_2O_5 and MoO_3 on TiO_2 led to the increase of the number of Brönsted acid sites and the strength of the Lewis acid sites, which showed high catalytic activity for reduction of NO_x with NH_3 due to the activation of NH_3 by adsorption on Lewis acid sites [41]. Reiche et al. also

reported that the deactivation of vanadium grafted on support materials (TiO_2, SiO_2, TiO_2-SiO_2) was observed due to the decrease in both Brönsted and Lewis acid sites [56].

1.4 Objectives and construction of this thesis

A few reports were discussed about Lewis acid property of non-supported reduced molybdenum and vanadium species. In contrast to the studies of Brönsted acid sites on V, and Mo based oxide catalysts, Lewis acid sites on reduced V and Mo oxides have not been studied extensively. Moreover, the reactions of oxygenated compound over reduced V and Mo oxide catalysts have not been reported. Recently, the conversion of oxygenated compounds derived from biomass has been attracted much attention. On the other hand, V and Mo supported catalysts have been widely studied for the conversion of oxygenated compounds. Elucidation of the catalytic activity using V and Mo supported oxides, however, could be difficult because catalytic properties of V and Mo species are very sensitive to the nature of support materials. Therefore, the Lewis acid nature of reduced V and Mo oxide catalysts for oxygenated compounds, such as alcohols, aldehydes and ketones, are still not clarified.

We found that the specific catalytic performances of reduced vanadium and molybdenum oxides were observed in the reaction of ethanol. Reduced vanadium and molybdenum oxides showed the formation of ethane and acetaldehyde in a 1:1 ratio in ethanol reaction. Recently, conversion of ethanol has attracted much attention due to use for the materials alternative to petroleum derived fuels (Fig.1-5) and model reaction [57], because ethanol is one of the most promising renewable platform molecules and converts to ethylene [58], diethyl ether [58], acetaldehyde [59], acetic acid [60] and propylene [61] related derivatives as shown in Fig. 1-6. Formation of ethane from ethanol is very interesting reaction as shown in Fig.1-4, because there are a few report for the describing the reaction mechanism for the formation of alkanes from alcohols. The formation of corresponding

toluene and benzaldehyde in 1:1 ratio was reported in the disproportionation of benzyl alcohols [62]. However, there is no report for the disproportionation of aliphatic alcohols. In the biomass conversion, deoxygenation of alcohols without use of hydrogen is one of the important issues.

In order to elucidate the catalytic property of reduced vanadium and molybdenum oxides, catalytic reaction of oxygenated compounds (alcohols and ketones) were performed over reduced V and Mo oxide catalyst.

In Chapter 2, the author discusses about the influence of the oxidation states of V and Mo oxides on the reaction of ethanol. V_2O_5, VO_2 and MoO_3 exhibited the induction period to form ethane in the reaction of ethanol, however, V_2O_3 and MoO_2 exhibited the formation of ethane and acetaldehyde with equal amount from the beginning of reaction. Moreover, crystal phase and surface oxidation states of V_2O_3 and MoO_2 did not change after ethanol reaction. Therefore, V_2O_3 and MoO_2 are identified to be active for the formation of ethane from ethanol.

In Chapter 3, the reaction mechanism of the formation of ethane and acetaldehyde in 1:1 ratio from ethanol over V_2O_3 and MoO_2 catalysts is discussed. Based on the kinetic isotope effects measured using C_2H_5OD and C_2D_5OD, the reaction scheme for the formation of ethane and acetaldehyde from ethanol was determined to takes place via hydrogen-transfer dehydration from 6-memberd transition states.

In Chapter 4, the author discusses the reaction of diols over V_2O_3 and MoO_2 catalysts. Corresponding aldehydes and ketones were formed as main products through dehydration of diols. However, the distributions of product are different between V_2O_3 or MoO_2 catalysts and solid acid or base catalysts. Therefore, the reaction mechanisms of the dehydration of vicinal diols to form corresponding aldehydes or ketones over V_2O_3 or MoO_2 catalysts are different from those of solid acid or base catalysts, and involve intramolecular hydrogen-transfer dehydration. Moreover, corresponding olefins were formed in diol reactions unlike in the reaction of mono-alcohols.

In Chapter 5, the author discusses reductive amination of ketones with ammonia over Pt-MoO_2/TiO_2 catalyst. One of the important issues of biomass conversion is synthesis of high valued compounds. Lewis acid sites of MoO_2 would interact with C=O bond of ketones and activates C=O bond. Touchy et al. reported that Pt-MoO_2/TiO_2 strongly interact with C=O bond of acetones compared to other support, such as TiO_2, Al_2O_3 [63].

The above results are summarized in Chapter 6. The contents of the thesis disclose a new aspect of catalytic properties attributed to Lewis acid sites on the reduced V and Mo oxides.

1. 5 References

[1] S. Surnev, M.G. Ramsey, F.P. Netzer, *Progress in Surface Science*, 20 (2008) 6396-6404.

[2] C. Wu, Y. Xie, E*nergy Environ. Sci.*, 2010, 3, 1191-1206.

[3] M. E. A. Warwick, R. Binions, *J. Mater. Chem. A*, 2 (2014) 3275-3292.

[4] C. Wu, F. Feng, Y. Xie, *Chem. Soc. Rev.*, 42 (2013) 5157-5183.

[5] P. D. Dernier, *J. Phys. Chem. Solids*, 31 (1970) 2569-2575.

[6] T. Leisegang, A. A. Levin, J. Walter, D. C. Meyer, Cryst. Res. Technol, 40 (2005) 95-105.

[7] D. O. Scanlon, G. W. Watson, D. J. Payne, G. R. Atkinson, R. G. Egdell, D. S. L. Law, *J. Phys. Chem. C* 114 (2010) 4636-4645.

[8] (a) R. Tesser, V. Maradei, M. Di Serio, E. Santacesaria, *Ind. Eng. Chem. Res*. 43 (2004) 1623-1633, (b) M. V. Ganduglia-Pirovano, C. Popa, J. Sauer, H. Abbott, A. Uhl, M. Baron, D. Stacchiola, O. Bondarchuk, S. Shaikhutdinov, H. J. Freund, *J. Am. Chem. Soc.* 132 (2010) 2345-2349, (c) B. Kilos, A. T. Bell, E. Iglesia, *J. Phys. Chem. C*, 113 (2009) 2830-2836.

[9] R. S. Mann M. K. Dosi, *J. Catal*., 28 (1973) 282-288.

[10] T.J. Yang, J. H. Lunsford, *J. Catal.* 103 (1987) 55-64.

[11] E. V. Kondratenko, O. Ovsitser, J. Radnik, M. Schneider, R. Kraehnert, U. Dingerdissen, *Applied Catal. A*, 319 (2007) 98-110.

[12] K. Chen, S. Xie, E. Iglesia, A. T. Bell, *J. Catal*., 189, (2000) 421-430.

[13] Y. Han, C. Lu, D. Xu, Y. Zhang, Y. Hu, H. Huang, *Applied Catal. A*, 396 (2011) 8-13

[14] T. Borowiecki, W. Gac, A. Denis, *Appl. Catal. A*, 270 (2004) 27-36

[15] T. Matsuda, H. Sakagami, N. Takahashi, *J. Chem. Soc., Faraday Trans.*, 93 (1997) 2225-2229

[16] F. Di-Grégorio, V. Keller, T. Di-Costanzo, J.L. Vignes, D. Michel, G. Maire, *Appl. Catal. A*, 218 (2001) 13-24

[17] Q. Liu, F. Gu, X. Lu, Y. Liu, H. Li, Z. Zhong, G. Xu, F. Su, *Applied Catal. A*, 488 (2014)

37-47.

[18] (a) S. A. Corr, M. Grossman, J. D. Furman, B. C. Melot, A. K. Cheetham, K. R. Heier, R. Seshadri, *Chem. Matter.* 20 (2008) 6396-6404, (b) S. A. Corr, M. Grossman, Y. Shi, K. R. Heier, G. D. Stucky, R. Seshadri, *J. Matter. Chem.* 19(2009) 4362-4367, (c) C. Wu, X. Zhang, J. Dai, J. Yang, Z. Wu, S. Wei, Y. Xie, *J. Matter. Chem.* 21(2011) 4509-4517, (d) S. R. Popuri, M. Miclau, A. Artemenko, C. Labrugere, A. Villesuzanne, M. Pollet, *Inorg. Chem.* 52 (2013) 4780-4785., (e) A. Bergerud, R. Buonsanti, J. L. Jordan-Sweet, D. J. Milliron, *Chem. Matter.* 25 (2013) 3172-3179.

[19] (a) C. Zheng, X. Zhang, S. He, Q. Fu, D. Lei, *J. Solid State Chem*., 170 (2003) 221-226, (b) K. Zhang, X. Sun, G. Lou, X. Liu, H. Li, Z. Su, *Mater. Lett.*, 59 (2005) 2729-2731, (c) Y. Bai, P. Jin, S. Ji, H. Luo, Y. Gao, *Ceramics International*, 39 (2013) 7803-7808, (d) F.Y. Kong, M. Li, D.B. Li, Y. Xu, Y.X. Zhang, G.H. Li, *J. Crystal Growth*, 346 (2012) 22-26, (e) C.V. Ramana, S. Utsunomiya, R.C. Ewing, U. Becker, *Solid State Commun*. 137 (2006) 645-649.

[20] A. I. Frenkel, E. A. Stern, F. A. Chudnovsky, *Solid State Commun*. 102 (1997) 637-641.

[21] H. Li, K. Jiao, L. Wang, C. Wei, X. Li, B. Xie, *J. Mater. Chem. A*, 2 (2014) 18806-18815.

[22] Y. Sun, S. Jiang, W. Bi, C. Wu, Y. Xie, *J. Power Sources* 196 (2011) 8644-8650.

[23] Z. Xu, J. Luo, K. T. Chuang, *ECS* 11 (2008) 1-17.

[24] T. Suzuki, *Appl. Catal.* 50 (1989) 15-25.

[25] (a) R. Thomas, E. M. Van Oers, V. H. J. D. Beer, J. Medea, J. A. Moulijn, *J. Catal.* 76 (1982) 241-253, (b) R. Thomas, E. M. Van Oers, V. H. J. D. Beer, J. A. Moulijn, *J. Catal.* 84 (1983) 275-287.

[26] J. Handzlik, J. Ogonowski, J. Stoch, M. Mikołajczyk, *Appl. Catal. A* 273 (2004) 99-104.

[27] (a) T. Hahn, E. V. Kondratenko, D. Linke, *Chem. Commun.* 50 (2014) 9060-9063, (b) T. Hahn, U. Bentrup, M. Armbrüster, E. V. Kondratenko, D. Linke, *ChemCatChem* 6 (2014) 1664-1672.

[28] D. P. Debecke, B. Schimmoeller, M. Stoyanova, C. Poleunis, P. Bertrand, U. Rodemerck, E. M. Gaigneaux, *J. Catal.* 277 (2011) 154-163.

[29] S. Lwin, I. E. Wachs, *ACS Cata*l. 4 (2014) 2505-2520.

[30] Y.S. Al-Zeghayer, P. Sunderland, W. Al-Masry, F. Al-Mubaddel, A.A. Ibrahim, B.K. Bhartiya, B.Y. Jibril, *Appl. Catal. A* 282 (2005) 163-171, (b) Y.S. Al-Zeghayer, B.Y. Jibril, *Appl. Catal. A* General 292 (2005) 287-294.

[31] Y. Okamoto, S. Ishihara, M. Kawano, M. Satoh, T. Kubota, *J. Catal.* 217 (2003) 12-22.

[32] F. Dumeignil, K. Sato, M. Imamura, N. Matsubayashi, E. Payen, H. Shimada, *Appl. Catal. A* 287 (2005) 135-145.

[33] H. Beuther , R. A. Flinn , J. B. McKinley, *Ind. Eng. Chem. 51* (1959) 1349-1350.

[34] S.-X. Zhuang, H. Magara, M. Yamazaki, Y. Takahashi, M. Yamada, *Appl. Catal. B* 24 (2000) 89-96.

[35] S. Damyanova, L. Petrov, M.A. Centeno, P. Grange, *Appl. Catal. A* 224 (2002) 271-284.

[36] Z. Li, X. An, P. Ren, W. Huang, K. Xie, *J. Natural Gas Chem.* 18(2009) 1-4.

[37] K. V. R. Chary, C. P. Kumar, D. Naresh, T. Bhaskar, Y. Sakata, *J. Mol. Catal. A* 243 (2006) 149-157.

[38] J. E. Herrera, T. T. Isimjan, I. Abdullahi, A. Ray, S. Rohani, *Appl. Catalysis A* 417–418 (2012) 13-18.

[39] S. Song, S. Jiang, R. Rao, H. Yang, A. Zhang, *Appl. Catal. A* 401 (2011) 215-219.

[40] Q. Liu, F. Gu, X. Lu, Y. Liu, H. Li, Z. Zhong, G. Xu,, F. Su, *Appl. Catal. A* 488 (2014) 37-47.

[41] M. Xue, H. Chen, J. Ge, J. Shen, *Microporous and Mesoporous Mater.* 131 (2010) 37-44.

[42] M.D. Soriano, J. J. Jiménez, P. Concepción, A. J. López, E. R. Castellón, J. M. L. Nieto, *Appl. Catal. B*, 92 (2009) 271-279.

[43] (a) T. Matsuda, Y. Hirata, H. Itoh, H. Sakagami, N. Takahashi, *Microporous and Mesoporous*

Materials 42 (2001) 337-344, (b) H. Sakagami, Y. Hirata,T. Ohno, N. Takahashi, H. Itoh, T. Matsuda, *Appl. Catal. A* 297 (2006) 189-197.

[44] A. Benadda, A. Katrib, A. Barama, *Appl. Catal. A* 251 (2003) 93-105.

[45] H. A. Kandari, F. A. Khorafi, H. Belatel, A. Katrib, *Catal. Commun*. 5 (2004) 225-229.

[46] T. Matsuda, H. Sakagami, N. Takahashi, *Appl. Catal. A* 213 (2001) 83-90.

[47] (a) T. Ohno, Z. Li, N. Sakai, H. Sakagami, N. Takahashi, T. Matsuda, *J. Mol. Catal. A*, 389 (2010) 52-59, (b) H. Sakagami, T. Ohno, N. Takahashi, T. Matsuda, *J. Catal*. 241 (2006) 296-303, (c) T. Matsuda, H. Sakagami, N. Takahashi, *Catal. Today* 81 (2003) 31-42.

[48] A. Katrib, P. Leflaive, L. Hilaire, G. Maire, *Catal. Lett* 38 (1996) 95-99.

[49] J. H. Song, P. Chen, S. H. Kim, G. A. Somorjai, R. J. Gartside, F. M. Dautzenberg, *J. Mol. Catal. A*, 184 (2002) 197-202.

[50] O. G. Marin Flores, Su Ha, *Appl. Catal. A* 352 (2009) 124-132.

[51] A. Corma, H. García, *Chem. Rev.* 102 (2002) 3837-3892.

[52] J.M. Tatibouët, J.E. Germain, *J. Catal.* 72 (1981) 375-378.

[53] X. Tang, D. Bumueller, A. Lim, J. Schneider, U. Heiz, G. Ganteför, D. H. Fairbrother, K. H. Bowen, *J. Phys. Chem. C*, 118 (2014) 29278-29286.

[54] R. B. Quincy, M. Houalla, A. Proctor, D. M. Hercules, *J. Phys. Chem.* 94 (1990) 1520-1526

[55] (a) G. Busca, L. Lietti, G. Ramis, F. Berti, *Appl. Catal. B* 18 (1998) 1-36, (b) I. Nova, L. Lietti, L. Casagrande, L. D.Acqua, E. Giamello, P. Forzatti, *Appl. Catal. B* 17 (1998) 245-258, (c) L. Lietti, I. Nova, G. Ramis, L. D.Acqua, G. Busca, E. Giamello, P. Forzatti, F. Bregani, *J. Catal.* 187 (1999) 419-435, (d) L. Casagrande, L. Lietti, I. Nova, P. Forzatti, A. Baiker, *Appl. Catal. B* 22 (1999) 63-77.

[56] M.A. Reiche, E. Ortelli, A. Baiker, *Appl. Catal. B* 23 (1999) 187-203.

[57] Renewable Fuel Standard 2

http://www.badgerstateethanol.com/fuel_independence_success.p.

[58] (a) J. Bi, X. Guo, M. Liu, X. Wang, *Catal. Today* 149 (2010) 143-147, (b) X. Zhang, R. Wang, X. Yang, F. Zhang, *Microporous Mesoporous Mater*.116 (2008) 210-215, (c) H. Xin, X. Li, Y. Fang, X. Yi, W. Hu, Y. Chu, F. Zhang, A. Zheng, H. Zhang, X. Li, J Catal. 312 (2014) 204-215, (d) J. Bi, X. Guo, M. Liu, X. Wang, *Catal. Today* 149 (2010) 143-147, (e) T. T .Ail, S.A. Al-Thabaiti, A.O. Alyoubi, M. Mokhtar, *Journal of Alloys and Compounds*, 496 (2010) 553-559, (f) S. Roy, G. Mpourmpakis, D. Y. Hong, D. G. Vlachos, A. Bhan, R. J. Gorte, *ACS Catal*. 2 (2012) 1846-1853.

[59] (a) Y. Guan, E. J. M. Hensen, *Appl. Catal. A* 361 (2009) 49-56, (b) N. Zheng, G. D. Stucky, *J. Am. Chem. Soc*. 128 (2006) 14278-1280, (c) E. O. G. Yañez, G. A. Fuentes, M. E. H. Teran, J. C. F. Gonzalez, *Appl. Catal. A* 464 (2013) 374-383, (d) Y. Gucbilmez, T. Gogu, *Ind. Eng. Chem. Res*. 45 (2006) 3496-3502, (e) J. H. Kwak, J. E. Herrera, J. Z. Hu, Y. Wang, C.H.F. Peden, *Appl. Catal. A* 300 (2006) 109-119, (f) R. Tesser, V. Maradei, M. D. Serio, *E.* Santacesaria, *Ind. Eng. Chem. Res*. 43 (2004) 1623-1633, (g) B. Kilos, A. T. Bell, E. Iglesia, *J.Phys. Chem*. 113 (2009) 2830-2836.

[60] (a) J. P. Breen, R. Burch, H. M. Coleman, *Appl. Catal. A* 39 (2002) 65-74, (b) J. Zhang, Z. Zhong, X. M. Cao, P. Hu, M. B. Sullivan, L. Chen, *ACS Catal.* 4 (2014) 448-456, (c) M. Scott, M. Goeffroy, W. Chiu, M. A. Blackford, H. Idriss, *Top Catal*. 51 (2008) 13-21, (d) S. M. de Lima, I. O. da, Cruz, G. Jacobs, B. H. Davis, L. V. Mattos, F. B. Noronha, *J Catal*. 257 (2008) 356-368.

[61] (a) H. Oikawa, Y. Shibata, K. Inazu, Y. Iwase, K. Murai, S. Hyodo, G. Kobayashi, T. Baba, *Appl. Catal A* 312 (2006) 181-185, (b) C. Duan, X. Zhang, Y. Hua, L. Zhang, J. Chen, *Fuel Process. Technol.* 108 (2013) 31-40, (c) T. Inoue, M. Itakura, H. Jon, Y. Oumi, A. Takahashi, T. Fujiatani, T. Sano, *Microporous Mesoporous Mater.* 122 (2009) 149-154, (d) W. Xia, A. Takahashi, I.

Nakamura, H. Shimada, T. Fujitani, *J. Mol. Catal. A* 328 (2010) 114-118, (f) M. Inaba, K. Muruta, I. Takahara, *React. Kinet. Catal. Lett*. 97 (2009) 19-26, (e) Y. Furumoto, N. Tsunoji, Y. Ide, M. Sadakane, T. Sano, *Appl. Catal. A* 417-418 (2012) 137-144.

[62] R. Sumathi, K. Johnson, B. Viswanathan, T. K. Varadarajan, *Appl. Catal. A* 172 (1998) 15-22.

[63] A. S. Touchy, S. M. A. H. Siddiki, K. Kon, K. Shimizu, *ACS catal.* 4, (2014) 3045–3050.

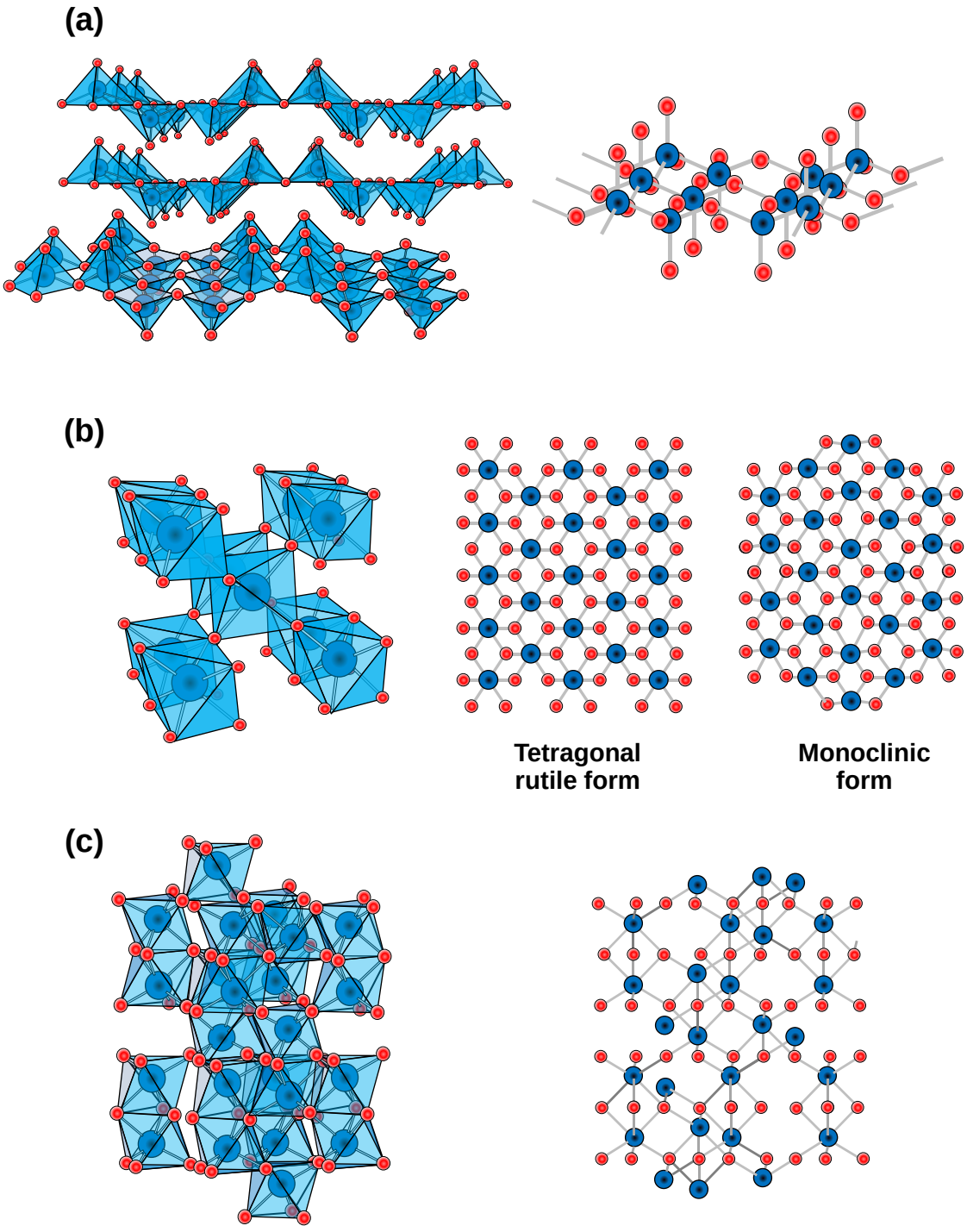

Fig. 1-1 Crystal structures of V_2O_5 (a), VO_2 (b) and V_2O_3 (c). Blue ball; vanadium, red ball; oxygen

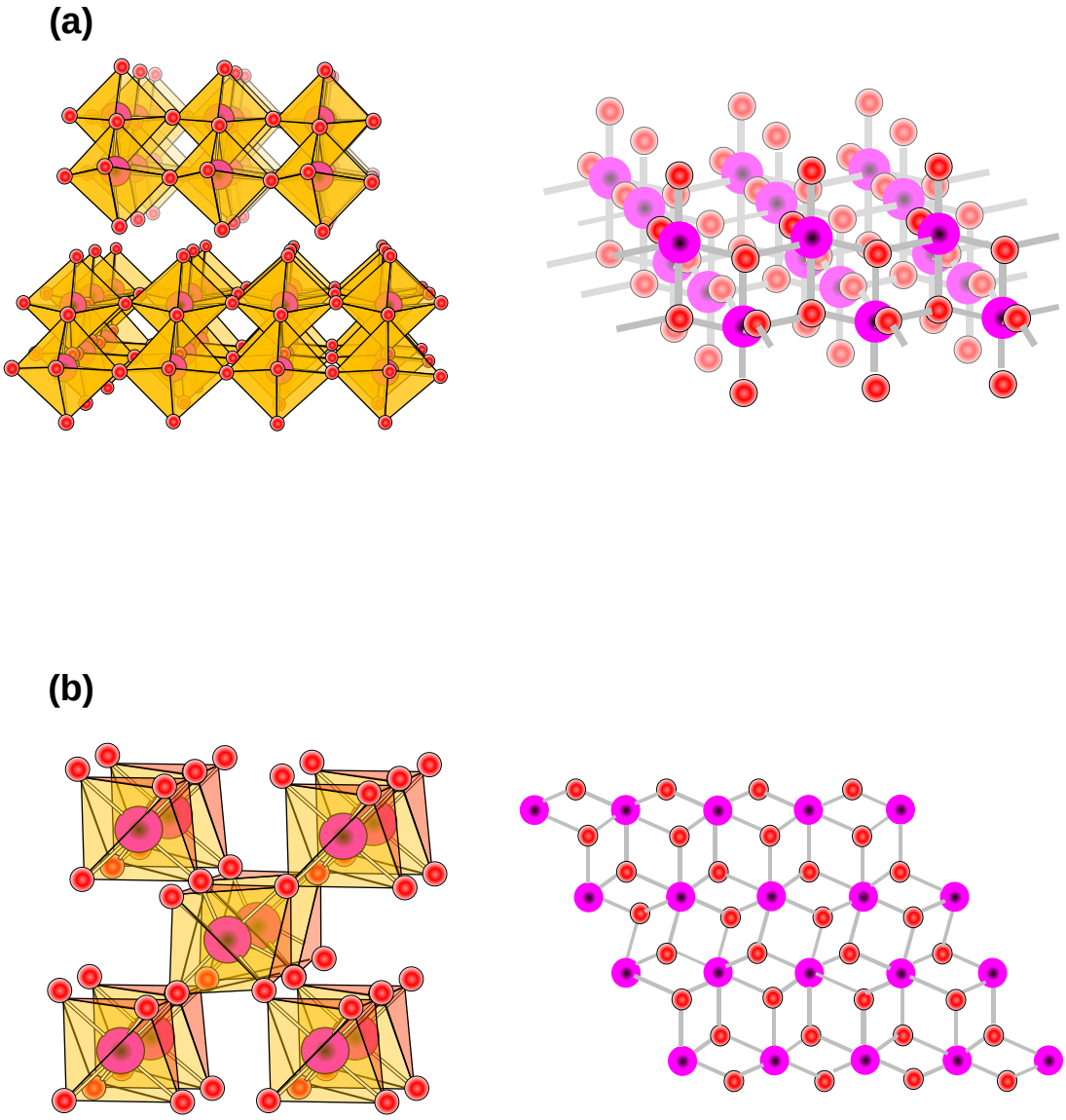

Fig. 1-2 Crystal structures of MoO_3 (a), MoO_2 (b). Pink ball; molybdenum, red ball; oxygen

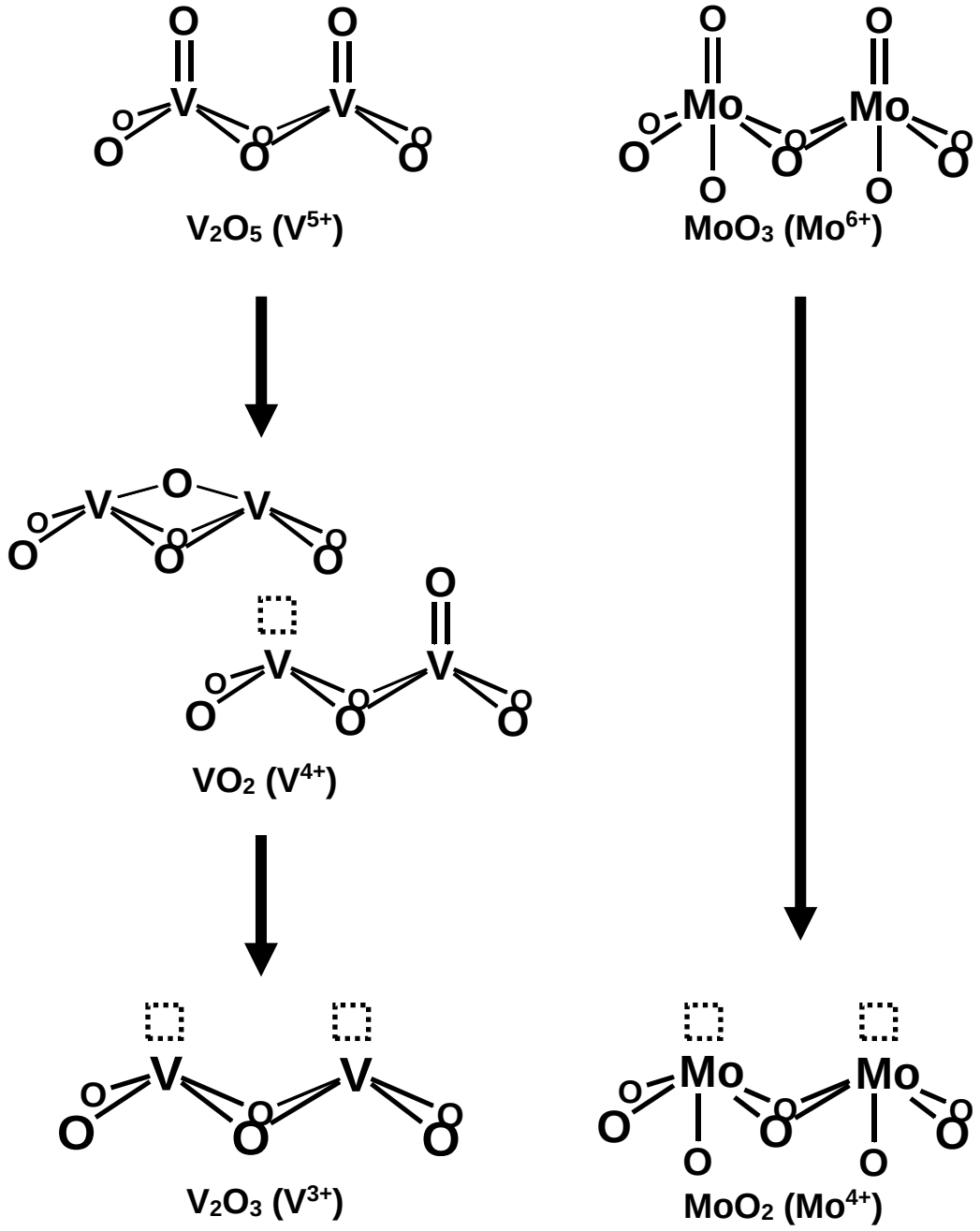

Fig. 1-3 Surface structures of V and Mo oxides with different oxidation states. ⬚ ; Coordinatively unsaturated sites

Table 1-1
Catalytic Reaction over V and Mo Oxide Catalysts.

Catalysts	Reactions
V_2O_5 VO_2	• Selective oxidation of alcohols and light alkanes • Dehydration of alcohols • Cracking, reforming and isomerization of light alkanes
V_2O_3	• Methanation of CO_2; $CO_2 + 4\,H_2 \longrightarrow CH_4 + 2\,H_2O$
MoO_3	• Selective oxidation of alcohols and light alkanes • Dehydration of alcohols • Cracking, reforming and isomerization of light alkanes
MoO_2	• Metathesis; 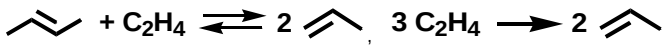 • Desulfurization; 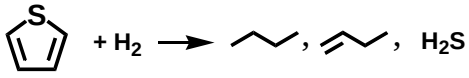

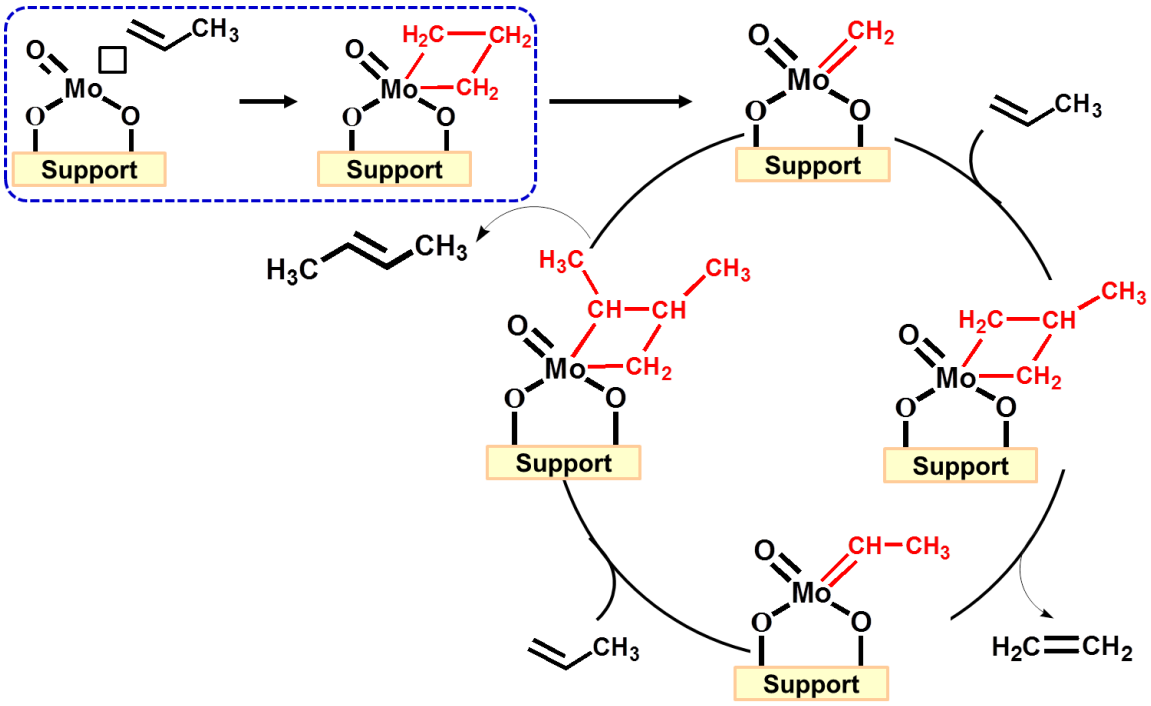

Fig. 1-4 Reaction schemes of metathesis of propylene to form ethylene and 2-butene on coordinatively unsaturated sites of supported MoO_2 catalysts [30].

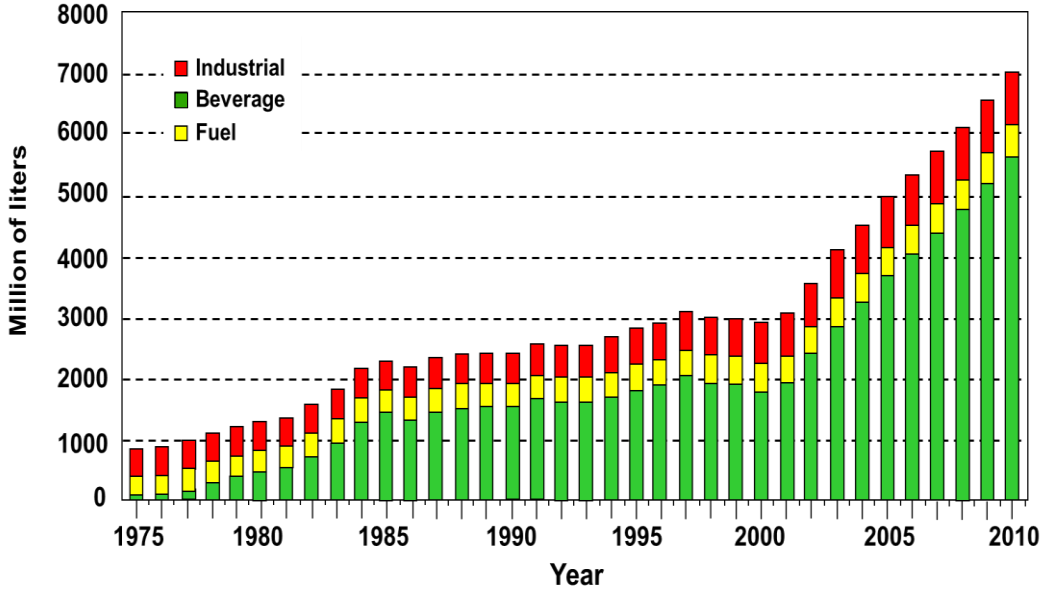

Fig. 1-5 Worldwide production of ethanol and its application over the period 1975-2010 [21].

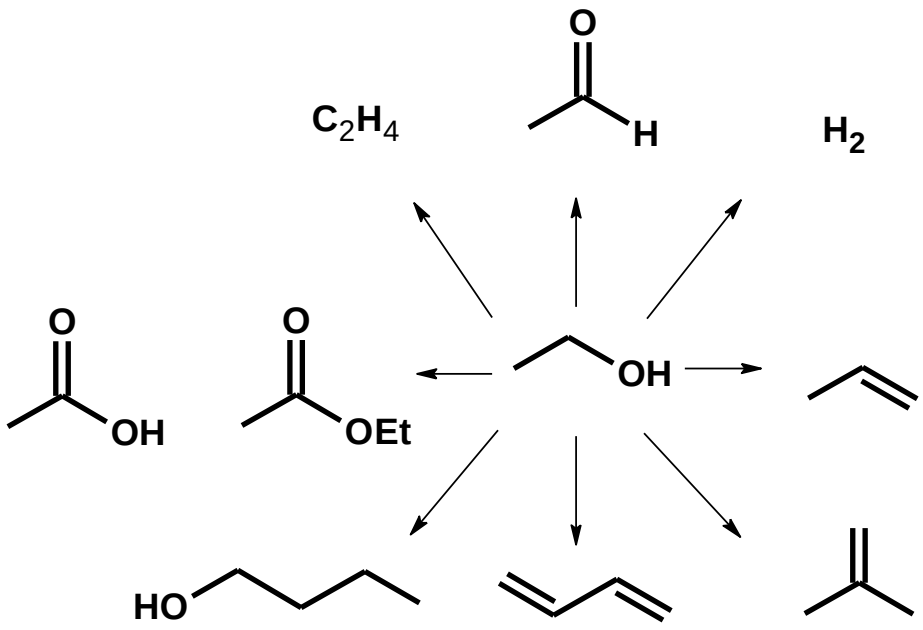

Fig. 1-6 A number of the important bulk chemicals that can be derived from ethanol.

Chapter 2
Ethanol reaction over vanadium and molybdenum oxide catalysts with different oxidation states

2. 1. Introduction

2. 1. 1 Catalytic systems for the formation of alkanes from corresponding alcohols

Vanadium and molybdenum oxides are used in industrial chemical processes as catalysts and their catalytic properties have been extensively investigated as catalysts for the partial oxidation of alkanes [1-3] and alcohols [4-7], dehydration of alcohols [8], isomerization[9], cracking and reforming of alkanes [10,11] to obtain important chemicals and to reduce environmental pollution. In the reports studying the reaction of ethanol over vanadium and molybdenum oxide catalysts, catalytic reactions were performed mostly in the presence of oxygen, and acetaldehyde, carboxylic acid and CO_2 were produced as major products, regardless of the catalyst oxidation states [12-15].

However, to the best of our knowledge, there are no reports describing the formation of ethane from ethanol over vanadium or molybdenum oxide catalysts. There are few reports describing the formation of alkanes from corresponding alcohols. In contrast to the studies of the dehydration and dehydrogenation of alcohols, the formation of alkanes from alcohols has not been studied extensively. The catalysts, reaction conditions and product distributions in the several alcohol reactions to form corresponding alkanes are listed in Table 2-1.

Mcmonagle and Moffat proposed that the formation of ethane from ethanol over 12-molybdophosphates takes place through secondary hydrogenation of ethylene formed by dehydration of ethanol, because the yield to the ethane increased in the presence hydrogen into the reaction stream, and the selectivity to acetaldehyde was always higher than that of ethane. In this report, Mo^{6+} in the catalyst was reduced to Mo^{5+} during the ethanol reaction [16]. The selectivities to ethane and acetaldehyde decreased while the selectivity to ethylene increased over the reduced catalyst due to the loss of active site for the dehydrogenation of ethanol.

Abu-Zied et al. proposed the four reaction pathways to form ethane from ethanol over Cd-Cr-O catalyst as shown in bellow [17].

$$(C_2H_5)_2O \rightarrow C_2H_6 + CH_3CHO \quad (1)$$

$$(C_2H_5)_2O + H_2 \rightarrow 2C_2H_6 + 2H_2O \quad (2)$$

$$C_2H_5OH \quad H_2 \rightarrow C_2H_6 + H_2O \quad (3)$$

$$C_2H_5OH \rightarrow C_2H_4 + H_2O$$

$$C_2H_4 + H_2 \rightarrow C_2H_6 \quad (4)$$

The first pathway is the disproportionation of diethyl ether formed by dehydration of ethanol (1), the second pathway is hydrogenolysis of diethyl ether (2), the third pathway is involved in the hydrogenolysis of ethanol (3) and the final reaction pathway is hydrogenation of ethylene formed by dehydration of ethanol (4). Hydrogen is formed by dehydrogenation of ethanol to acetaldehyde. They reported that hydrogenation of ethylene is the mainly pathway to form ethane from ethanol over Cd-Cr-O catalyst because the selectivity to ethane increased with an increase in the selectivity to acetaldehyde and with a decrease in the selectivity to ethylene, and also because diethyl ether was not observed. Moreover, chromia is known to form hydride species, Cr-H, which was active species for the hydrogenation of ethylene. In this reaction, they also showed that the influence of the oxidation state of Cr in the catalyst on the selectivity to products. Chromia was reduced from Cr^{6+} to Cr^{3+} during the catalyst usage due to the absence of oxygen in the reaction stream. This reduced cromia was active for the dehydration reaction due to the increase of Lewis acidity.

Other reports also showed the relation between the selectivity to alkanes and oxidation state of catalysts. Mohamed et al. showed that the ethane and methane were formed as rather main products from ethanol, compared to acetaldehyde and acetone over Fe ion exchanged mordenite. They proposed that the alkane formation from ethanol was due to a high O-abstraction affinity from alcohol of the Fe^{3+} in the catalysts because ethane was produced in the absence of H_2 and an appreciable amount of Fe^{2+} species was observed [18]. Methane was formed as a result of decomposition reaction at high reaction temperature.

Kagiya et al. reported that the ethane was formed by hydrogenation of hemiacetal using acidified ethanol over TiO_2-PtO_2 in the post-irradiation dark reaction, because the yield of ethane increased with decreasing of yields of acetal and H_2 [19].

Rintramee et al. showed that the formation of ethane was observed in ethanol temperature-programmed desorption (TPD) profiles of Pt catalyst at high temperature and proposed hydrogenation of ethylene to form ethane from ethanol [20]. Ochoa et al. also showed that ethane, acetaldehyde and water were observed at low temperature in the ethanol TPD profiles over ferrite catalyst, however, they suggested that the reaction mechanism for the formation of ethane is ethanol disproportionation and coupling of the methyl species formed by the dissociation of acetaldehyde [21].

Miller reported the almost same selectivity to propanal and propane obtained from 1-propanol over Pt supported catalyst (Pt/Al_2O_3, Pt/Ce_2O_3, Pt/TiO_2), and proposed the reaction pathway through the hydrodeoxygenation of 1-propanol [22]. Hydrogen was formed by dehydrogenation and decomposition of propanol in the propanol reforming reaction. They indicate that hydrogenation of propylene and OH shifting were less likely possibility because propylene and diols were not observed in either the gas or liquid phase products. The Pt-Ti catalyst showed the highest 1-propanol conversion rate per gram of catalyst followed by the Pt-Al, Pt-Ce catalysts, however, the selectivity to products were almost the same in all of the catalysts (the selectivity to propan 10-13 % and to propanal 10-15 %).

Jin et al. showed that butane was formed from 2-butanol over Fe_2O_3, Fe_2O_3–ZrO_2 and Fe_2O_3–ZnO. They indicated that the formation of butane from butanol was via nucleophilic substitution (S_N2) of hydroxyl ion in alcohols by a hydride ion. In the nucleophilic mechanism, the source of hydride ion may be a heterolytically adsorbed hydrogen produced by the dehydration of butanol [23].

R. Sumathi shows that the reducibility of B site of $ABB'O_3$ (A = Ba, B = Pb, Ce, Ti and B' = Bi,

Cu, Sb) –type perovskite oxides plays an important role in catalytic activity and the selectivity in the selective oxidation of benzyl alcohol [24]. They showed that toluene was formed through hydrogenation of benzyl alcohol, produced by dehydrogenation of benzyl alcohol. The possibility of adsorbed hydrogen species (from dehydrogenation of benzyl alcohol) taking up lattice oxide ion increased, as the reducibility of B site was decreased, leading to the reduction of catalyst, instead of interacting with benzyl alcohol to produce toluene. $BaPbO_3$ exhibited the highest selectivity toward toluene and Cu containing perovskite was highly reducible and the low selectivity to toluene.

The formation of toluene from benzyl alcohol has been known to take place over several kinds of catalysts [25~31]. Table 2-2 shows the summary of the catalysts and reaction conditions in the benzyl alcohol reaction to produce toluene and benzaldehyde.

Molybdophosphoric acid based catalysts showed the formation of benzaldehyde and toluene from benzyl alcohol [25-28]. In all of the above reports describing the formation of toluene from benzyl alcohol over molybdophosphoric acid catalysts, the selectivity to toluene was much lower than that to benzaldehyde because the oxidation of benzyl alcohol to form benzaldehyde was dominant due to the presence of oxygen into the reaction stream. Vanadium substituted 12-molybdophosphoric acid was also reported to enhance the catalytic activity to produce benzaldehyde [26~28].

Pillai's group investigated the catalytic activity of alumina catalyst in the benzyl alcohol reaction. They indicated that toluene and benzaldehyde were produced in an equal amount from benzyl alcohol over alumina catalyst [29], and Ganesan et al. indicated that disproportionation of ether is also pathway to form the toluene and benzaldehyde in a 1:1 ratio in addition to the disproportionation of benzyl alcohol. The reaction mechanism on the surface of alumina to produce toluene was proposed based on the reaction of substituted benzyl alcohol. The mechanism was via direct hydride transfer from one surface benzyloxy species to a neighboring positive charged on the benzylic carbon atom as hydride acceptor. They also studied the effect of the acid-base property of

alumina catalysts for the disproportionation of benzyl alcohol. They used alumina doped with Na ion. The yields of toluene and benzaldehyde on the Na ion doped alumina catalysts was the lower while the yield of dibenzyl ether as higher than that observed for pure alumina catalyst. They suggested that the disproportionation reaction to produce toluene and benzaldehyde required relatively strong acidity than the ether formation.

Mathew et al. reported that the conversion of benzyl alcohol and the selectivity to toluene and benzaldehyde on molybdenum supported $Al(OH)_3$ were higher than those formed on support ($Al(OH)_3$), suggesting that Mo species enhance the formation of active site for the disproportionation of benzyl alcohol to form toluene and benzaldehyde [30]. CaO, MgO and $Zr(OH)_4$ also have been used as support for the preparation of supported Mo catalysts. These pure support also showed poor and almost no activity for the benzeladehyde and toluene formation, however, the conversion of benzyl alcohol to benzaldehyde and toluene was depending on the type of support used. Mo on basic supports such as MgO and CaO exhibited very low activity, and $Al(OH)_3$ exhibited the highest activity to produce benzaldehyde and toluene from benzyl alcohol due to a strong interaction of metal-oxo species with the support that possess the strongly basic hydroxyl groups.

Hutching's group also showed that Au-Pd led to the equivalent formation of toluene and benzaldehyde in solvent-free oxidation of benzyl alcohol under He and disproportionation of benzylalchol was proposed to be main pathway to form toluene and benzalldehyde [31]. Au sites do not catalyze the disproportionation reaction and Au sites are much less active for the oxidation than Pd sites.

2. 1. 2 Objective

The disproportionation reaction on the acid site of catalysts is favored in the benzyl alcohol reaction because the dehydration of benzyl alcohol to produce olefin compound can not take place.

Most of the catalysts for the benzyl alcohol mentioned above may act as acid catalysts to produce olefins through the dehydration reaction in the reactions of aliphatic alcohol. In the present study, we found that the formation of ethane from ethanol over V_2O_5 and MoO_3 catalysts under N_2. Furthermore, the oxidation states of these catalysts were reduced during the ethanol reaction. The objective of the present study is to understand the catalytic properties of vanadium and molybdenum oxides in relation with their oxidation states for the formation of alkanes from the corresponding alcohols.

2. 2. Experimental

2. 2. 1 Catalyst preparation

V_2O_5 was prepared by the calcination of NH_4VO_3 (99 % Wako Pure Chemical Industries) at 773 K for 2 h in air. VO_2 (99 % Wako Pure Chemical Industries) was purchased from Wako Pure Chemical Industries. V_2O_3 was then prepared by the reduction of the prepared V_2O_5 (0.3 g) in a tubular furnace under H_2 stream (30 ml/min) at 773 K for 2 h. The reduced samples were then exposed to air when they cooled at room temperature before use as catalysts. MoO_3 was prepared by the calcination of $(NH_4)_6Mo_7O_{24}$ (99 % Wako Pure Chemical Industries) at 773 K for 2 h in air. MoO_2 was prepared by the reduction of the obtained MoO_3 (0.3 g) in a tubular furnace under H_2 stream (30 ml/min) at 773 K for 2 h, subsequently the reduced molybdenum oxide samples were exposed to air once after they cooled at room temperature and then the sample was treated again in a tubular furnace under 5 % H_2/Ar stream (30 ml/min) at 773 K for 2 h. Finally, the reduced sample was cooled to room temperature, followed by exposure to air. Thus obtained MoO_2 was used for the reactions.

2. 2. 2 Catalytic tests

Catalytic reactions were carried out in a continuous flow fixed bed reactor (Pyrex). A similar volume mixture of the catalyst (0.15 g) and SiO_2 sands (2.6 g) as a diluent was placed in the reactor and heated to a desired reaction temperature (533~633 K) under a N_2 flow (21.4 ml/min). Then, the catalytic reaction was started by the introduction of ethanol (99.5 %, Wako Pure Chemical Industries) with N_2 carrier into the reactor. The 1.8 mol%. Two gas chromatographs, Shimadzu GC-8A equipped with a thermal conductivity detector and a packed column Porapack-QS and GC-380 equipped with a thermal conductivity detector and a flame-ionization detector and two packed columns, Unicarbon and molecular sieve 5A, were used. N_2 gas was used as internal standard for quantitative GC analysis. Ethanol conversion, the product selectivity, and carbon balance were defined as the following equations (1) and (2), respectively.

$$Conversion(\%) = \frac{X\ /mol}{X_0/mol} \times 100 \quad (1)$$

$$Selectivity(\%) = \frac{A\ /\ mol}{X/mol} \times 100 \quad (2)$$

where X_0, X, and A refer to the molar concentration of the reactant, consumption of substrate, and molar concentration of the products, respectively.

2. 2. 3 Characterization

Powder X-ray diffraction (XRD) measurements were performed with a RINT Ultima+ diffractometer (Rigaku) with Cu-Kα radiation (Kα =0.1540nm) and X-ray power of 40 kV / 20 mA. Specific surface areas were measured by the BET method from N2 adsorption at 77 K using a BELSORP MAX (BEL Japan Inc.). XPS measurements were performed using a JPS-9010 MC (JEOL). An Mg- Kα radiation source (1253.3 eV) operated at a power of 100 W (10 kV, 10 mA) was employed. Vacuum in the analysis chamber was < 5×10^{-6} during all measurements. Pass energy

of 30 eV was used to acquire all survey scans. The binding energy (BE) was corrected for surface charging by taking the C1s peak of carbon as a reference at 248.7 eV. Data were analyzed using the SpecSurf including Shirley background subtraction and fitting procedure. Quantification of the components for the surface oxidation state of vanadium and molybdenum was made using the SpecSurf. The binding energies of 517.2, 516.0 and 515.2 eV were attributed to V^{5+}, V^{4+} and V^{3+}, respectively, in the V_2O_3[15 ,16]. Mo^{6+}, Mo^{5+} and Mo^{4+} oxidation states were identified at 235.8, 234.7 and 232.2 eV for Mo3d3/2, and 231.7, 230.1 and 229.1 eV for Mo3d5/2, respectively[17, 18].

2. 3 Results and Discussion

2. 3. 1 Ethanol reaction over V_2O_5 and MoO_3 catalysts

Fig.2-1 and Fig.2-2 showed the product distribution in the ethanol reaction on vanadium and molybdenum oxide catalysts with different oxidation states. In the ethanol reaction over V_2O_5, no formation of ethane was observed, however, the high selectivity to acetaldehyde with 64.7 % was observed with complete transformation of ethanol at a 0.1 h time on stream. After 0.1 h time on stream, the conversion of ethanol and the selectivity to ethylene decreased to 74.5 % and 43.7 %, respectively at 2 h time on stream and constant for 14 h time on stream. The formation of ethane was observed at 1 h time on stream. The selectivity to ethane increased accompanied by the decrease in the selectivity to acetaldehyde with increase in the time on stream until 4 h. At the time on stream of 4 h, the selectivities to ethane and acetaldehyde reached in equal values, 45.3 % and 44.7 %, respectively. After 4 h time on stream, the selectivities to ethane and acetaldehyde kept unchanged until 14 h time on stream, even though the selectivity to acetaldehyde was slightly lower than that of ethane.

MoO_3 catalyst showed the catalytic behavior similar to V_2O_5 catalyst. In the beginning of the time on stream, ethanol was completely converted to products, however, no formation of ethane was

obtained. The main products were acetaldehyde with 65.5 % selectivity and ethylene with 30.7 % selectivity. In addition the small amount of diethyl ether with 6.7 % selectivity was also obtained. The selectivity to ethylene was higher than that to diethyl ether in all time on stream, suggesting that there are relatively strong acid site to produce olefin on the molybdenum oxide catalyst. The conversion of ethanol and the selectivity to acetaldehyde drastically decreased while the selectivity to ethane increased with increase in time on stream. The conversion of ethanol also decreased from 98.7 % at 0.1 h time on stream to 48.9 % at 5 h time on stream, and kept unchanged for 14 h time on stream. The conversion of ethanol was about two-third compared to that observed for the V_2O_5 catalyst at steady state. In addition, the selectivites to ethane and acetaldehyde were 26.7 % and 32.1 %, respectively at 5 h time on stream and kept constant until 14 h time on stream. In addition, the selectivity to ethylene also slightly increased from 0.1 h time on stream to 14 h time on stream. However, the selectivity to diethyl ether did not change in all time on stream. The Ohno et al. reported that H_xMoO_3 phase is formed by partial reduction of MoO_3 with H_2 and it is active for the dehydration of 2-propanol [14]. Therefore, in the present case, H_xMoO_3 phase seems to be formed on MoO_x during the ethanol conversion and it may act as protonic acid sites for the promotion of dehydration of ethanol. The formation of H_xMoO_3 phase was observed in the XRD and XPS analysis, and discuss later. The formation of ethylene and diethyl ether on MoO_3 catalyst was due to the relatively high acidic property of MoO_x catalyst compared with V_2O_x.

Other minor products for both the V_2O_5 and MoO_3 catalysts are attributed to C4 compounds, which is non-identified by GC (equipped with Porapack QS and Unicarbon packed column). The formation of C4 compounds such as ethyl acetate, n-butanol, crotonaldehyde and 2-butanone as condensation reaction of acetaldehyde were observed on GC-Mass analysis (equipped with ZB-1 column). The selectivity to others mentioned above over V_2O_5 catalyst and the CH_3CHO/C_2H_6 ratio were higher than that observed over MoO_3 catalyst, suggesting that the condensation reaction of

acetaldehyde was relatively favored on V_2O_5 catalyst. Decrease in the selectivity to acetaldehyde with increase of time on stream over V_2O_5 and MoO_3 catalysts was caused by the reduction of vanadium and molybdenum oxide. In the initial time on stream, the preferential formation of acetaldehyde took place as dehydrogenation of ethanol with concomitant removal of lattice oxygen of V_2O_5 and MoO_3 catalysts because the reaction was carried out under N_2, suggesting that V_2O_5 and MoO_3 catalysts were reduced during the catalytic reaction. This result indicates that the catalyst states of V_2O_5 and MoO_3 catalysts at steady state of ethanol reaction was different from those in the initial period of reaction.

In addition, increase in the surface area and pore volume of mesopores were observed for the V_2O_5 catalysts after use for the ethanol reaction for 14 h. Reduction of V_2O_5 led to the increase of surface area because lattice oxygen atoms of vanadium oxide were removed and formed porous structure. MoO_3 also showed increase of the surface area after ethanol reaction, suggesting that MoO_3 reduced during ethanol reaction. Increase in surface are of MoO_3 by reduction with H_2 was also reported by Matsuda's group. These observation were supported to the concept for the reduction of V_2O_5 and MoO_3 catalysts during ethanol reaction.

2. 3. 2 Ethanol reaction over VO_2, V_2O_3 and MoO_2 catalysts

In order to elucidate the relationship between the oxidation states of vanadium and molybdenum oxide catalysts and the catalytic activity, the ethanol reaction was carried out over VO_2, V_2O_3 and MoO_2 catalysts. Fig.s 2-3, 2-4 and 2-5 shows the conversion of ethanol and the product distribution as a function of time on stream in the ethanol reactions over VO_2, V_2O_3 and MoO_2 catalysts, respectively.

The ethanol reaction over VO_2 produced a large amount of acetaldehyde with 82.8 % selectivity and the small amount of ethane with 7.7 % selectivity at 0.1 h time on stream. In addition, a trace

amount of ethylene was also obtained. This result indicates that the degree of reduction of vanadium was not enough to form the equivalent amount of ethane and acetaldehyde in the initial period of reaction. The selectivity to ethane was still lower than that to acetaldehyde until 5 h time on stream, then almost the same selectivities to ethane with 42.7% and acetaldehyde with 44.4 % were observed at 5 h time on stream. After 5 h time on stream, the selectivity to each products was constant for 9 h time on stream. However, the conversion of ethanol gradually increased with increase of time on stream. This observation suggests that the initial crystal phase of the catalyst was changed to the other crystal phase which has more active sites for the ethanol reaction to produce ethane and acetaldehyde in an equal amount.

Compared to the VO_2 catalyst, V_2O_3 catalyst showed the formation of ethane and acetaldehyde in a 1 : 1 ratio in the initial period of reaction at 0.1 h time on stream, even though the conversion of ethanol slightly decreased from 22.3 % at 0.1 h time on stream to 15.3 % at 1 h time on stream. The selectivity to ethane and acetaldehyde did not change by increase of time on stream until 10 h time on stream, suggesting that the catalytic state of V_2O_3 catalyst was constant during the ethanol reaction. In other words, the V_2O_5 and VO_2 catalyst were reduced during the ethanol reaction to the same surface oxidation states as that of V_2O_3 to show the activity that forms ethane and acetaldehyde in the equal amount.

On the other hand, MoO_2 catalyst also showed a high performance for the equivalent formation of ethane and acetaldehyde, and the ratio C_2H_6/CH_3CHO was more close to 1 (the selectivity to ethane with 48.4 % and the acetaldehyde with 48.5 %) from the beginning of the ethanol reaction and stable for 10 h time on stream with the better conversion of ethanol compared with V_2O_3 catalyst. The conversion of ethanol was about three times higher than that of V_2O_3 catalyst and slightly decreased from 47 % to 41 % at 2 h time on stream. Obviously, intrinsic activity the MoO_2 catalyst for the ethanol reaction seems higher than that of the V_2O_3 catalyst, since the surface area of the V_2O_3 (17

m^2/g as shown in Table 2-3) is higher than that of MoO_2 (5 m^2/g as shown in Table 2-4). The selectivity to the other products (attributed to non-identified compounds) such as C4 compounds and carbon deposited, was less than 12 %. From these results, we can conclude that V^{3+} and Mo^{4+} species are active for equivalent formation of ethane and acetaldehyde from ethanol.

It is noteworthy that the amount of ethylene was very small and the formation of diethyl ether was not obtained over V_2O_3 and MoO_2 catalysts. This fact indicates that no acid sites, which can promote dehydration of ethanol to ethylene and diethyl ether, exist on the surfaces of the (low valence of) V_2O_3 and MoO_2 catalysts. The formation of equivalent amounts of toluene and benzaldehyde via the disproportionation of benzyl alcohol over $Mo/Al(OH)_3$, Mo/Al_2O_3 and $Mo/Zr(OH)_4$ was reported [29,30] by Mathew et al. and this reaction took place on the strong acid sites on the catalysts. Therefore, the formation of ethane and acetaldehyde in an equal amount from ethanol over the V_2O_3 and MoO_2 catalysts was not through the disproportionation reaction of ethanol that would occur of the strong acid site on the catalysts.

2. 3. 3 XRD measurements of V_2O_5 and MoO_3 catalysts

To study the relation between the oxidation states of catalysts and the activity for the formation of ethane and acetaldehyde, XRD examination was carried out for the V_2O_x and MoO_x used for various times on stream (0 h, 0.1 h, 2 h, 6 h, 13 h time on stream).

Fig.2-8 shows the XRD patterns of V_2O_5 with various times on stream (0 h, 0.1 h, 2 h, 6 h, 13 h time on stream). Before ethanol reaction, V_2O_5 catalyst provided XRD patterns corresponding only to the V_2O_5 phase and kept it until 0.1 h time on stream as a main phase. Small phase ascribed to V_4O_9 phase were observed at 0.1 h time on stream, suggesting that the reduction of V_2O_5 started at this time on stream. At 2 h time on stream, the peak intensity of the V_2O_5 phase decreased while the intensity of the V_4O_9 phase increased, and the VO_2 phase appeared. After 6 h time on stream, only

the diffraction lines due to the tetragonal and monoclinic VO_2 phases were observed and after 14 h time on stream only the tetragonal VO_2 phase remained. From this result, V_2O_5 phase of parent vanadium oxide catalyst was reduced to the VO_2 phase during the ethanol reaction.

Fig.2-9 shows the XRD patterns for the VO_2 and V_2O_3 samples before and after ethanol reaction. Monoclinic VO_2 phase including a small amount of V_6O_{13} phase (Fig.2-9 (c)) changed to tetragonal VO_2 phase, V_5O_9 phase and V_2O_3 phase after ethanol reaction. This result indicates that VO_2 also reduced during the ethanol reaction. However, the typical XRD patterns of the V_2O_3 phase were observed without other crystal phase after the ethanol reaction, suggesting that V_2O_3 catalyst did not reduce and catalytic states was constant during the ethanol reaction.

In the case of molybdenum oxide catalyst (Fig.2-10), only the diffraction lines due to the MoO_3 phased was detected on MoO_x catalyst until 0.1 h time on stream. The MoO_3 phase disappeared while the Mo_4O_9 phase and MoO_2 phase were observed at 2 h time on stream. With further increase of time on stream, the diffraction patterns corresponding to Mo_4O_9 phase decreased while the intensity of the diffraction lines for MoO_2 phase increased. In addition, the two diffraction lines corresponding to the MoO_xH_y at 2θ = 38.9 and 44.4° were observed on MoO_x after 6 h time on stream [31]. Moreover, some new peaks, which were non-identified were present at 2θ = 14.3, 29.1, 33.0 and 45.8° and their intensities increased with increase of time on stream.

Matsuda's group have also reported that MoO_3 was reduced by H_2 accompanied by an increase in surface area. They suggested on the basis of the results of XRD measurements that an increase of the surface area could be related to the formation of MoO_xH_y phase, for which a XRD diffraction lines appears at 2θ = 38.9° and 44.5°. The structure of MoO_xH_y phase is considered to be similar to that of molybdenum oxycarbide phase, MoO_xC_y, in which carbon atoms fill oxygen vacancies generated by reduction. The formation of MoO_xH_y phase was also detected by the result of XPS, and catalytic reaction, which will be discussed later.

Fig.2-11 shows the XRD patterns of MoO_2 samples before and after ethanol reaction. MoO_2 also showed no characteristic peaks to any impurities such as H_xMoO_3 [31] and no other molybdenum oxides were detected in the molybdenum oxides after ethanol reaction. This result indicates that the catalytic state of MoO_2 did not change during the ethanol reaction as well as V_2O_3 catalyst.

From these results, V_2O_3 and MoO_2 catalysts were active and stable for the formation of ethane and acetaldehyde in the ethanol reaction. It is indicated that vanadium oxide and molybdenum oxides, if started with different states, change their states to V_2O_3 and MoO_2, respectively, during the reaction of ethanol to be stabilized and showed the activity for the formation of ethane and acetaldehyde.

2. 3. 4 Surface oxidation states of V_2O_5 and MoO_3 catalysts in ethanol reaction

To obtain further insight into the oxidation state of V_2O_5 and MoO_3 in the ethanol reaction, the effect of time on stream on the oxidation state of catalyst was studied by X-ray photoelectron spectroscopy (XPS) analysis as shown in Fig.s 2-12 and 2-13. XPS analysis is a good tool for the investigation of the composition and oxidation states of the surface elements. The binding energy (BE) was corrected for surface charging by taking the C s1 peak of carbon as a reference at 248.7 eV.

The XPS spectrum of the $V2p_{3/2}$ in the V_2O_x catalyst and composition of valence state of vanadium by deconvolution of the XPS spectrum of the $V2p_{3/2}$ are shown in Fig. 2-12. In addition, the composition of surface of V_2O_5 as a function of time on stream is shown in Fig.2-14 and Table 2-5. The binding energies of V^{5+}, V^{4+} and V^{3+} used for the deconvolution were 517.2, 516.0 and 515.2 eV$\pm$0.2 eV, respectively [28,29], in the V_2O_x as shown in Table 2-5.

As could be observed in Fig.2-12 (a), the peak top was sifted from 516.5 eV to the low binding energy region as the time on stream increased, suggesting that the surface oxidation state was reduced during the ethanol reaction. At 6 h time on steam, the binding energy region of the peak for

$V2p_{3/2}$ was 516.5 eV and did not change until 14 h time on stream. However, the intensity of this peak was weaker and became broader than that of peak before reaction. This result clearly indicates that the vanadium species were mixed 5^+, 4^+ and 3^+ valence states on the catalyst surface after beginning of the reaction.

The double peak for Mo3d was also shifted to lower binding energy region with an increase of time on stream to 2 h time on stream as shown in Fig.2-13, but the region of this peak did not change after 2 h time on stream. There are three valence states of Mo speices on the MoO_x at 2 h time on stream because the peak shape became broader than that of pristine molybdenum oxide catalyst. However, the doublet peak for Mo3d became sharp at 6 h time on stream and did not change for 14 h time on stream, suggesting that the MoO_3 was also reduced during the ethanol reaction.

The compositions of surface oxidation states for V_2O_x and MoO_x as a function of time on stream are shown in Fig.2-14 and Fig.2-15, respectively. The composition of the surface oxidation states of vanadium and molybdenum oxides are calculated by fitted with Gaussian – Lorentzian curves after Shirley background subtraction of the spectra for $V2p_{3/2}$ and $Mo3d_{5/2}$ as shown in Table 2-5, 2-6. The calculation of the composition of surface oxidation states for vanadium oxide (Fig.2 (a)) indicates that the surface oxidation states were mainly V^{5+} (at 517.2 eV 90.1 %), followed by V^{4+} (at 515.8 eV 4.9 %) and V^{3+} (at 515.2 eV 5.0 %) on the surface of V_2O_x catalyst before reaction. However, the composition of V^{4+} and V^{3+} increased while the composition of V^{5+} decreased with an increase of time on stream and reached the maximum values at 6 h time on stream. Then, the composition of each oxidation states for vanadium was constant for 14 h time on stream, even though the V^{5+} species slightly decreased at 14 h time on stream. Curve fitting using respective binding energies showed the presence of three V_2O_5, VO_2 and V_2O_3 states on the surface of V_2O_x catalyst at steady state.

In the case of molybdenum oxide, the only Mo^{6+} species was observed on the surface of molybdenum oxide catalyst before ethanol reaction. At 0.1 h time on stream, the composition of Mo^{5+} slightly increased to 16.7 % while Mo^{6+} slightly decreased 83.3 %, but no Mo^{4+} species was detected. In time on stream of 2h, the composition of Mo^{6+} drastically decreased to 31.1 % and Mo^{5+} and Mo^{4+} increased to 37.8 % and 31.1 %, respectively. The maximum values for the composition of Mo^{5+} species was obtained at this time on stream. The composition both of Mo^{6+} and Mo^{5+} species decreased while the composition of Mo^{4+} species increased at 6 h time on stream and kept unchanged until 14 h time on stream. The induction period was observed on the Mo^{4+} species, suggesting that the step by step reduction of Mo species took place.

For both V_2O_x and MoO_x catalysts, the tendencies of the increase in the compositions of V^{4+} and V^{3+} on vanadium oxides and those of Mo^{5+} and Mo^{4+} on molybdenum oxides as a function of time on stream is correlated well with the increase of the selectivity to ethane in the ethanol reaction over V_2O_x and MoO_x. From this result, reduced vanadium and molybdenum species are active for the formation of ethane from ethanol.

On the other hand, the peak for the O 1s (530.5 eV) on molybdenum oxide sample was shifted to lower binding energy after 2 h time on stream. This result supports that oxygen of MoO_3 was reduced during the ethanol conversion after 2 h time on stream. The reduction of oxygen of molybdenum oxides was caused by the formation of hydrogen bonding with lattice oxygen and hydrogen produced by dehydrogenation of ethanol.

This idea was supported by observation of shoulder peak on the XPS spectra corresponding to O 1s at higher binding energy region after 2 h time on stream on the MoO_x (Fig.2-16). An additional spectrum beside the main O1s spectra at 530.5 eV was observed after 2 h time on stream over MoO_x oxide and revealed the presence of shoulder around 532 eV (Fig.2-16). Moreover, the relatively low intensity of spectral line of O 1s at 530.5 eV was observed from this time on stream. This result

indicates that parent oxygen attributed to lattice oxygen of MoO_3 catalyst, which is attributed to binding energy region at 530.5 eV, was partial changed to another type of oxygen surface on molybdenum oxide. Kandari et al. indicated that this shoulder peak around 532.0 eV was assigned to the formation of Brönsted acidic group Mo-OH on the surface of the sample following dissociation of H_2 by the metallic function of MoO_2 [10]. Therefore, $MoO_x(H)_{ac}$ was formed during the ethanol conversion by adsorption of hydrogen produced by dehydrogenation of ethanol on surface. The formation of $MoO_x(H)_{ac}$ resulted in the increase in acidity of sample and enhanced the production of ethylene by dehydration of ethanol. As a result, the selectivity to ethylene was increased as increase of time on stream because dehydration of alcohol proceeded on the Brönsted acid site. This result is supported by the change in XPS spectra for $V2p_{2/3}$ of V_2O_5 as a function of time on stream. The additional peak similar to MoO_3 beside the main O 1s peak of V_2O_5 was not detected for all the samples. Therefore, the selectivity to ethylene was decreased with increase of time on stream due to no formation of the Brönsted acidic group V-OH during the ethanol reaction.

Reduced vanadium and molybdenum oxides have oxygen-defect structure compared with V_2O_5 and MoO_3. Reduction of V_2O_5 and MoO_3 occurred by interaction between hydrogen produced by dehydrogenation of ethanol and terminal oxygen of V_2O_5 and MoO_3. As a result, terminal oxygen was disappeared and lead to form the cation site on the reduced vanadium and molybdenum oxides. Therefore, this cation site was active for the formation of ethane from ethanol.

2. 3. 5 Surface oxidation states of VO_2, V_2O_3 and MoO_2 catalysts before and after ethanol reaction.

Fig.2-17 showed the XPS spectra corresponding to the $V2p_{3/2}$ of VO_2 and V_2O_3, and Mo3d of MoO_2 before and after ethanol reaction. The composition of the surface oxidation states for VO_2, V_2O_3 MoO_2 are also shown in Table 2-7. The binding energy region for $V2p_{3/2}$ of VO_2 shifted to

lower binding energy region after ethanol reaction as well as that of V_2O_3. The binding energy region for $V2p_{3/2}$ of V_2O_3 did not change after ethanol reaction. Moreover, the composition of surface oxidation states of VO_2 were changed to the same as that of V_2O_3 after ethanol reaction, but V_2O_3 did not change after ethanol reaction. The composition of surface oxidation states of MoO_2 was almost the same after ethanol reaction, even though Mo^{6+} was slightly low as shown in Fig.2-18.

These results clearly indicate that exposure of V_2O_5, VO_2 and MoO_3 catalysts to reaction stream at 573 K results in the reduction of the surface oxidation states to the same surface oxidation state of V_2O_3 and MoO_2, respectively. From this result, the surface oxidation states of V_2O_3 and MoO_2 are active and stable for the formation of ethane from ethanol, even though vanadium and molybdenum species are mixed V^{4+} and V^{3+} valence states, Mo^{6+}, Mo^{5+} and Mo^{4+} valence states.

2.4 Conclusion

Catalytic tests for ethanol conversion were performed on vanadium and molybdenum oxides with different oxidation states. Ethane and acetaldehyde were formed in 1:1 ratio over all of the vanadium and molybdenum oxide catalysts. To the best of our knowledge, this is the first time to observe the formation of ethane from ethanol over vanadium and molybdenum oxide catalysts.

V_2O_5 and MoO_3 exhibited no formation of ethane at 0.1 h time on stream, even though the same selectivities to ethane and acetaldehyde were obtained in the long time on stream period. VO_2 also produced the very low amount of ethane from ethanol in the beginning of the time on stream. On the other hand, the equivalent amounts of ethane and acetaldehyde were formed over V_2O_3 and MoO_2.

The results of XRD and XPS shows that the crystal phase and surface oxidation states of V_2O_5, VO_2 and MoO_3 were changed after the ethanol reaction, however, for both the V_2O_3 and MoO_2 catalysts did not change. The surface oxidation states of V_2O_5 and VO_2 were changed to the similar

that of V_2O_3 catalyst.

Based on these results, we can conclude that V_2O_3 and MoO_2 are active and stable for the ethanol reaction to produce ethane and acetaldehyde in unity.

2. 5 References

[1] H. Nair, J. E. Gatt, J. T. Miller, C. D. Baertsch, *J. Catal*. 279 (2011) 144-154.

[2] E.V.Kondratenko, O. Ovsitser, J. Radnik, M. Schneider, R. Kraehnert, U. Dingerdissen, *Appl. Catal. A* 319 (2007) 98-110.

[3] Y.Sakurai, T. Suzaki, K. Nakagawa, N. Ikenaga, H. Aota, T. Suzuki, *J. Catal*. 209 (2002) 16-24.

[4] R. Tesser, V. Maradei, M. D. Serio, E. Santacesaria, *Ind. Eng. Chem. Res*. 43 (2004) 1623-1633.

[5] S. T. Oyama, W. Zhang, *J. Am. Chem. Soc*. 118 (1996) 7173-7177.

[6] M. R. Maurya, A. K. Chandrakar, S. Chand, *J. Mol. Catal. A* 263 (2007) 227-237.

[7] M. Niwa, J. Igarashi, *Catal. Today* 52 (1999) 71-81.

[8] A. Benadda, A. Katrib, A. Barama, *Appl. Catal. A* 251 (2003) 93-105.

[9] T. Ohno, Z. Li, N. Sasaki, H. Sakagami, N. Takahashi, T. Matsuda, *Appl. Catal. A* 389 (2010) 52-59.

[10] S. Al-Kandari, H. Al-Kandari, F. Al-Kharafi, A. Katrib, *Appl. Catal. A* 341 (2008) 160-167.

[11] J. H. Song, P. Chen, S. H. Kim, G. A. Somorjai, R. J. Gartside, F. M. Dautzenberg, *J. Mol. Catal. A* 184 (2002) 197-202.

[16] J. B. Mcmonagle, J. B. Moffat, *J. Catal.* 91 (1985) 132-141

[17] B. M. Abu-Zied, A. M. El-Awad, *J. Mol. Catal. A: Chem.* 176 (2001) 227-246

[18] M. M. Mohamed, *J. Mol. Catal. A: Chem.* 200 (2003) 301-3137

[19] B. Ohtani, M. KAkimoto, S. Nishimoto, T, Kagiya, *J. Photochem. Photobiol.a: Chem.* 70 (1993) 265-272

[20] K. Rintramee, K. Fottinger, G. Rupprechter, J. Wittayakun, *Appl. Catal. B* 115 (2012) 225-235

[21] J.V. Ochoa, C. Trevisanut, J. M.M Millet, G. Busca, F. Cavani, *J. Phys. Chem. C* 117 (2013) 23908-23918

[22] R. Lobo, C. L. Marshall, P.J. Dierich, F. H.Ribeiro, C. Akatay, E. A.Stach, A. Mane, Y. Lei, J. Elam, J. T. Miller, *ACS Catal*. 2 (2012) 2316-2326

[23] T. Jin, H. Hattori, K. Tanabe, *Chem. Lett*. 1 (1981) 533-1534

[24] R. Sumathi, K. Johnson, B. Viswanathan, T. K. Varadarajan, *Appl. Catal. A* 172 (1998) 15-22

[25] D. R. Park, J. H. Song, S. H. Lee, S. H. Song, H. Kim, J. C. Jung, I. K. Song, *Appl. Catal. A* 349 (2008) 222-228

[26] N. Lingaiah, K. M. Reddy, N. S. Babu, K. N. Rao, I. Suryanarayana, P. S. S. Prasad, *Catal. Commun*. 7 (2006) 245-250

[27] P. S. N. Rao, K. T. V. Rao, P. S. S. Prasad, N. Lingaiah, *Catal. Commun*. 11 (2010) 547-550

[28] K. M. Reddy, M. Balaraju, P. S. S. Prasad, I. Suryanarayana, N. Lingaiah, *Catal. Lett*. 119 (2007) 304-310

[29] (a) S. Mathewa, C. S. Kumara, N. Nagaraju, *J. Mol. Catal. A* 255 (2006) 243-248, (b) S. Mathew, J.B. Nagy, N. Nagaraju, *Catal. Commun*. 7 (2006) 177-183, (c) S. Mathew, H. Kathyatini, J. B. Nagy, N. Nagaraju, Catal. Commun. 10 (2009) 1043-1047

[30] (a) M. Jayamani, C.N. Pillai, J. Catal. 82 (1983) 485-488, (b) M. Jayamani, N. Murugasen, C.N. Pillai, J. Catal. 85 (1984) 527-529, (c) K. Ganesan, C. P. Pillai, J. Catal. 119 (1989) 8-13

[31] (a) M. Sanker, E. Nowicka and G. J. Hutchings, *Faraday Discuss* 145 (2010) 341-356, (b) M. Sanker, E. Nowicka, R. Tiruvalam, Q. He, S. H. Taylor, C. J. Kiely, D. Bethell, D. W. Knight, G. J. Hutchings, *Chem. Eur. J*. 17 (2011) 6524 – 6532, (c) E. Cao, M. Sanker, E. Nowicka, Q. He, M. Morad, P. J. Miedziak, S. H. Taylor, D. W. Knight, D. Bethell, C. J. Kiely, A. Gavriilidis, Catal. Taday 203 (2013) 146-152

Table 2-1. The reaction of various alcohols over various kinds of catalysts to produce corresponding alkanes and aldehydes.

Catalyst	Reactant	T	Conv.	Selectivity (%)			Other	Ref
		(K)	(%)	Alkane	Alkene	Aldehyde	Products	
$(NH_4)_3PMo_{12}O_{40}$	C_2H_5OH	498	38.3	32.9	15.3	51.8	—	[16]
Cd-Cr-O	C_2H_5OH	673	58.0	5.5	5.0	73.0	—	[17]
Fe ion exchanged mordenite	C_2H_5OH	673	68.0	68.0	—	7.0	CH_4, $(C_2H_5)_2O$	[18]
TiO_2-PtO	C_2H_5OH	r.t	—	2.6	—	3.7	Hemi acetal	[19]
Pt-Al	C_3H_7OH	523	—	13.0	—	12.0	H_2	[22]
Pt-Ti	C_3H_7OH	523	—	12.0	—	10.0	H_2	[22]
Pt-Ce	C_3H_7OH	523	—	10.0	—	15.0	H_2	[22]
Fe_2O_3	2-Butanol	523	8.8	16.8	7.7	76.5	—	[23]
Fe_2O_3-ZnO	2-Butanol	523	24.9	2.4	3.2	94.4	—	[23]
Fe_2O_3-ZrO_2	2-Butanol	523	8.5	13.8	11.9	85.3	—	[23]
V_2O_3	C_2H_5OH	573	16.5	39.9	< 1	41.7	—	This work
MoO_2	C_2H_5OH	573	42.9	45.6	1.3	47.1	—	This work

Table 2-2. The reactions of benzyl alcohol produce toluene and benzaldehyde over various kinds of catalysts.

Catalyst	T (K)	Carrier	Conversion (%)	Selectivity (%)			Ref
					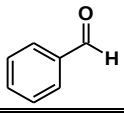	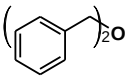	
$H_3PMo_{12}O_{40}$	573	O_2	< 65	< 5	< 97	—	[25]
$H_3PMo_xW_{12-x}O_{40}$ $H_6P_2Mo_xW_{18-x}O_{62}$	573	O_2	< 65	< 7	> 90	—	[25]
15 % $AMPV_2/NbO_2$ [a]	523	O_2	41.1	< 10	88.0	—	[26]
$(NH_4)_4PMo_{11}VO_{40}$	523	O_2	< 60	< 20	< 80	—	[27]
HSiWO	626	—	97.0	25.7	17.5	7.2	[29]
HPWO	626	—	96.0	25.0	22.9	5.2	[29]
HY-zeolite	573	—	90.0	36.7	35.3	—	[29]
$Al(OH)_3$	663	—	47.0	1.4	10.1	88.5	[29]
Al_2O_3	663	—	—	43.0	43.0	17.0	[29]
$Mo/Al(OH)_3$	reflux	—	98.0	41.0	51.0	6.0	[30]
Mo/Al_2O_3	reflux	—	64.0	30.0	34.0	—	[30]
$Mo/Zr(OH)_4$	reflux	—	41.0	—	2.0	—	[30]
Mo/CaO	reflux	—	21.0	7.0	14.0	—	[30]
Mo/MgO	reflux	—	2.0	7.0	14.0	—	[30]
Au-Pd / TiO_2	353	He	27.0	45.4	54.6	—	[31]

[a] Vanadium incorporated molybdophosphoric acid

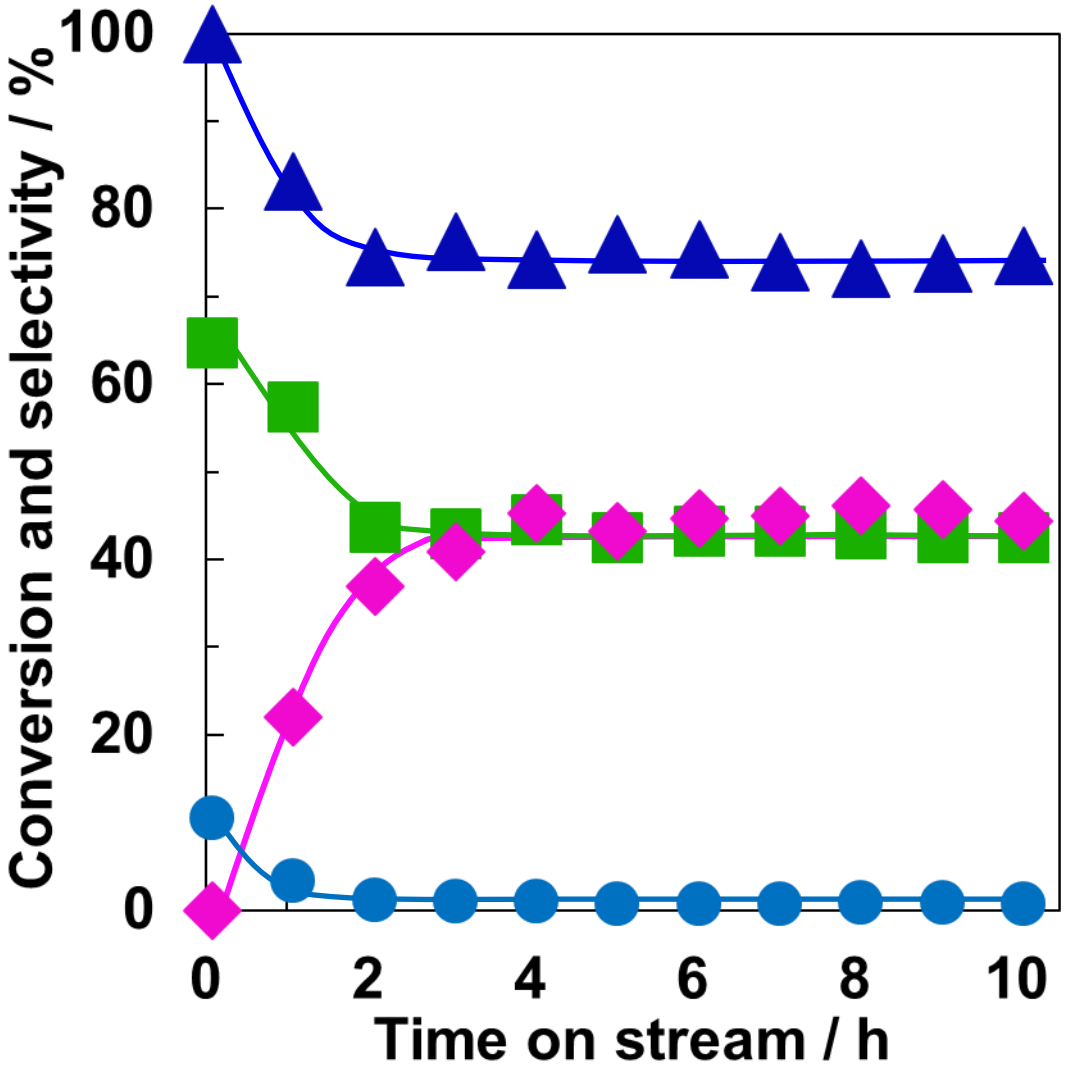

Fig.2-1 Ethanol conversion to ethane and acetaldehyde as the function of time on stream over V_2O_5 at 573 K under N_2. V_2O_5 0.15g, SiO_2 2.5g, flow rate: N_2 21 ml/min, ethanol 0.39 ml/min. (▲) conversion of ethanol, selectivity to (◆) ethane, (●) ethylene, (■) acetaldehyde.

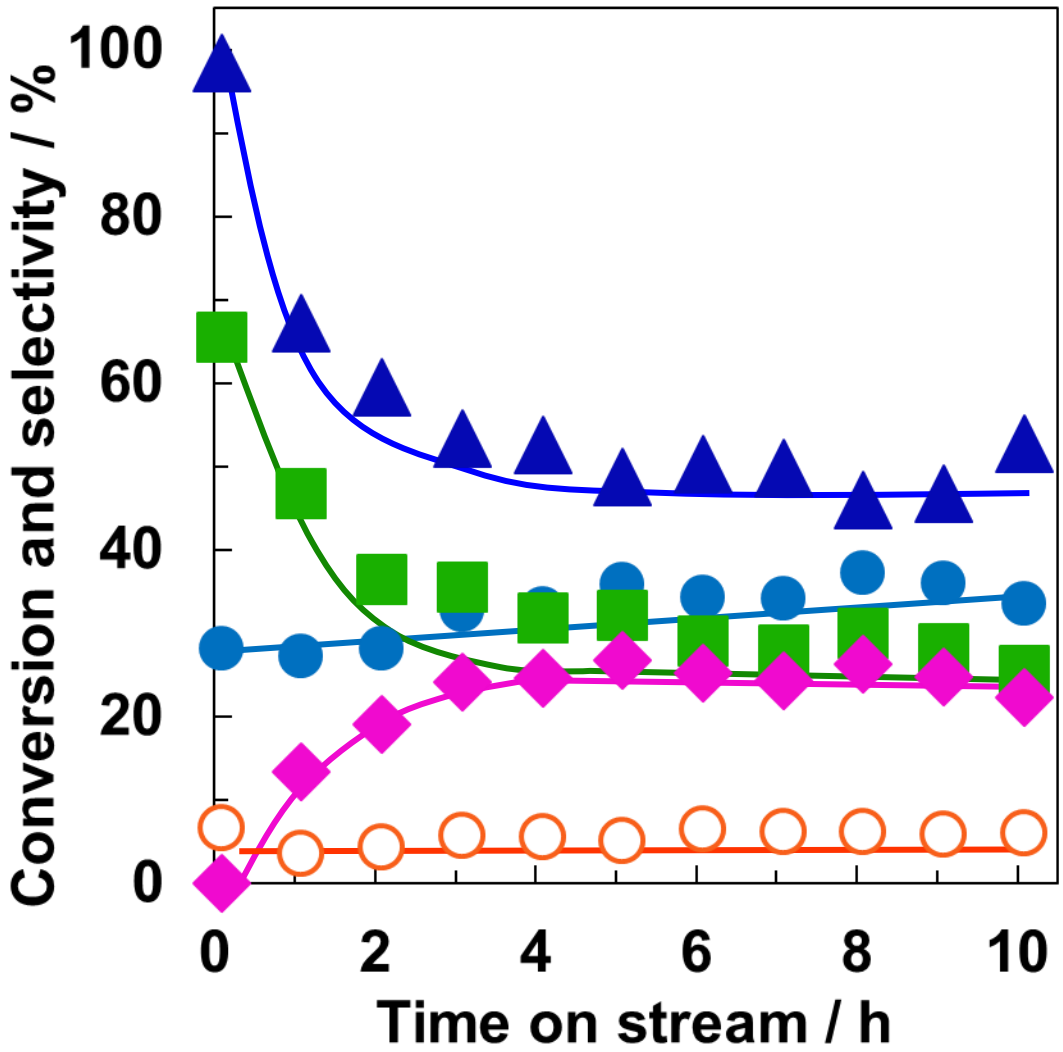

Fig.2-2 Ethanol conversion to ethane and acetaldehyde as the function of time on stream over MoO_3 catalyst at 573 K under N_2. MoO_3 0.15g, SiO_2 2.5g, flow rate: N_2 21 ml/min, ethanol 0.39 ml/min. (▲) conversion of ethanol, selectivity to (◆) ethane, (●) ethylene, (■) acetaldehyde, (○) diethyl ether.

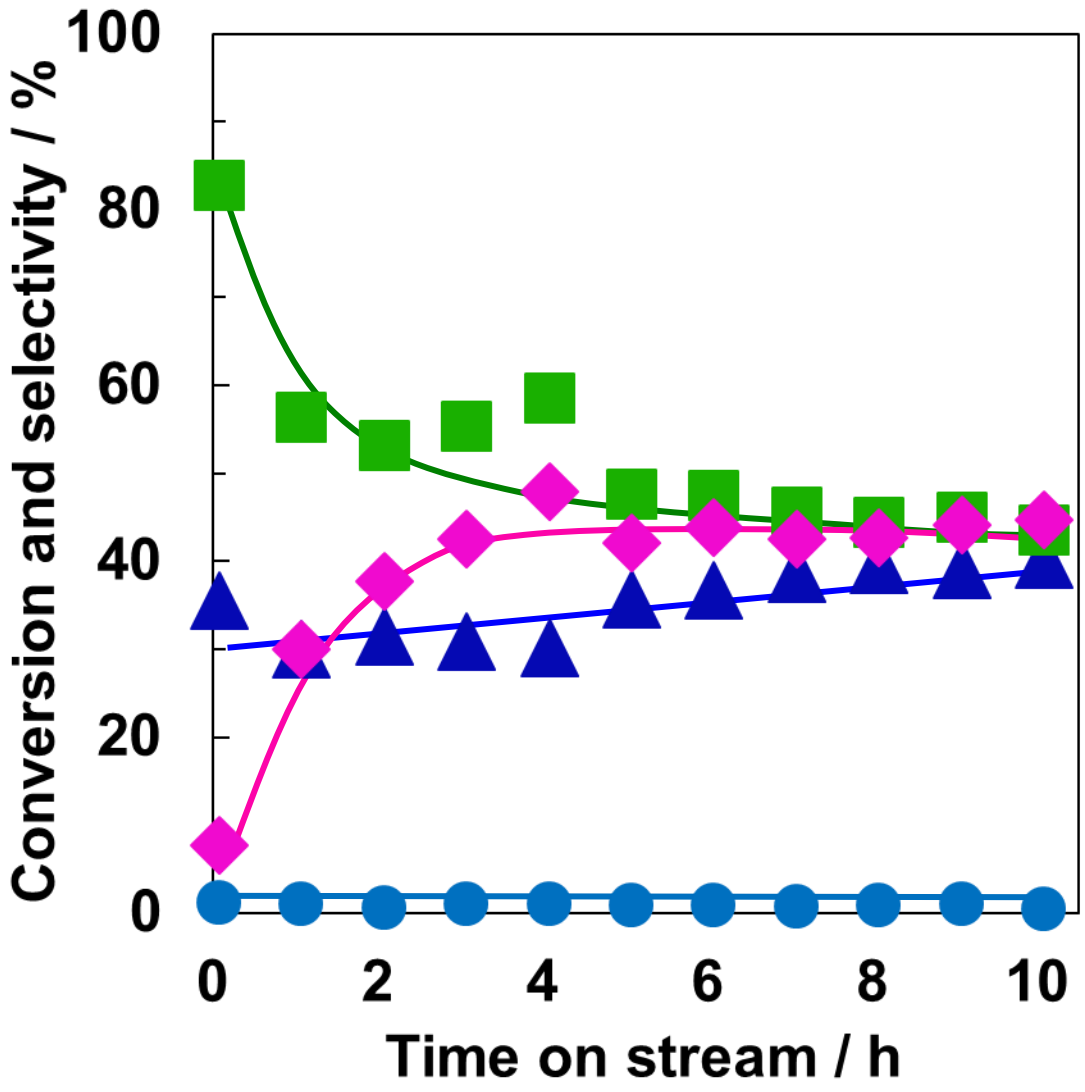

Fig.2-3 Ethanol conversion to ethane and acetaldehyde as the function of time on stream over VO_2 catalysts at 573 K under N_2. VO_2 0.15g, SiO_2 2.6 g, 5 h time on stream, flow rate : N_2 21 ml/min, ethanol 0.39 ml/min, (▲) conversion of ethanol, selectivity to (◆) ethane, (●) ethylene, (■) acetaldehyde

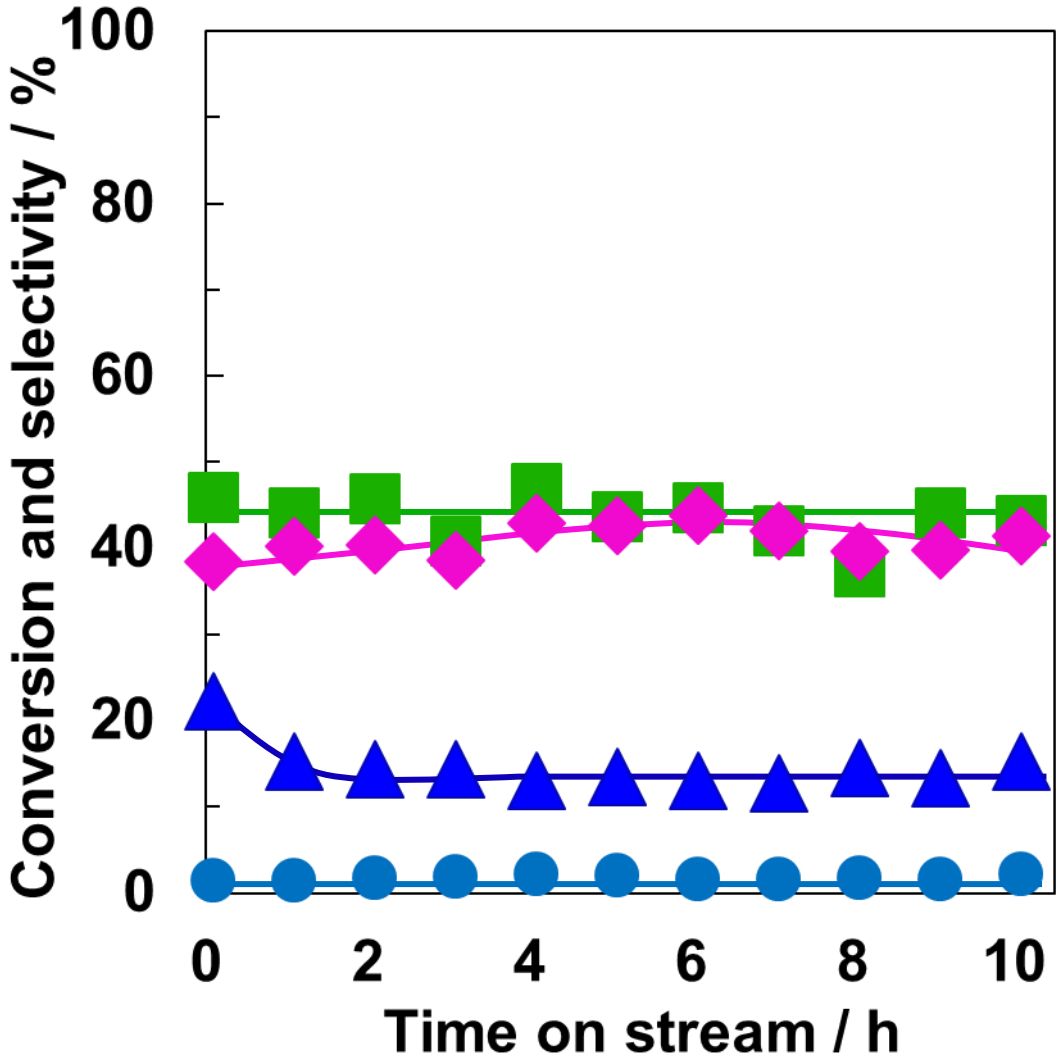

Fig.2-4 Ethanol conversion to ethane and acetaldehyde as the function of time on stream over V_2O_3 catalysts at 573 K under N_2. Reaction condition: V_2O_3 0.15g, SiO_2 2.6 g, 5 h time on stream, flow rate : N_2 21 ml/min, ethanol 0.39 ml/min, (▲) conversion of ethanol, selectivity to (◆) ethane, (●) ethylene, (■) acetaldehyde

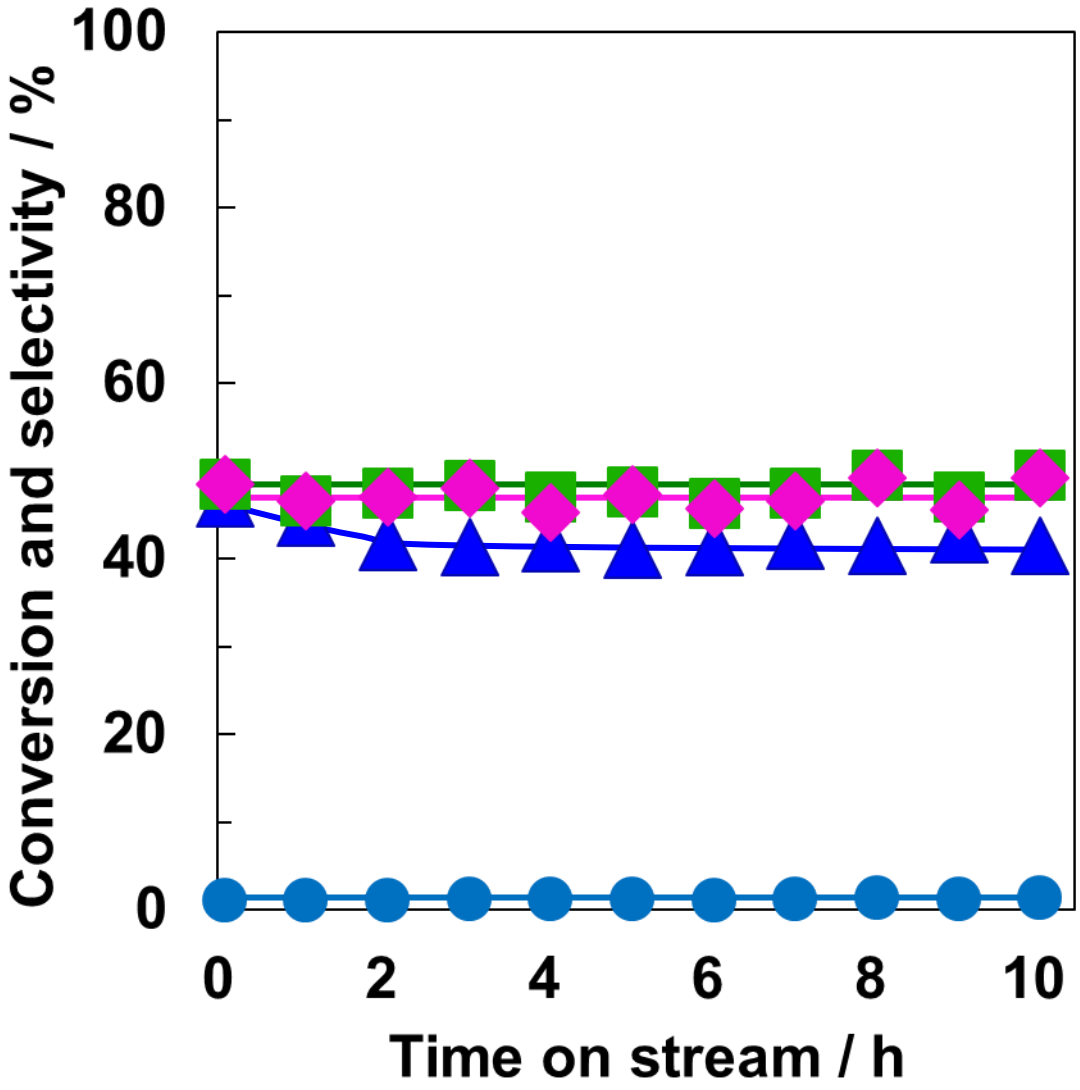

Fig.2-5 Catalytic performance of MoO_2 at 573 K. HT-MoO_2 0.15g, SiO_2 2.5g, flow rate: N_2 21 ml/min, ethanol 0.24 ml/min. (▲) conversion of ethanol, selectivity to (◆) ethane, (●) ethylene, (■) acetaldehyde

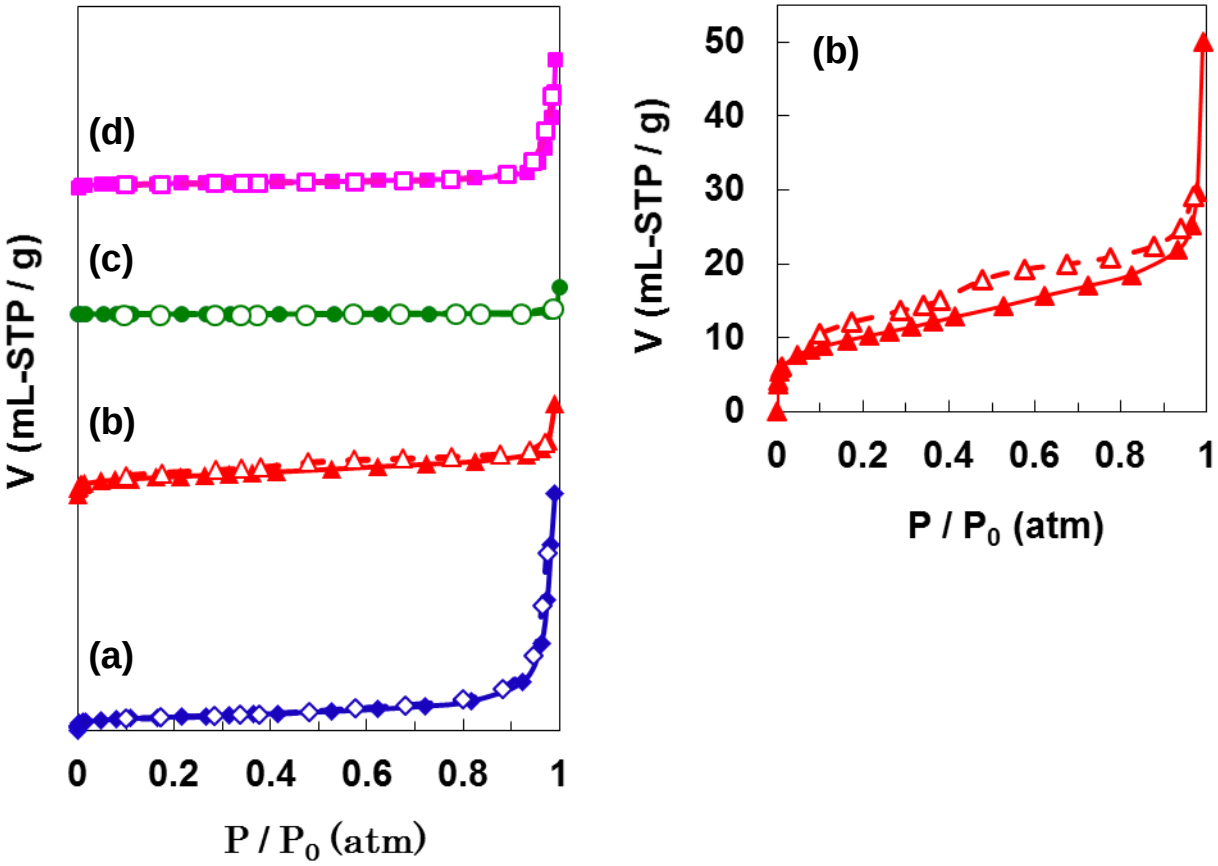

Fig.2-6 N_2 adsorption isotherms at 77 K for the V_2O_5 (a), used-V_2O_5 (after 13 h time on stream) (b), VO_2 (c) and V_2O_3 (d). Open symbol; adsorption of N_2, closed symbol; desorption of N_2

Table 2-3. Surface are of V_2O_5, used-V_2O_5 (after 13 h time on stream) and V_2O_3.

Sample name	Surface area / m^2 g^{-1}
V_2O_5	57
used-V_2O_5 (13 h time on stream)	94
V_2O_3	14

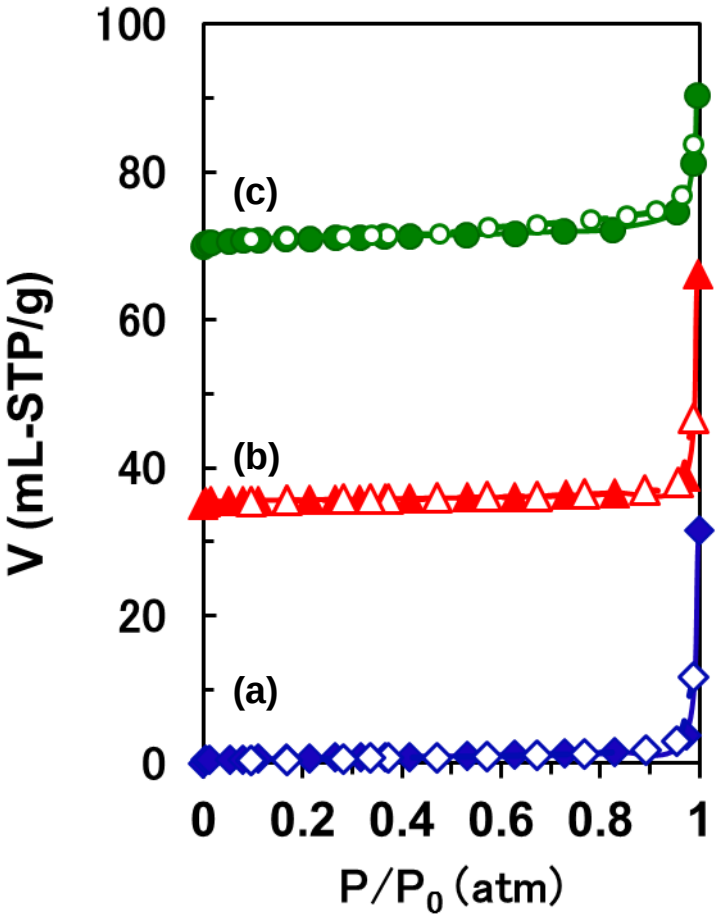

Fig.2-7 N_2 adsorption isotherms at 77 K for the MoO_3 (a), used-MoO_3 (after 13 h time on stream) (b) and MoO_2 (c). Open symbol; adsorption of N_2, closed symbol; desorption of N_2

Table 2-4. Surface are of MoO_3, used- MoO_3 (13 h after time on stream) and MoO_2.

Sample name	Surface area / m^2 g^{-1}
MoO_3	6
Used-MoO_3(13 h time on stream)	9
MoO_2	5

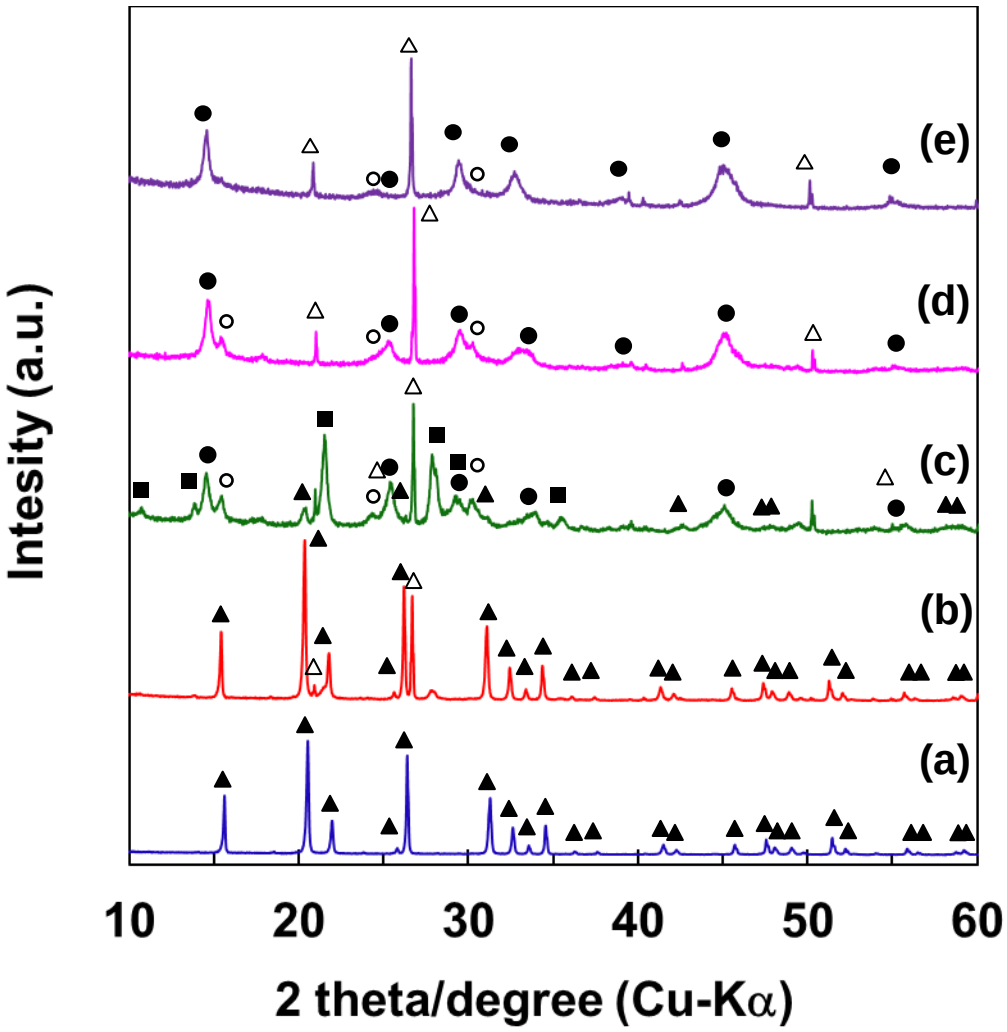

Fig.2-8 Comparison of XRD patterns of the V_2O_5 catalysts at different time on stream. Time on stream of (a) 0 h (fresh V_2O_5), (b) 0.1 h, (c) 2 h, (d) 6 h and (e) 13 h. Reaction condition: V_2O_5 0.15g, SiO_2 2.0 g, reaction temperature 573 K, flow rate: N_2 21 ml/min, ethanol 0.24 ml/min. (▲)V_2O_5, (■)V_4O_9, (●)tetragonal-VO_2, (○)monoclinic-VO_2, (△) SiO_2

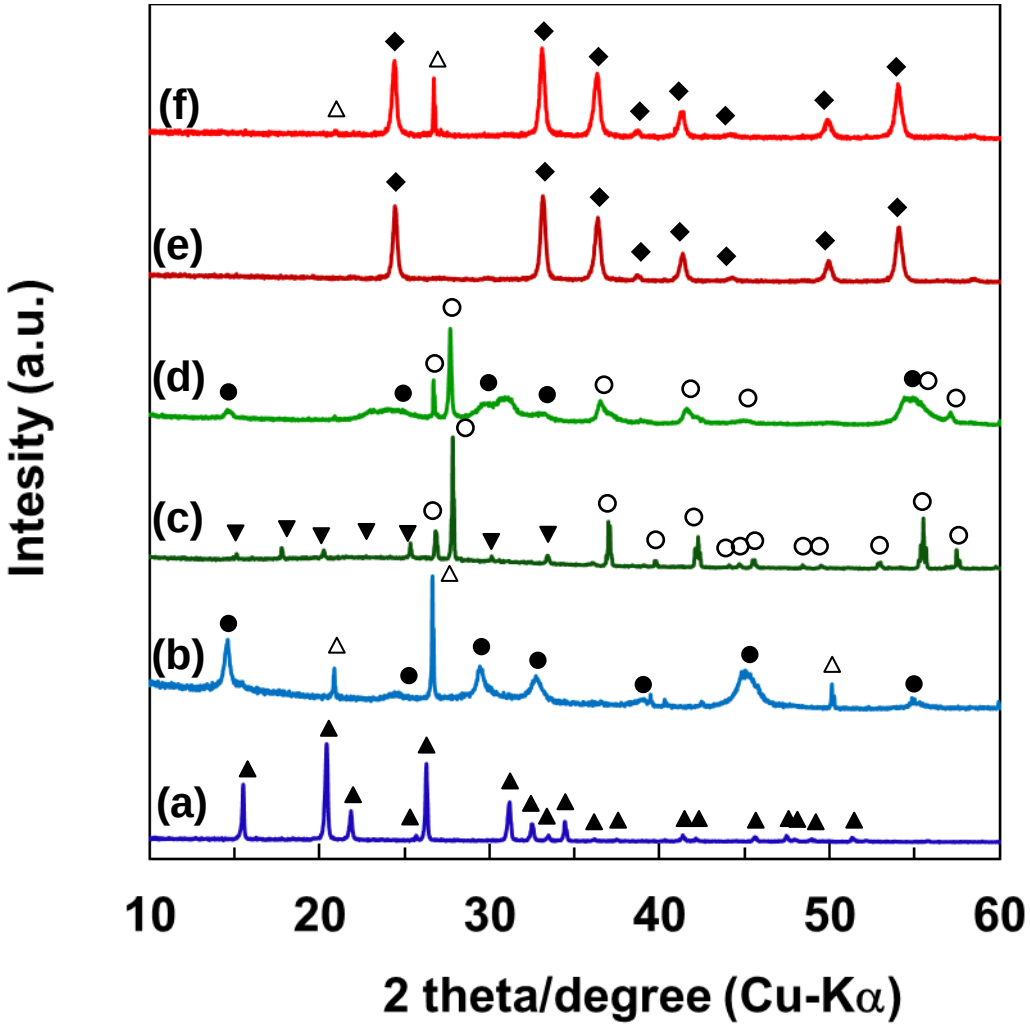

Fig.2-9 Comparison of XRD patterns of the VO_x before and after ethanol reaction. (a) V_2O_5 before reaction, (b) V_2O_5 after reaction, (c) VO_2 before reaction, (d) VO_2 after reaction, (e) V_2O_3 before reaction and (f) V_2O_3 after reaction. Reaction condition: V_2O_5 0.15g, reaction temperature 573 K, flow rate: N_2 21 ml/min, ethanol 0.24 ml/min. (▲) tetragonal V_2O_5, (●) tetragonal-VO_2, (○)monoclinic-VO_2, (▼)V_6O_{13}, (◆)V_2O_3, (△) SiO_2

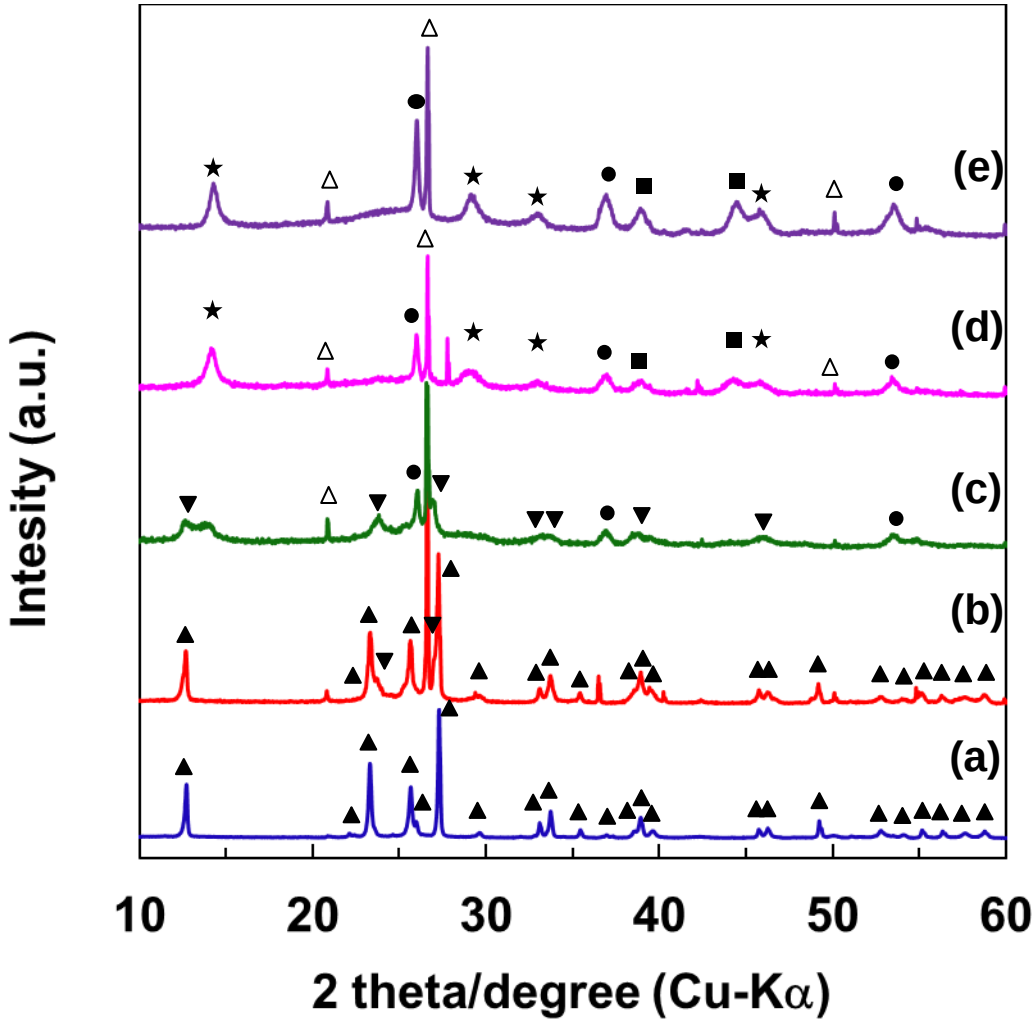

Fig.2-10 Comparison of XRD patterns of the MoO_3 catalysts at different time on stream. Time on stream (a) 0 h (fresh MoO_3), (b) 0.1 h, (c) 2 h, (d) 6 h and (e) 13 h. Reaction condition: MoO_3 0.15g, SiO_2 2.0 g, reaction temperature 573 K, flow rate: N_2 21 ml/min, ethanol 0.24 ml/min. (▲)monoclinic MoO_3, (▼) orthorhombic MoO_3, (●)MoO_2, (■)MoO_xH_y, (★)unknown, (△) SiO_2

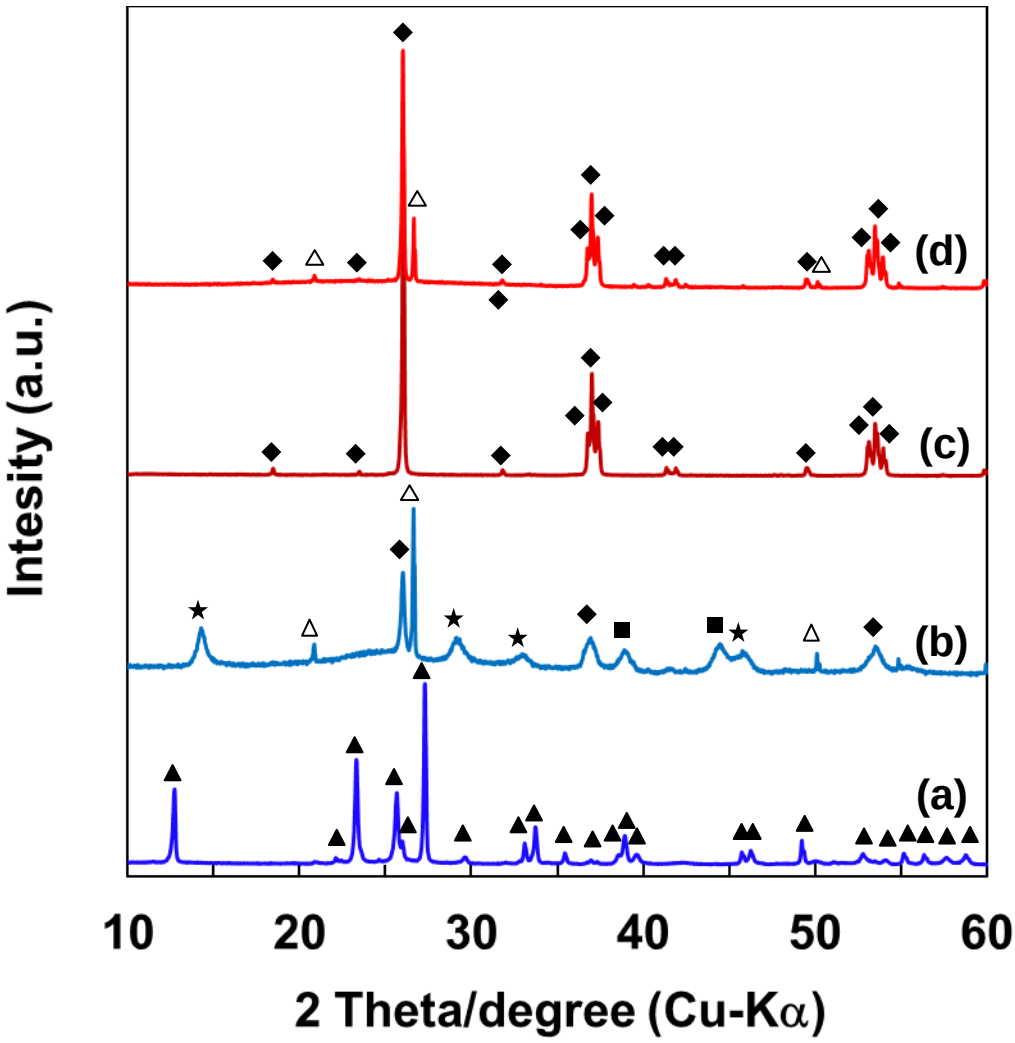

Fig.2-11 Comparison of XRD patterns of the MoO_x before and after ethanol reaction. (a) MoO_3 before reaction, (b) MoO_3 after reaction, (c) MoO_2 before reaction and (d) MoO_2 after reaction. Reaction condition: V_2O_5 0.15g, reaction temperature 573 K, flow rate: N_2 21 ml/min, ethanol 0.24 ml/min. (▲) monoclinic MoO_3, (■) MoO_xH_y, (◆) MoO_2, (★) unknown, (△) SiO_2

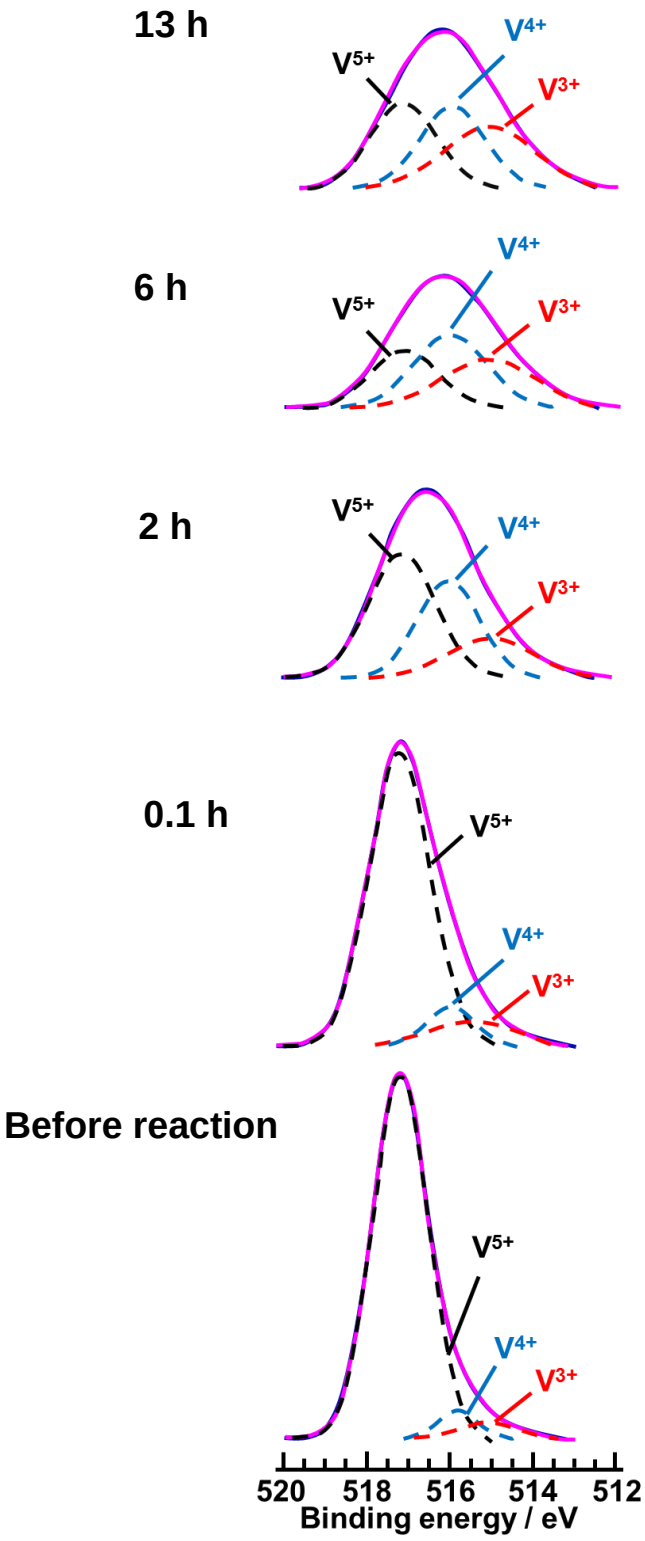

Fig.2-12 XPS spectra corresponding to V $2p_{3/2}$ of V_2O_5 samples as a function of time on stream

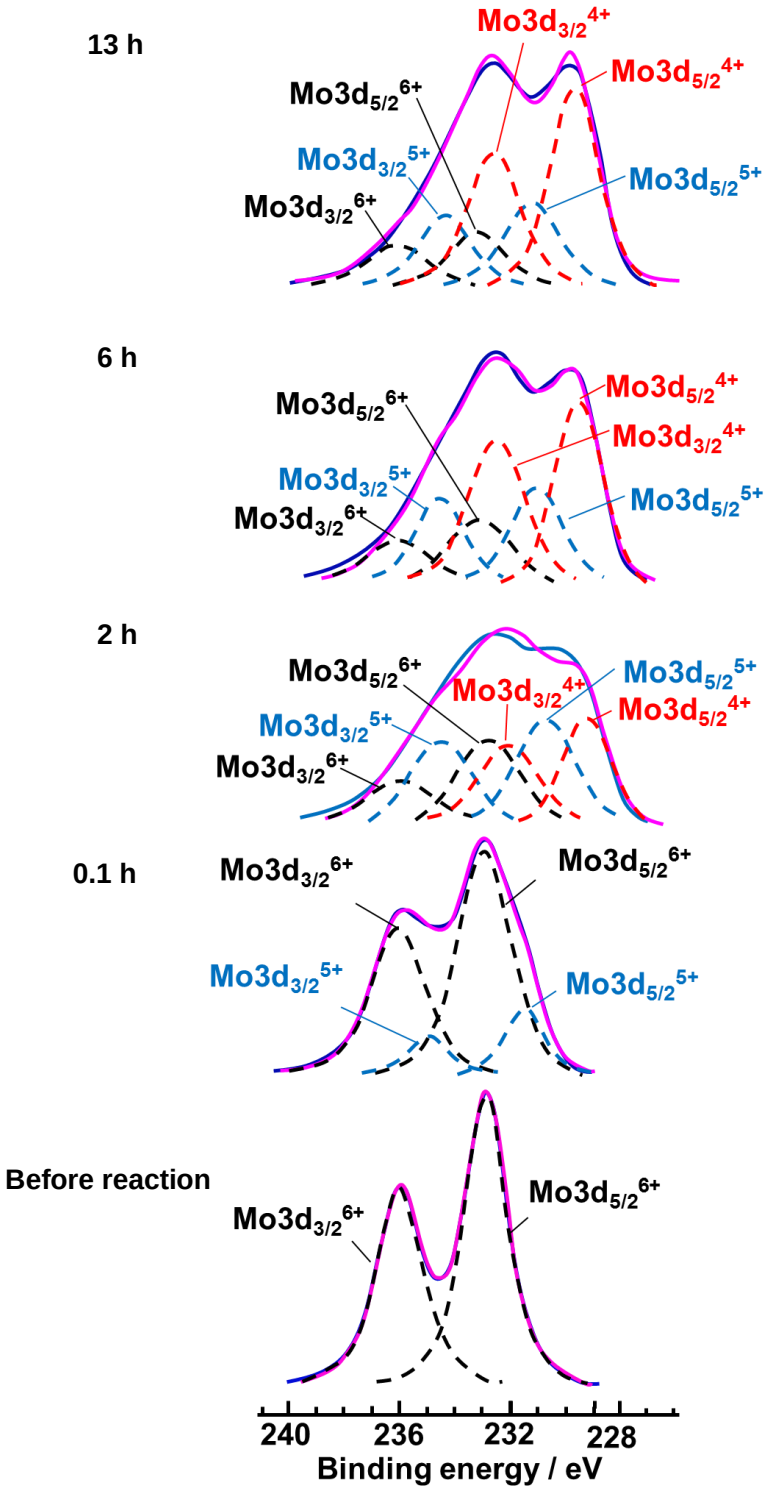

Fig.2-13 XPS spectra corresponding to Mo $3d_{3/2}$ and $3d_{5/2}$ of MoO_3 samples as a function of time on stream.

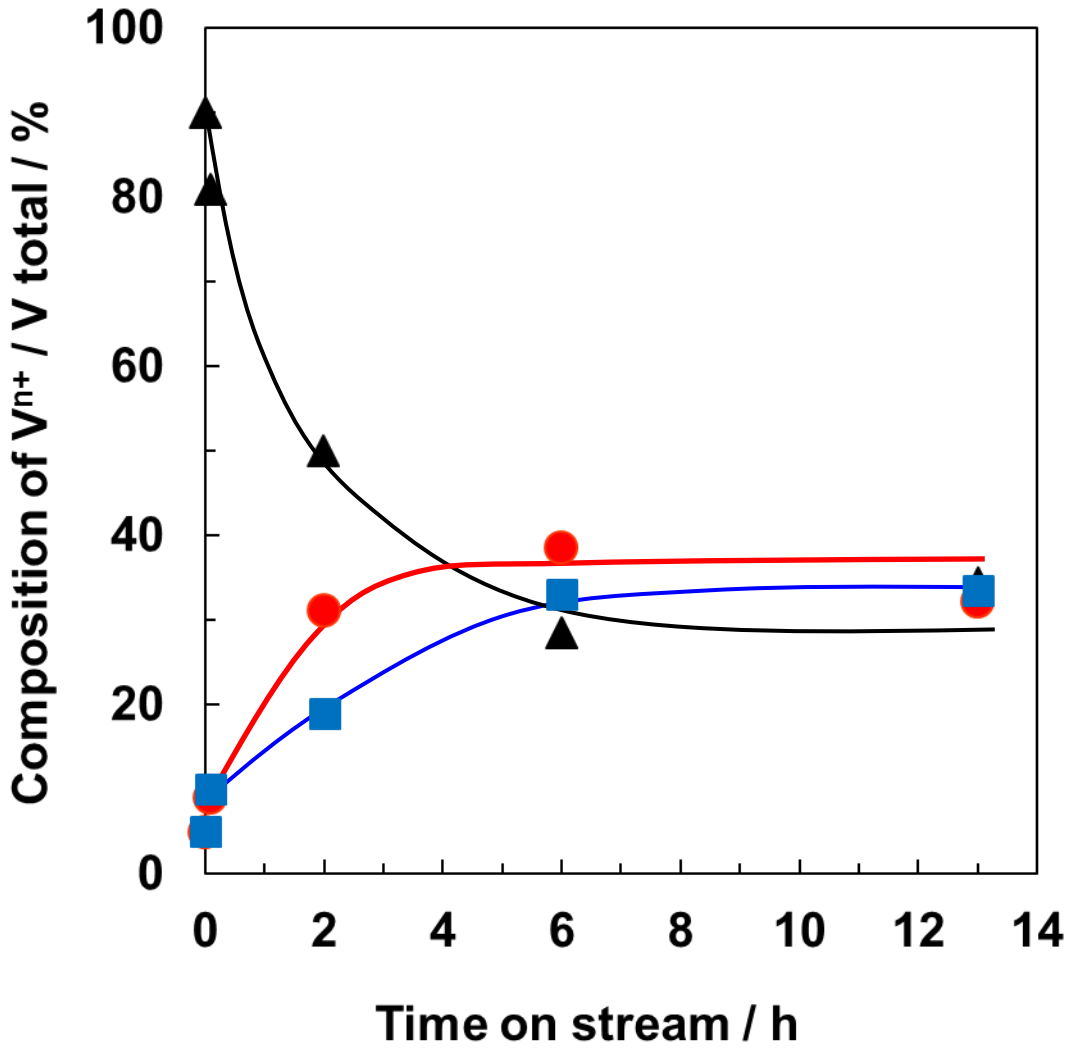

Fig.2-14 The compostion of V^{5+}, V^{4+} and V^{3+} obtained by deconvolution of the V $2p_{3/2}$ for V_2O_5 catalysts as function of time on stream. Reaction condition: reaction temperature 573 K, V_2O_5 0.50 g, SiO_2 2.0 g, flow rate: N_2 21 ml/min, ehanol 0.24 ml/min, (▲) V^{5+}/V_{total}, (●) V^{4+}/V_{total}, (■) V^{3+}/V_{total}

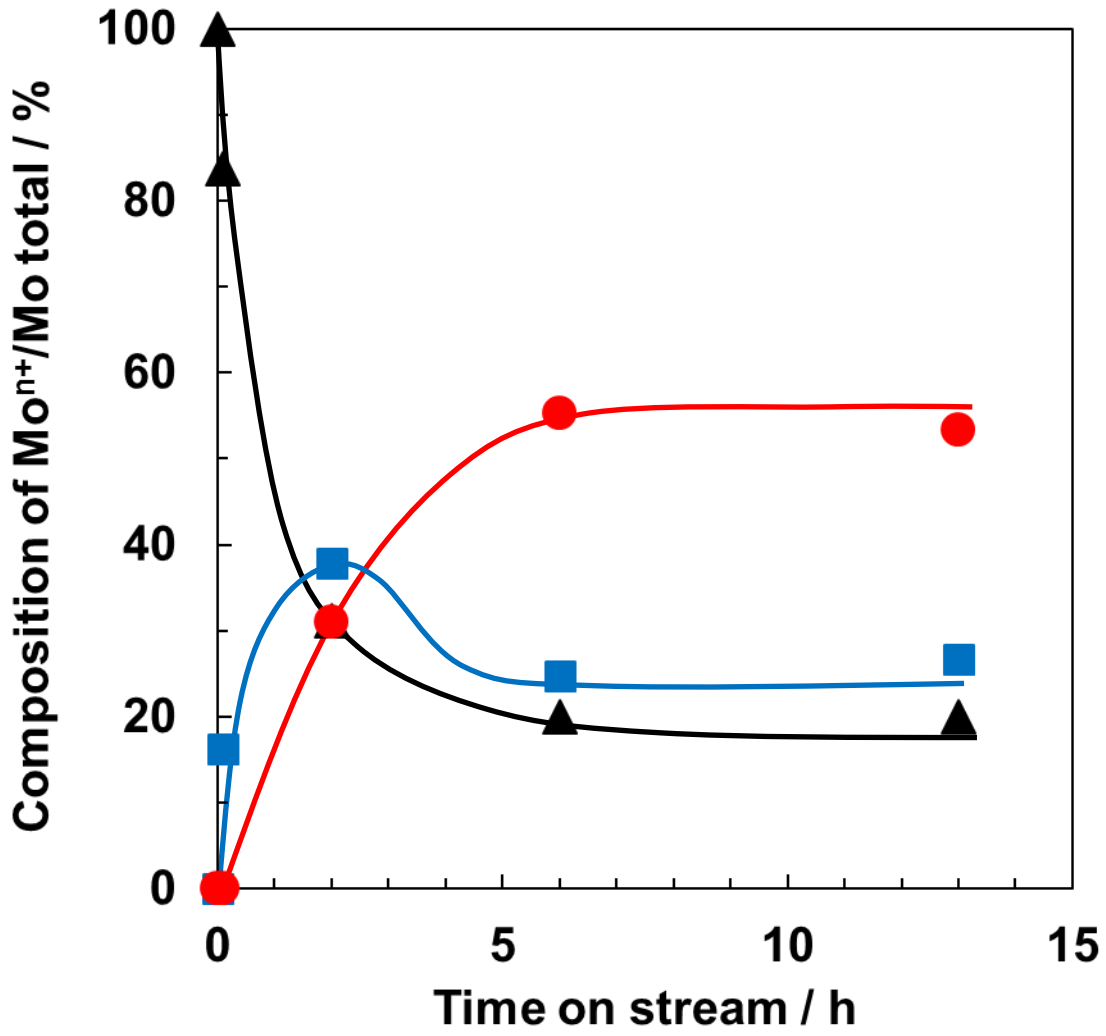

Fig.2-15 The compostion of Mo^{6+}, Mo^{5+} and Mo^{4+} obtained by deconvolution of the $Mo3d_{5/2}$ for MoO_3 catalysts as function of time on stream. Reaction condition: reaction temperature 573 K, V_2O_5 0.15 g, SiO_2 2.6 g, flow rate: N_2 21 ml/min, ethanol 0.39 ml/min, (▲) Mo^{6+}/Mo_{total}, (●) Mo^{5+}/Mo_{total}, (■) Mo^{4+}/Mo_{total}

Table 2-5. Calculation of relative ratio for V^{5+}, V^{4+} and V^{3+} based on deconvolution of V $2p_{3/2}$.

Reaction time	Ratio of V^{n+} / V total / %		
	V^{5+} $2p_{3/2}$ / 517.2±0.2 eV	V^{4+} $2p_{3/2}$ /515.8 eV±0.2 eV	V^{3+} $2p_{3/2}$ /515.2 eV±0.2 eV
before reaction	90.0	5.0	5.0
0.1 h	81.0	9.0	10.0
2 h	49.9	31.1	19.0
6 h	28.4	38.5	33.1
14 h	34.4	32.1	33.5

Table 2-6. Calculation of relative ratio for Mo^{6+}, Mo^{5+} and Mo^{4+} based on deconvolution of Mo $2d_{5/2}$

Reaction time	Ratio of Mo^{n+} / Mo total / %		
	Mo^{6+} $2d_{5/2}$ / 232.5±0.2 eV	Mo^{5+} $2d_{5/2}$ /231.2 eV±0.2 eV	Mo^{4+} $2d_{5/2}$ /229.3 eV±0.2 eV
before reaction	100.0	0	0
0.1 h	83.3	16.7	0
2 h	31.1	37.8	31.1
6 h	19.9	24.9	55.2
14 h	20.0	26.6	53.4

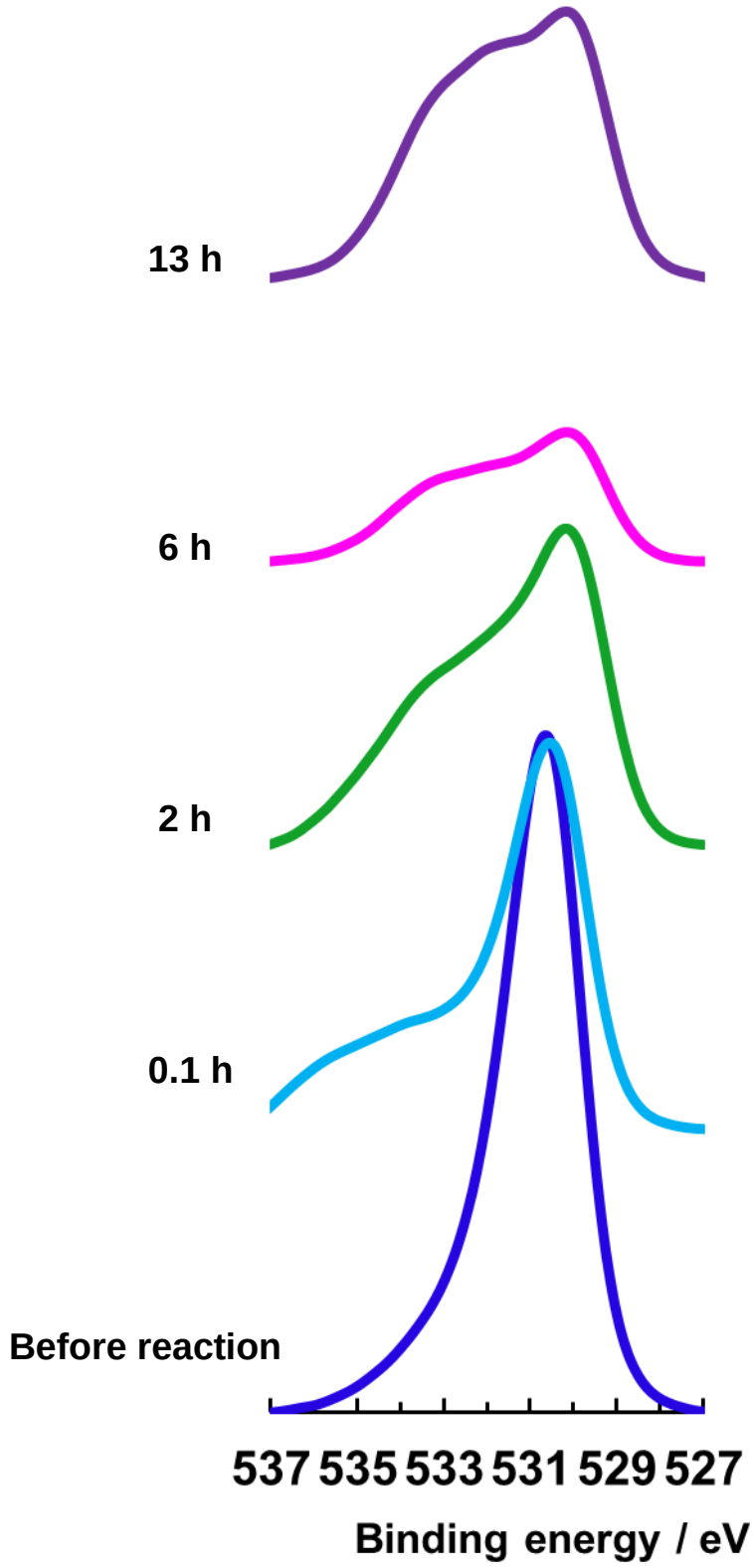

Fig.2-16 XPS spectra for O 1s binding energy on MoO_x as a function of time on stream

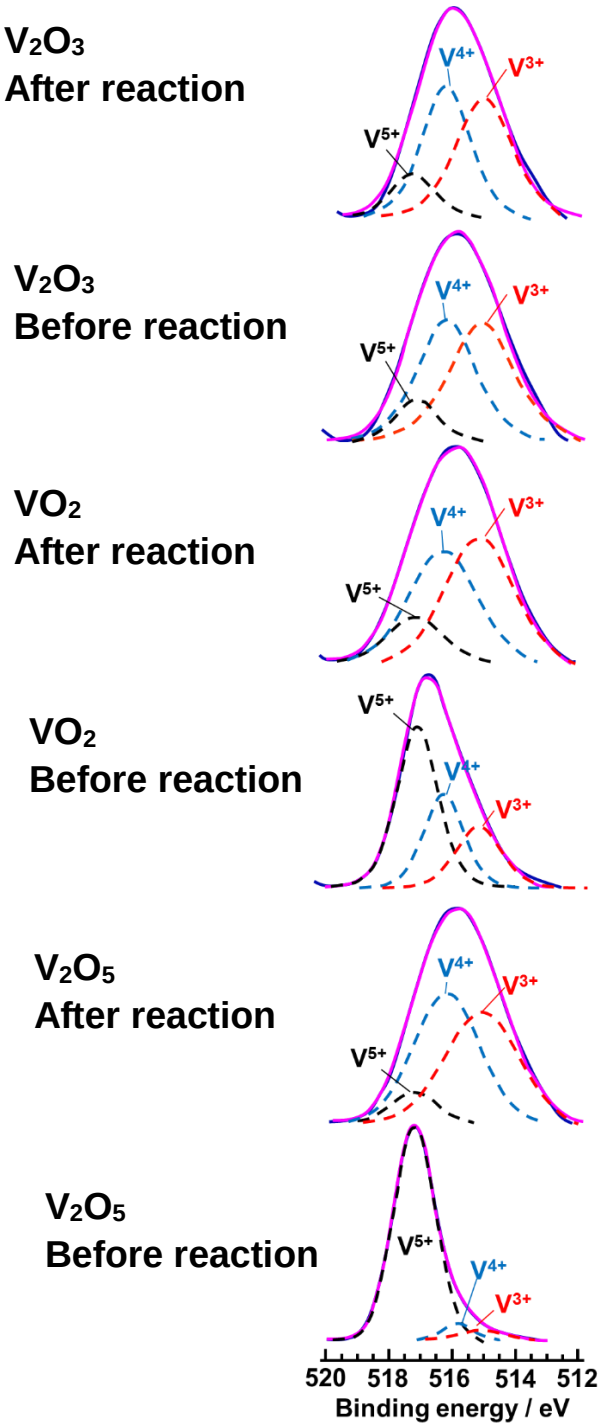

Fig.2-17 XPS spectra corresponding to V $2p_{3/2}$ of V_2O_x catalysts before and after ethanol reaction. V_2O_x 0.15g, SiO_2 2.6 g, 10 h time on stream, flow rate: N_2 21 ml/min, ethanol 0.39 ml/min

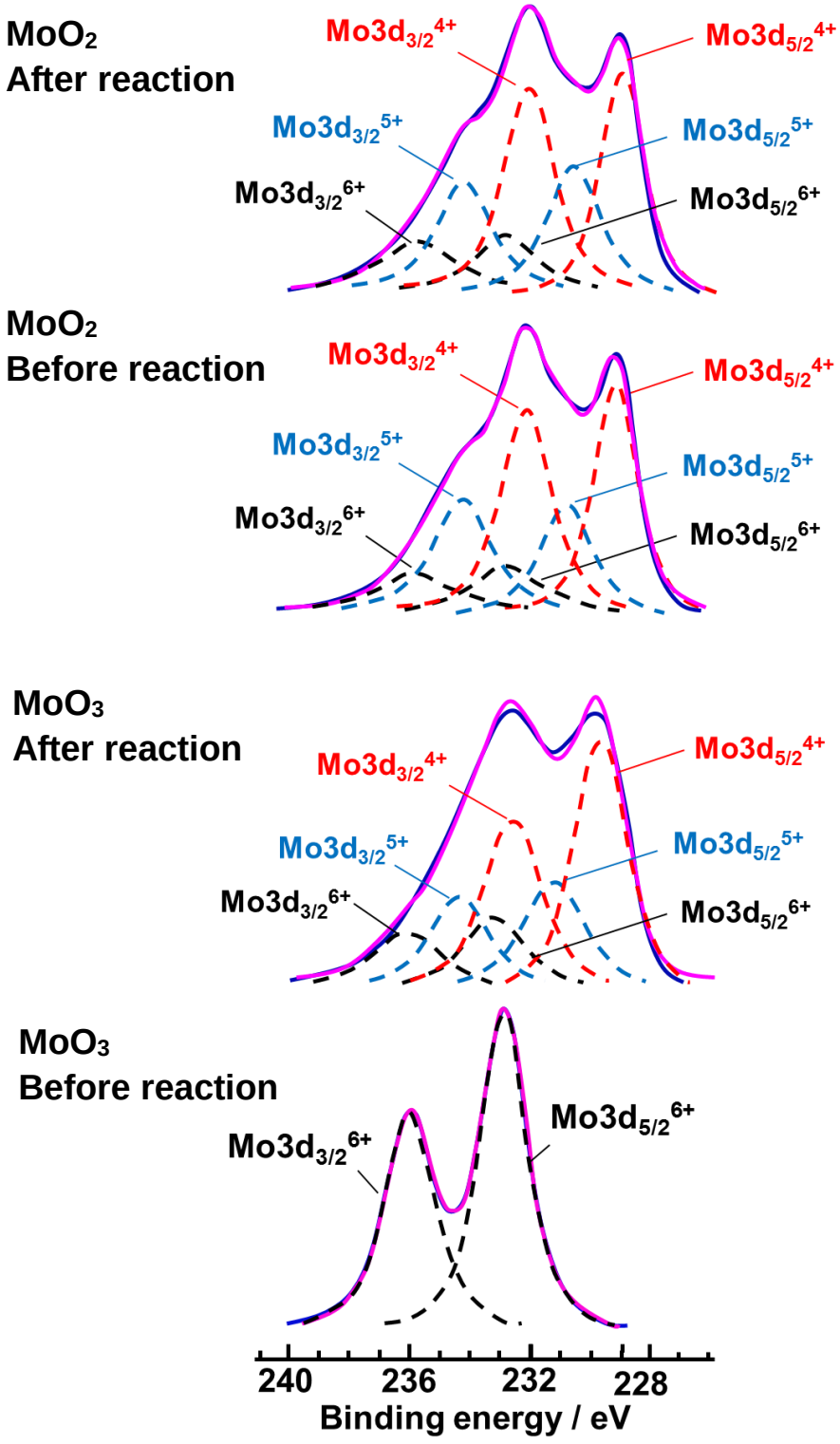

Fig.2-18 XPS spectra corresponding to Mo $3d_{3/2}$ and $Mo3d_{5/2}$ of MoO_x catalysts before and after ethanol reaction. MoO_x 0.15g, SiO_2 2.6 g, 10 h time on stream, flow rate: N_2 21 ml/min, ethanol 0.39 ml/min

Table 2-7. Calculation of composition for V^{5+}, V^{4+} and V^{3+} based on deconvolution of $V2p_{3/2}$, Mo^{6+} , Mo^{5+} and Mo^{4+} based on deconvolution of Mo $2d_{5/2}$

Catalysts	Composition of V^{n+} and Mo^{n+} / %					
	V^{5+} $2p_{3/2}$ / 517.2 eV	V^{4+} $2p_{3/2}$ /515.8 eV	V^{3+} $2p_{3/2}$ /515.2 eV	Mo^{6+} $2d_{5/2}$ / 232.7 eV	Mo^{5+} $2d_{5/2}$ /231.2 eV	Mo^{4+} $2d_{5/2}$ /229.3 eV
V_2O_5 fresh	90.0	5.0	5.0	—	—	—
V_2O_5 after reaction	7.5	47.6	44.9	—	—	—
VO_2 fresh	51.8	27.0	21.2	—	—	—
VO_2 after reaction	13.0	43.9	43.1	—	—	—
V_2O_3 fresh	10.9	42.8	46.3	—	—	—
V_2O_3 after reaction	12.3	44.4	43.3	—	—	—
MoO_3 fresh	—	—	—	100.0	0	0
MoO_3 after reaction	—	—	—	12.6	54.7	32.7
MoO_2 fresh	—	—	—	29.8	34.0	36.2
MoO_2 after reaction	—	—	—	20.0	38.3	41.7

Chapter 3
Investigation of the reaction scheme for the formation of ethane and acetaldehyde from ethanol over V_2O_3 and MoO_2 catalysts

3. 1 Introduction

In the chapter 3, we discussed the catalytic activity of V_2O_3 and MoO_2 for the formation of ethane and acetaldehyde in the ethanol reaction, however, the reaction scheme was not cleared. Several reports showed the formation of alkanes from corresponding alcohols as shown in introduction of Chapter 2, but the proposed reaction scheme was different in all of these reports. Therefore, the objective of the present study in this chapter is to understand the reaction scheme for the formation of ethane from ethanol over V_2O_3 and MoO_2 catalysts. Here, we describe the catalytic activity of V_2O_3 and MoO_2 catalysts with several reaction conditions. The reactions of methanol, 1-propanol and 2-propanol also produced the corresponding alkanes and aldehydes in a 1:1 ratio.

The reaction mechanism leading alkanes and aldehydes is proposed, in which hydrogen-transfer dehydration occurs between two ethanol molecules adsorbed on the adjacent metal cation-O anion pair sites through the six membered transition states. Proposed reaction scheme is supported on the basis of kinetic isotope effect obtained by use of C_2H_5OD and C_2D_5OD.

3. 2 Experimental

3. 2.1 Catalyst preparation

The preparation of V_2O_3 and MoO_2 catalysts were also showed in Chapter 3. Other oxide catalysts belong in 5 and 6 groups were prepared by calcination of ammonium salt and acidic compounds in air. Tungsten oxide (WO_3) was prepared by calcination of 1.5 g of ammonium metatungstate hydrate ($(NH_4)_6H_2W_{12}O_{40}\cdot xH_2O$, NIPPON INORGANIC COLOR & CHEMICAL Co., LTD.) at 773 K in air. Nb_2O_5 and Ta_2O_5 were prepared by calcination of 0.5 g of niobium acid (70.8 %, SOEKAWA Chemicals. Co., LTD) and tantalic acid at 673 K in air, respectively.

Base catalysts (MgO, CuO and Fe_2O_3) were prepared by calcination of hydrate compounds under N_2. Nitrate salt of Mg, Cu and Fe (99 - 99.9%, Wako Pure Chemical Industries) 62.5 mmol was

dissolved in 25 ml distilled water, subsequently 14 % ammonium solution were added drop wise, then hydrates as precipitates were obtained. In the case of copper, 7 % ammonium solution were used to precipitate coppers as hydroxide. The precipitates were filtrated and washed by 50 ml of distilled water. Then the samples were dried overnight at 353 K. The samples were treated under N_2 at 773 K for 2 h.

3. 2. 2 Catalytic tests

Catalytic test procedures were similar as shown in Chapter 2. Catalytic reactions were carried out in a continuous flow fixed bed reactor (Pyrex). A similar volume mixture of the catalyst (0.03~1.5 g) and SiO_2 sands (1.3~2.6 g) as a diluent were placed in the reactor and heated to a desired reaction temperature (533~633 K) under a N_2 flow (21.4 ml/min).

Then, the catalytic reaction was started by the introduction of ethanol (99.5 %, Wako Pure Chemical Industries) with N_2 carrier into the reactor. The base catalysts (MgO. CuO, NiO and Fe_2O_3) were treated again under N_2 at 773 K for 2 h in the reactor before the ethanol reaction, then cooled to the reaction temperature and started by the introduction of ethanol as mentioned above. The total flow rate of the reactant gas (N_2+alcohols) was kept constant (21.4 ml/min) for all the reactions. Ethanol concentration was changed from 1.8~7.5 mol%. The concentrations of methanol (99.8 %, Wako Pure Chemical Industries), 1-propanol (99.5 %, Wako Pure Chemical Industries) and 2-propanol (99.7 %, Wako Pure Chemical Industries) were 2.7, 1.7, and 4.3 mol%, respectively. For study on kinetic isotopic effect, two types of isotope-labeled ethanol, CH_3CH_2OD (99 %, Wako Pure Chemical Industries) and CD_3CD_2OD (99 %, Wako Pure Chemical Industries), were used as reactant. The reaction products were analyzed by gas chromatography. Two gas chromatographs, Shimadzu GC-8A equipped with a thermal conductivity detector and a packed column Porapack-QS and GC-380 equipped with a thermal conductivity detector and a flame-ionization detector and two

packed columns, Unicarbon and molecular sieve 5A, were used. N_2 gas was used as internal standard for quantitative GC analysis. Alcohol conversion, the product selectivity, and carbon balance were defined as the following equations (1) and (2), respectively.

$$Conversion(\%) = \frac{X\ /mol}{X_0/mol} \times 100 \quad (1)$$

$$Selectivity(\%) = \frac{A\ /\ mol}{X/mol} \times 100 \quad (2)$$

Where X_0, X, and A refer to the molar concentration of the reactant, consumption of substrate, and molar concentration of the products, respectively.

3. 2. 3 Characterization

Powder X-ray diffraction (XRD) measurements were performed with a RINT Ultima+ diffractometer (Rigaku) with Cu-Kα radiation (Kα =0.1540nm) and X-ray power of 40 kV / 20 mA. XPS measurements were performed using a JPS-9010 MC (JEOL). An Mg- Kα radiation source (1253.3 eV) operated at a power of 100 W (10 kV, 10 mA) was employed. Vacuum in the analysis chamber was < 5×10^{-6} during all measurements. Pass energy of 30 eV was used to acquire all survey scans. The binding energy (BE) was corrected for surface charging by taking the C1s peak of carbon as a reference at 248.7 eV. Data were analyzed using the SpecSurf including Shirley background subtraction and fitting procedure. Quantification of the components for the surface oxidation state of vanadium and molybdenum was made using the SpecSurf. The acid and base amounts of catalysts were measured by NH_3-TPD and CO_2-TPD, respevtively, with TPD apparatus (BEL Japan Inc.) The sample was pretreated at 773 K under He (50 ml/min) with temperature rising rate 10 °C/min for 2 h. Subsequently, the temperature decreased to 373 K then 30 Torr of ammonia was equilibrated with pretreated sample at 373 K. The physical adsorbed ammonia was removed under He (50 ml/min) for 30 min. The TPD date measured by increasing the temperature at a rising rate 10 K/min to 973 K

under He (50 ml/min). A mass spectrometer (ANELVA-100 OA-F) was used to measure the desorbed NH_3 (at m/z = 16). The samples were pretreated at 773 K under He (50 ml/min) with rising rate 10 ℃/min for 2 h. Subsequently, the temperature decreased to 323 K then Torr of carbon dioxide equilibrated with pretreated sample at 373 K for 5 min. The physical adsorbed CO_2 was removed under He (50 ml/min) for 30 min at 323 K. The TPD date measured by increasing the temperature at a rising rate 10 K/min to 873 K under He (50 ml/min). A mass spectrometer (ANELVA-100 OA-F) was used to measure the desorbed CO_2 (at m/z = 44) The acid and base amounts are calculated based on the acid amount of H-ZSM5(JRC-Z5-90H) and the desorption amount of CO_2 from decomposition of $MgCO_3$.

3. 3 Results and discussion

3. 3. 1 Catalytic activity of on 5, 6 group metal oxides in the ethanol reaction

Vanadium and molybdenum belong to the 5 and 6 groups in the periodic table. Therefore, the ethanol reaction was carried out using the other single metal oxide catalysts composed of the elements in the 5 and 6 groups, such as WO_3, Nb_2O_5 and Ta_2O_5 to investigate the catalytic property of 5 and 6 group metal oxides. The results are shown in Fig.3-1. These catalysts are known as oxidation and dehydration catalysts for alcohol conversion and there has been no report on the formation of alkane from corresponding alcohols.

WO_3 catalyst showed predominant formation of ethylene with 88.9 % selectivity, diethyl ether with 11.1 % selectivity due to the strong acidity and Brönsted acid sites on the surface. Nb_2O_5 and Ta_2O_5 catalysts also showed the formation of ethylene and diethyl ether. Diethyl ether was found in 60 % selectivity and ethylene in 33 % selectivity over Nb_2O_5 catalyst, while over Ta_2O_5 catalyst, diethyl ether and ethylene were formed in 34.7 % and 35.7 %, respectively. These catalysts showed the formation of fluoroethane as other compounds, which was analyzed from GC-mass analysis,

caused by addition reaction between ethylene and fluorine including in raw material as impurity. In addition, Nb_2O_5 and Ta_2O_5 exhibited the low conversion of ethanol compared to the other catalysts, because the acid property on the surface of these catalysts is very week using by itself.

Based on these results, the catalytic features of vanadium and molybdenum oxide to produce ethane and acetaldehyde were not observed for the other group 5 and 6 metal oxides.

Low oxidation states of V and Mo oxides were active for the formation of ethane from ethanol. In order to elucidate the effect of oxidation states of 5 and 6 group metal oxides in ethanol reaction, catalytic performance of NbO (Nb^{2+}) was examined. Fig. 3-2 showed the comparison of catalytic properties of Nb_2O_5 and NbO in ethanol reaction. Nb_2O_5 (Nb^{5+}) showed the formation of diethyl ether and ethylene as main products via dehydration. On the other hand, NbO (Nb^{2+}) showed the formation of ethylene as a main product with the formation of ethane and acetaldehyde to a considerable extent. The formation of diethylether was not detected. The selectivity to ethane and acetaldehyde were 13 % and 9 %, respectively. The ratio 13% to 9% is close to unity with an error of 40%. Considering the results obtained with reduced V and Mo oxides, it can be stated that the reduction phase of 5 and 6 group metal oxides are active for the formation of ethane in a nearly equal amount from ethanol.

3. 3. 2 Catalytic activity of the ethanol reaction on various base catalysts

Vanadium and molybdenum oxide catalysts have been known as dehydrogenation of alcohol to produce aldehyde, regardless of their oxidation states. Therefore, the active site for the equivalent formation of ethane and acetaldehyde over V_2O_3 and MoO_2 may correlate with the basic sites of the catalysts like some base catalyst. To study the reaction scheme, the comparison of the catalytic activities of V_2O_3 and MoO_2 with those of MgO, ZnO, CuO and Fe_2O_3 was performed as shown in Fig. 3-3.

For both the ZnO and CuO catalysts showed that the formation of ethane was observed with moderate selectivity in the range of 21-31 %, however, acetaldehyde was also formed as major product with 52.6 % and 62 % selectivity, respectively. Some reports showed that the ethane was slightly formed as a by-product from ethanol on copper oxide catalysts, however, little attention has been paid to this point. To the best of our knowledge, this work focuses on the formation of ethane from ethanol over CuO and ZnO catalysts for the first time. Fe_2O_3 showed the similar selectivity to ethane (21.5 %), and acetaldehyde (33.1 %). However, nearly equal amount of ethane and acetaldehyde as well as V_2O_3 and MoO_2 catalysts were not observed for all of the base catalysts. NiO showed no formation of ethane and acetaldehyde from ethanol. Methane and CO_2 were formed as major products by reforming reaction of ethanol.

MgO showed the formation of ethane with 18.2 % selectivity and acetaldehyde with 4.9 % selectivity in the initial period of reaction, even though others attributed to heavy compounds formed by condensation reaction of acetaldehyde were major products. Moreover, the small amount of the formation of ethylene as dehydration of ethanol and C4 olefines such as 1-butane, 2-butane and 1.3-butadiene by condensation of acetaldehyde were also observed. However, the amount of ethane gradually decreased while the amount of ethylene and acetaldehyde increased with increase of time on stream, and the selectivity to ethane reached to 4 % at 5 h time on stream in the ethanol reaction. Moreover, the conversion of ethanol also drastically decreased with increase of time on stream, and the color of the catalyst changed from white to black, suggesting that the carbon deposit occurred on the catalysts and led to the decrease of the conversion of ethanol. Therefore, the decrease of the selectivity to ethane was also caused by covering of the active site to form ethane with carbon deposit.

Most of these catalysts showed that the ethane and acetaldehyde were produced from ethanol. However, the active sites of these base catalysts for the formation of ethane from ethanol were

different from those of the reduced vanadium and molybdenum oxides because the selectivity ratios of ethane to acetaldehyde were not 1, preferential formation of acetaldehyde was observed over all base catalysts. Fe_2O_3 indicated that a similar selectivity to ethane and acetaldehyde (the ratio of selectivity to ethane/acetaldehyde = 0.66) was obtained at 623 K. However, the product distribution to ethane and acetaldehyde was changed with decrease of reaction temperatures to 573 K as shown in Fig. 3-4, which is different from the results of ethanol reaction over V_2O_3 and MoO_2 catalysts with different reaction temperatures as discussed in detail later. Therefore, the formation of ethane and acetaldehyde over Fe_2O_3 catalyst took place via consecutive reaction or parallel reaction. Based on these results, the basic sites on V_2O_3 and MoO_2 catalysts, which are lattice oxygen, were not probably involved in the equivalent formation of ethane and acetaldehyde from ethanol. This means that the reaction pathway for the formation of ethane and acetaldehyde over V_2O_3 and MoO_2 catalysts was differed from that proceeded over base catalysts as reported previously.

3. 3. 3 XRD patterns of the various base catalysts before and after ethanol reaction

To study the relation between the crystallines structure catalyst states of MgO, ZnO, CuO and Fe_2O_3 and the catalytic activity in the ethanol reaction, the comparison of XRD patterns for these catalysts were measured before and after the ethanol reaction as shown in Fig. 3-5. ZnO catalyst did not change the crystal phase corresponding to ZnO at 2θ = 31.8, 34.4, 36.3, 47.5 and 56.6° after ethanol reaction, even though the intensity of these diffraction lines increased after ethanol reaction (Fig. 3-5 (a, b)). In the case of CuO catalyst (Fig. 3-5 (c, d)), however, the CuO phase (at 2θ = 32.5, 35.6, 38.7, 48.7, 53.5 and 58.3°) disappeared and new diffraction lines due to the Cu metal phase at 2θ = 43.3 and 50.4° appeared after ethanol reaction, suggesting that CuO was completely reduced to Cu metal during ethanol reaction. Fe_2O_3 catalyst also showed the diffraction peaks of Fe_3O_4 at 29.9, 35.3 and 56.9° (Fig. 3-5 (e,f)).

3. 3. 4 XPS spectra for the various base catalyst before and after ethanol reaction

The surface oxidation states on ZnO, CuO and Fe_2O_3 before and after ethanol reaction were studied by XPS analysis as shown in Fig.3-6. In the case of ZnO (Fig 3-6 (a)), the XPS peak at 1021.9 eV attributed to Zn^{2+} [1] did not change after ethanol reaction, suggesting that ZnO did not change the oxidation states not only in the bulk but also on the surface of ZnO during the ethanol reaction. The XPS spectrum of $Cu2p_{3/2}$ (Fig. 3-6 (b)) for CuO catalyst showed that the peak for Cu^{2+} (at 933.8 eV) shifted to 932.5 eV ascribed to Cu metal [2]. The XPS spectra of $Fe2p_{3/2}$ for Fe_2O_3 did not change after ethanol reaction (Fig. 3-6 (c)) [3], even though the bulk of Fe_2O_3 was reduced to Fe_3O_4 from XRD measurement.

In the catalyst which produced ethane from ethanol, monometallic oxides with high reducibility of metal provided relatively high selectivity to ethane. CuO and Fe_2O_3 catalysts, which showed the relatively high selectivity to ethane, were reduced during ethanol reaction except for NiO, suggesting that the reduced metal species is important for the formation of ethane from ethanol. Moreover, CuO was most reduced during the ethanol reaction and showed the highest selectivity to ethane. From these results, the catalytic activity for the formation of ethane from ethanol seems to be relation with the reducibility of the metal and high reducibility of metal on oxide shows high selectivity to ethane from ethanol. Fe_2O_3 has been known to act as catalyst for the production of alkanes from corresponding alcohols. Indicated that formation of toluene proceed via O-abstracting of benzyl alcohol on Fe^{3+}. In the present study, however, the Fe_2O_3 (Fe^{3+}) was reduced to Fe_3O_4 ($Fe^{2+,3+}$). This result indicates that the mechanism for the formation of ethane from ethanol on Fe_2O_3 is not O-abstracting of ethanol.

3. 3. 5 Acid-base properties of the active surface on V and Mo oxides for the formation of ethane

In order to investigate the effect of acid-base property on the catalytic activity of the reduced vanadium and molybdenum oxide catalysts, the poisoning test by addition of base compounds (such as pyridine and tri-ethylamine) and TPD study were performed.

Pyridine and tri-ethylamine compounds are known to be adsorbed onto Lewis acid sites and inhibit the dehydration reaction. If Lewis acid sites on V_2O_3 and MoO_2 as active sties for the formation of ethane interacted with these base compounds, the selectivity to ethane and acetaldehyde might decrease by introduction of these base compounds. The poisoning tests were carried out on V_2O_5 and MoO_3 by introduction of the base substrates after the reaction reached steady states. The results are shown in Fig. 3-7 for V_2O_3 and 3-8 for MoO_2. The selectivities to ethane and acetaldehyde and the conversion of ethanol over V_2O_5 catalysts did not change for 2 h time on stream after addition of pyridine. Subsequently addition of tri-ethylamine also showed no effects on the conversion of ethanol and the selectivity to products. In the reaction of ethanol over MoO_3, the decrease in conversion of ethanol and the selectivity to ethylene while the increase of the selectivity to ethane and acetaldehyde were observed immediately after addition of pyridine and tri-ethylamine. The immediate changes caused by the introduction of the basic compounds restored with the time on stream. The poisoning effects were reversible. It is noted that the C_2H_6/CH_3CHO ratio kept constant while the dehydration activity was reversibly retarded by the introduction of basic compounds. Therefore, it is concluded that the active sites for the formation of ethane and acetaldehyde are different from those active for dehydration of ethanol, and the active sites for the formation of ethane and acetaldehyde are unaffected by these amines.

Fig. 3-9 shows the NH_3-TPD and CO_2-TPD profiles of V_2O_3 and MoO_2 catalysts. For both the V_2O_3 and MoO_2 catalysts, negligible amount of NH_3 (m/z = 16) was observed over the all desorption temperature range, suggesting that there are no acid sites on both the V_2O_3 and MoO_2 catalysts and acid property of the catalysts did not correlate with the catalytic performance. The TPD profile

shows that the CO_2 (m/z = 44) desorption was observed in the range of high desorption temperature (above 300 °C), however, no desorption of CO_2 was observed under 300 °C, suggesting that CO_2 was adsorbed on the surface of V_2O_3 and MoO_2 during the ethanol reaction. The selectivity to ethane and acetaldehyde in a 1:1 ratio was obtained over V_2O_3 and MoO_2 catalysts pre-treated at 778 K under N_2, and the conversion of ethanol over the pretreated MoO_3 was the same as that of the MoO_2 catalyst without pretreatment. These results indicate that basic sites on the catalyst are not involved in the formation of ethane and acetaldehyde from ethanol.

Moreover, these results clearly indicate that the acid sites (oxygen defect site as Lewis acid), are very weakly acidic and could not interact with ammonia, pyridine and tri-ethylamine.

3. 3. 6 Effect of introduction of H_2 and C_2H_4 into reaction stream

The secondary hydrogenation of primarily formed ethylene was thought to be a possible pathway to ethane formation, since both ethylene (from dehydration) and hydrogen (from dehydrogenation to aldehyde) were produced from the primary reaction. Moreover, some reports showed that hydrogenation of alcohols were proposed for the formation of alkanes from corresponding alcohols. To study the effect of the presence of hydrogen in the reaction stream, ethanol conversion was performed under H_2 after steady states. Moreover, ethanol was thought to be hydrogen source for hydrogenation of ethylene. Therefore H_2 (1.0 ml/min) and C_2H_4 (1.0 ml/min) were introduced into the reaction stream when the reaction became steady state and total flow rate was adjusted to 21.4 ml/min by changing the N_2 flow rate to 20 ml/min.

The product distributions in the presence of H_2 and C_2H_4 into the reaction stream over V_2O_3 and MoO_2 catalysts are listed in Table 3-1. If the hydrogenation of ethylene or ethanol occurred in the main pathway to form ethane, co-feeding of ethylene and that of hydrogen would increase the selectivity to ethane. However, for both the V_2O_3 and MoO_2 catalysts, the conversion of ethanol and

the selectivities to all kind of products did not change on introduction of H_2 into the reaction stream. Therefore, it is concluded that hydrogen molecules are not involved in the formation of ethane from ethanol. In addition, the introduction of C_2H_4 had also no effect on the conversion of ethanol and the selectivities to products. These results suggest that the hydrogenation of ethylene and hydrogenolysis of ethanol are not the pathway for the formation of the equivalent amount of ethane and acetaldehyde from ethanol over V_2O_3 and MoO_2 catalysts. Therefore, other reaction pathway occurred to form the ethane and acetaldehyde over reduced vanadium and molybdenum oxides.

3. 3. 7 Investigation of the reaction pathway for the formation of ethane and acetaldehyde from ethanol

To investigate the reaction pathway for the formation of ethane and acetaldehyde over V_2O_3 and MoO_2 catalysts, catalytic reaction was carried out under different reaction conditions, in which reaction temperature, contact time and reactant were changed.

The effects of the reaction temperature on the selectivities to ethane and acetaldehyde were examined over V_2O_3 and MoO_2 catalysts in the temperature range from 533 K to 653 K as shown in Fig.s 3-10 and 3-11. V_2O_3 (Fig. 3-10) showed the selectivities to ethane and acetaldehyde of 43.4 % and 45.3 %, respectively, at low reaction temperature (573 K). The selectivities to these products did not change even when the reaction temperature was increased until 653 K, at which the selectivity to ethane and acetaldehyde were 44.7 % and 40.5 %, respectively at 653 K in high conversion range. The selectivities to these products were constant in the reaction temperature range 533-653 K. even though the small amounts of ethylene with the selectivity 1.3 % was obtained at 603 K and increased to 3.7 % at 653 K. The similar catalytic behavior was observed over MoO_2 catalyst. MoO_2 showed no remarkable temperature effect on the selectivity to ethane and acetaldehyde (Fig.3-11). The selectivities to ethane and acetaldehyde were 44 ~ 46 % and 45 ~ 48 %, respectively, in all reaction

temperature range. In addition, the formation of ethylene with 1.7 % selectivity was observed at 594 K and increased to 3.8 % at 634 K in the high conversion range.

Fig.s 3-12 and 3-13 show the Arrhenius plots for the formation of ethane and acetaldehyde over V_2O_3 and MoO_2 catalysts, respectively. Apparent activation energies ($E_{a,\,app}$) of ethane and acetaldehyde formation were calculated to be 100 kJ/mol and 106kJ/mol, respectively, for V_2O_3 catalyst and the 90 kJ/mol and 96 kJ/mol, respectively, for MoO_2 catalyst as listed in Table 3-2. The $E_{a,app}$ values for ethane and acetaldehyde formation were similar over both V_2O_3 and MoO_2, but the $E_{a,app}$ value over V_2O_3 was slightly higher than that of MoO_2. In the oxidative dehydrogenation of ethanol to acetaldehyde, the apparent activation energies of 46 kJ/mol over $VO_x/TiO_2/SiO_2$ catalyst [8] and 17~23 kJ/mol over MO_x/Al_2O_3 (M = V, Mo, W) catalysts [9] were reported. These values are obviously much lower than those observed in the present ethanol reaction over V_2O_3 and MoO_2 which is a non-oxidative reaction. This comparison may suggest that the equimolar formation of ethane and acetaldehyde from ethanol takes place without accompanying a reduction-oxidation process of the V_2O_3 and MoO_2 catalysts. Moreover, the reaction order on V_2O_3 and MoO_2 are under 0.5 as shown in Fig.s 3-14 and 3-15, respectively.

The effects of the contact time on the selectivity to ethane and acetaldehyde were also investigated over V_2O_3 and MoO_2 catalysts as shown in Fig.s 3-16 and 3-17, respectively. Ethane and acetaldehyde were formed in a 1 :1 ratio at the low W/F (0.023 g・min/ml) over V_2O_3 catalyst. As W/F increased, the selectivity to ethane kept constant while the selectivity to acetaldehyde constantly decreased to 34.9 % at a W/F of 0.07 g・min/ml. MoO_2 catalyst revealed similar catalytic behavior to the V_2O_3 catalyst. The selectivity to acetaldehyde linearly decreased with an increase of contact time, from 50.9 % at 0.03 g・min/ml to 39.4 % at 0.07 g・min/ml, however, the selectivity to ethane kept unchanged over the all of contact time. The observed decrease in the selectivity to acetaldehyde was caused by the enhancement of the consecutive condensation reaction of acetaldehyde formed

dehydrogenation of ethanol because the concentration of acetaldehyde was increased due to the high conversion of ethanol under longer contact time.

These results indicate that the formation of ethane and acetaldehyde occurred simultaneously because the reaction rates for the formation of ethane and acetaldehyde were the same. By summarizing all the data collected under the different reaction conditions, it is evident that the product selectivities are practically independent of the reaction temperature and the conversion of ethanol. If ethane and acetaldehyde were formed by successive steps, the selectivities to ethane and acetaldehyde would vary with the reaction temperature or conversion unless the activation energies for the formation of ethane and acetaldehyde were the same for these steps. The observed these results suggest that ethane and acetaldehyde form in a single step from a common intermediate.

3. 3. 8 Various alcohol reactions over V_2O_3 and MoO_2 catalysts

In order to further study the equimolar formation of alkanes and aldehydes, the reactions of methanol, 1-propanol, 2-propanol were carried out over V_2O_3 and MoO_2 oxide catalysts. Results are shown in Fig.s 3-18 and 3-19, for V_2O_3 and MoO_2, respectively. Formation rates of the products of each alcohol were calculated by using the data summarized in Table 3-3. As can be seen in Fig.s 3-16 and 3-17, almost the same selectivities to alkanes and corresponding aldehydes were observed in all kinds of tested alcohols for both V_2O_3 and MoO_2 oxide catalysts as well as ethanol reaction, though a large amount of propylene in the reaction of 2-propanol as dehydration was obtained. This result indicates that the equivalent formation of alkanes and aldehydes occurs regardless of the alcohols, even though the selectivity to others is slightly higher in methanol reaction than in the reaction of the other alcohols because condensation reaction is favorable in a lower alcohol reaction. In the reaction of 2-propanol, V_2O_3 showed the low selectivity to propylene with 17.9 % than that of propane and propionaldehyde. In the reaction of 2-propanol over MoO_2 the selectivity to propylene

(41.9 %) was higher than that of propane (26.2 %) and propionaldehyde (32.0 %). The high selectivity to propylene resulted from relatively high acidity of MoO_2 as compared with V_2O_3. Moreover, propylene would be formed via E1 mechanism because the formation of olefin was observed only secondary alcohol. In general, the secondary alcohol is favored for dehydration by E1 mechanism than primary alcohols.

The conversion rates of the different alcohols on V_2O_3 were as follows: 2-propanol > ethanol > 1-propanol > methanol shown as in Table 3-3. In the case of MoO_2, the conversion rates were as follows: 2-propanol > methanol > ethanol > 1-propanol shown as shown in Table 3-3. There are difference in the order between two catalysts but the order among normal alcohols seem to have less meaning, since the rates of these alcohols are more or less similar. It is clear that the reactivity of 2-propanol is about one order of magnitude higher than that of the other alcohols for both the V_2O_3 and MoO_2 catalysts. The higher reactivity of 2-propanol as compared to other alcohols is assumed to be due to a higher negative charge on the H_α atom. The H_α transfers to the C atom as a hydride and, therefore, transferring to the high positive charged C occurs faster. Moreover, carbocation formed by elimination of H_α as hydride ion in methylene group is more stables in 2-propanol compared with other alcohols. Therefore, hydride transfer of α-hydrogen is involved in the rate-determining step for the co-formation of alkanes and aldehydes from corresponding alcohols. Moreover, it is noteworthy that methane was obtained from methanol even though the selectivity to other products was slightly high as compared with other alcohols. This result strongly supports that the equivalent formation of alkanes and corresponding aldehydes from alcohols is not via the formation of olefin.

3. 3. 9 Kinetic investigation for the formation of ethane and acetaldehyde from ethanol

Study of H-D kinetic isotope effects (KIE) has been conducted to understand the reaction mechanism. KIE was measured using CH_3CH_2OD and CD_3CD_2OD with respect to CH_3CH_2OH. The

results are shown in Table 3-4. The KIE values in the conversion of C_2H_5OD (KIE; $r_{C_2H_5OH} / r_{C_2H_5OD}$) is 1.09 for V_2O_3 and 1.12 for MoO_2 catalysts. On the other hand, a slightly high KIE value for MoO_2 (KIE; $r_{C_2H_5OH} / r_{C_2D_5OD}$ is 1.32) was observed when C_2D_5OD are used as reactant. Very differently V_2O_3 showed an inverse isotope effect (KIE; $r_{C_2H_5OH} / r_{C_2D_5OD}$ is 0.84). There are two possibilities to obtain the inverse kinetic isotope effect on V_2O_3. First possibility is that the difference in the zero point energy of C-H bond is larger for the transition state than for ground state; i.e. the H atom that is transferring is strongly bound to two C atoms of ethanol molecules adjacently adsorbed. High activation energies for the formation of ethane and acetaldehyde over V_2O_3 catalyst is obtained compared with MoO_2 catalyst. Transfer reaction of the hydrogen in methylene group takes place easily over MoO_2 catalysts because the distance between the hydrogen in methylene group and the adjacent carbon is short compared with V_2O_3 catalyst, suggesting that the mechanism of the transfer of hydrogen in methylene group is different MoO_2 and V_2O_3 catalysts. The relatively short distance of hydrogen in methylene group and adjacent carbon over MoO_2 catalyst led to taking place the hydrogen transfer reaction through non-linear like transition state. On the other hand, the hydrogen transfer occurred via linear like transition state over V_2O_3 because the distance between the hydrogen in methylene group and adjacent carbon is relatively long compared with MoO_2 catalyst. Form this reason, the interaction of the hydrogen in methylene group with the adjacent carbon is stronger over V_2O_3 catalyst than that over MoO_2 catalyst. As a result, the difference in the zero point energy of C-H bond is large over V_2O_3, and the inverse isotope effect was observed when C_2D_5OD was used. The other possibility is the high concentration of C_2D_5OD on the surface of V_2O_3 due to the strong adsorption of C_2D_5OD as compared with C_2H_5OH. At the present stage, it is not clear which reason is correct. Therefore, other studies are needed to clarify the reaction mechanism.

In this work, the theoretical KIE values of isotope effects were estimated on the assumption that

the O-H and C-H bonds are completely cleaved in the transition state of the rate determining step. The theoretical values of KIE were 3.1 and 2.8 for $r_{C_2H_5OH} / r_{C_2H_5OD}$ and $r_{C_2H_5OH} / r_{C_2D_5OD}$, respectively, at 573 K for C-H cleavage (α-H elimination), however, experimental KIE values of 0.80 and 1.32 for V_2O_3 and MoO_2, respectively, were much lower than those of estimated value (entry 1, 2 in Table 3-4).

The experimental KIE value for the oxidative dehydrogenation of ethanol over VO_x/Al_2O_3 ($r_{C_2H_5OH} / r_{C_2D_5OD}$ = 4.9, entry 3 in Table 3-4) was reported to be very close to the estimated KIE value as primary isotope effect (KIE = 5.0), suggesting that C-H bond in methylene group is completely cleavaged on VO_x/Al_2O_3 [34]. However, V_2O_3 and MoO_2 in this work showed rather small KIE value. It is suggested that the mechanism of hydrogen elimination is different from oxidative dehydrogenation of ethanol. Ru/Carbon catalyst indicated much lower KIE value than that of estimated value, suggesting that α-hydrogen elimination is not involved in the rate-determining step [11]. Hydroxyapatite [12], Al-complex [13] and Zr-complex [14] also showed the rather small KIE values as primary isotope effect for the cleavage of C-H bond and these catalysts were reported to be active catalysts for hydrogen transfer reaction. All of these reports indicate that C-H and C-D bonds are not completely cleavaged in the transition states and the hydride transfer occurs by concerted mechanism [11-14]. The experimental KIE values ($r_{C_2H_5OH} / r_{C_2D_5OD}$) for the V_2O_3 and MoO_2 catalysts are similar to those of these reports, even though slightly small values were obtained in this work due to a higher reaction temperature. Therefore, hydrogen in methylene group and hydroxyl group were not completely cleavaged in the transition states over V_2O_3 and MoO_2 catalysts. Moreover, hydride transferred occurred by concerted mechanism and the hydride transfer is rate determining step for the equivalent formation of ethane and acetaldehyde from ethanol over V_2O_3 and MoO_2 catalysts.

3. 3. 10 Adsorbed models of two ethanol molecules on the V_2O_3 and MoO_2 catalysts

To examine how it is possible to form ethane and acetaldehyde in a single step via hydrogen transfer reaction, adsorption models of two ethanol molecules on (0 1 2) plane of V_2O_3 and (-1 1 1) plane of MoO_2 are drawn in Fig. Fig. 3-20. A hexagonal crystal structure of the V_2O_3 catalyst grew in the direction to (0 1 2) plane [15], and the preferential orientation effect is observed along (1 1 *l*) direction for the MoO_2 catalyst [16]. The distances of H_a-O_b are almost the same for V_2O_3 (2.30 Å) and MoO_2 (2.37 Å) catalysts and the distance of H_a-C_b for V_2O_3 catalyst (2.21 Å) is greater than that for MoO_2 catalyst (1.61 Å). The model can help to reasonably explain the observed various kinetic results by assuming that simultaneously formation of ethane and acetaldehyde proceeds via hydrogen transfer dehydration between two ethanol molecules adsorbed on the adjacent metal cation-oxygen anion pair sites via formation of six-membered transition states on the V_2O_3 and MoO_2 catalysts.

3. 3. 11 Reaction scheme for the co-formation of ethane and acetaldehyde from ethanol over V_2O_3 and MoO_2 catalysts

Based on the kinetic isotope effect and the model of two ethanol molecules adsorbed on (0 1 2) plane of V_2O_3 and (-1 1 1) plane of MoO_2, we proposed a plausible reaction scheme for the co-formation of ethane and acetaldehyde from ethanol as shown in scheme 3-1. Simultaneous formation of ethane and acetaldehyde proceeds via the hydrogen transfer through 6-membered cyclic intermediated, which is concerted process where two ethanol molecules are adsorbed at V-O and Mo-O sites on the surface of the catalysts. In this case, the first step of the process involves chemisorption of two ethanol molecules at metal cation sites on V_2O_3 and MoO_2, and the H atoms in the hydroxyl groups may be stabilized by hydrogen bonding with lattice oxygen atoms in V_2O_3 and MoO_2 catalysts. The rather small KIE values for $v_{C_2H_5OH} / v_{C_2D_5OD}$ indicates that α-hydrogen is

eliminated by concerted mechanism and hydrogen transfer reaction takes place via formation of nonlinear transition structure. The KIE value in hydrogen transfer reaction exceeds 6 when the reaction takes place in linear transition structure [17], and nonlinear transition structure gives the decreasing of the KIE value as low as $2^{1/2}$ [18]. Based on this consideration, H_a adsorbed on lattice oxygen interacts with O_b of $-O_bH$ in ethanol adjacent adsorbed hydroxyl group and H_a in methylene group also interact with C_b in adjacent methylene group. As a result, six-membered transition state similar to that of scheme 1 was formed. Subsequently, H_a in hydroxyl group adsorbed on lattice oxygen transfers as proton to the hydroxyl group adsorbed at adjacent site ($-O_bH$). H_a in the methylene group also transfers as hydride ion to the C_b in methylene group of another ethanol adsorbed on the adjacent site accompanied by cleavage of C_b-O_b bond. Therefore, ethane and acetaldehyde are simultaneously formed. Cation sites of certain catalysts are known to act as Lewis acid sites and active for the hydrogen transfer reaction between alcohols and aldehydes through six-membered transition state [19.20].

In this reaction scheme, alkanes are formed from corresponding alcohols without hydrogen, because alcohols act as hydrogen sources by itself. Deoxygenation of alcohols without use of hydrogen is one of the important issues in biomass conversion technology. Therefore, it is suggested that V_2O_3 and MoO_2 act as deoxygenation catalysts without hydrogen sources.

3.4 Conclusion

The selectivity to ethane and acetaldehyde were almost independent of the reaction temperature in the range of 533 – 653 K and contact time in the range 0.0014 - 0.07 g· ml· min^{-1}, confirming the equimolar formation scheme. Both over the V_2O_3 and MoO_2 catalysts, the reactions of methanol, 1-propanol and 2-propanol also produced the equivalent amount of corresponding alkanes and

aldehydes. The reaction over the V_2O_3 and MoO_2 catalysts is generally applicable for aliphatic alcohols. The formation of methane strongly supports that olefin is not an intermediate in the co-formation of alkanes from aliphatic alcohols. Kinetic isotope effects for C_2H_5OD and C_2D_5OD respect to C_2H_5OH were rather small for both the V_2O_3 and MoO_2 catalysts. It is concluded that plausible reaction mechanism for the co-formation of ethane and acetaldehyde from ethanol is a hydrogen transfer reaction between two ethanol molecules adsorbed on metal-O_2-metal sites of V_2O_3 and MoO_2 atalysts surface *via* formation of six-membered transition states. This reaction itself and catalytic function of low valence V and Mo in metal oxide form seem quite unique in catalysis field and interesting for further application.

3. 5 References

[1] C. Freitas, S. Damyanova, D.C. Oliveira, C.M.P. Marques, J.M.C. Bueno, J. Mol. Catal. A 381 (2014) 26-37.

[2] A. P. Grosvenor, M. C. Biesinger, R. St.C. Smart, N. S. McIntyre, *Surf. Sci.* 600 (2006) 1771–1779.

[3] V. Bilovol, S. Ferrari, D. Derewnicka, F.D. Saccone, *Mater. Chem. Phys*. 146 (2014) 269-276.

[4] F. C. Marı´n, A. Mueden, C. M. Castilla, *J. Phys. Chem. B* 102 (1998) 9239-9244.

[5] N. Takezawa, C. Hanamaki, H. Kobayashi, *J Catal*. 38 (1975) 101-109.

[6] K. Kanoun, M.P. Astier, G.M. Pajonk, *Appl. Catal.* 70 (1991) 225-236.

[7] Y.C. Lin, C.H. Chang, C.C. Chen, J.M. Jehng, S.G. Shyu, *Catal. Communication*, 9 (2008) 675.

[8] B. Beck, M. Harth, N.G. Hamilton, C.Carrero, J.J.Uhlrich, A. Trunschke, S. Shailhutdinov, H. Schubert, H.J.Freund, R.Schlogl, J.Sauer, R. Schomacker, *J. Catal*. 296 (2012) 120-131.

[9] H. Nair, C.D. Baerthsch, *J. Catal*. 258 (2008) 1-4.

[10] B. Kilos, A. T. Bell, E. Iglesia, J. *Phys. Chem. C* 113 (2009) 2830-2836.

[11] M. Yamashita, T. Kawamura, M. Suzuki, Y. Saito, *Bull. Chem. Soc. Jpn.* 64 (1991) 272-278.

[12] C. L. Kibby, W. K. Hall, *J. Catal.* 31(1973) 65-73.

[13] (a) R. Cohen, C. R. Graves, S. T. Nguyen, J. M. L. Martin, M. A. Ratner, *J. Am. Chem. Soc*. 126 (2004) 14796-14803, (b) P. Nandi, Y. I. Matvieiev, V. I. Boyko, K. A. Durkin, V. I. Kalchenko, A. Katz, *J. Catal.* 284 (2011) 42-49.

[14] Y. Umekawa, S. Sakaguchi, Y. Nishiyama, Y. Ishi, J. Org. Chem. 62 (1997) 3409-3412.

[15] Y. Bai, P. Jin, S. Ji, H. Luo, Y. Gao, *Ceramics International* 39 (2013) 7803-7808.

[16] T. Leisegang, A. A. Levin, J. Walter, D. C. Meyer, *Crest. Res. Technol*. 40 (2005) 95-105.

[17] F. H. Westheimer, *Chem. Rev*. 61 (1961) 265-273.

[18] H. Kwart, Acc. *Chem. Res*. 15 (1982) 401-408.

[19] Y. Zhu, G. Chuah, S. Jaenicke, *J. Catal*. 2004, 227, 1-10.

[20] J. M. Hidalgo, C. J. sanchidrian, J. R. Ruiz, *Appl. Catal. A* 470 (2014) 311-317.

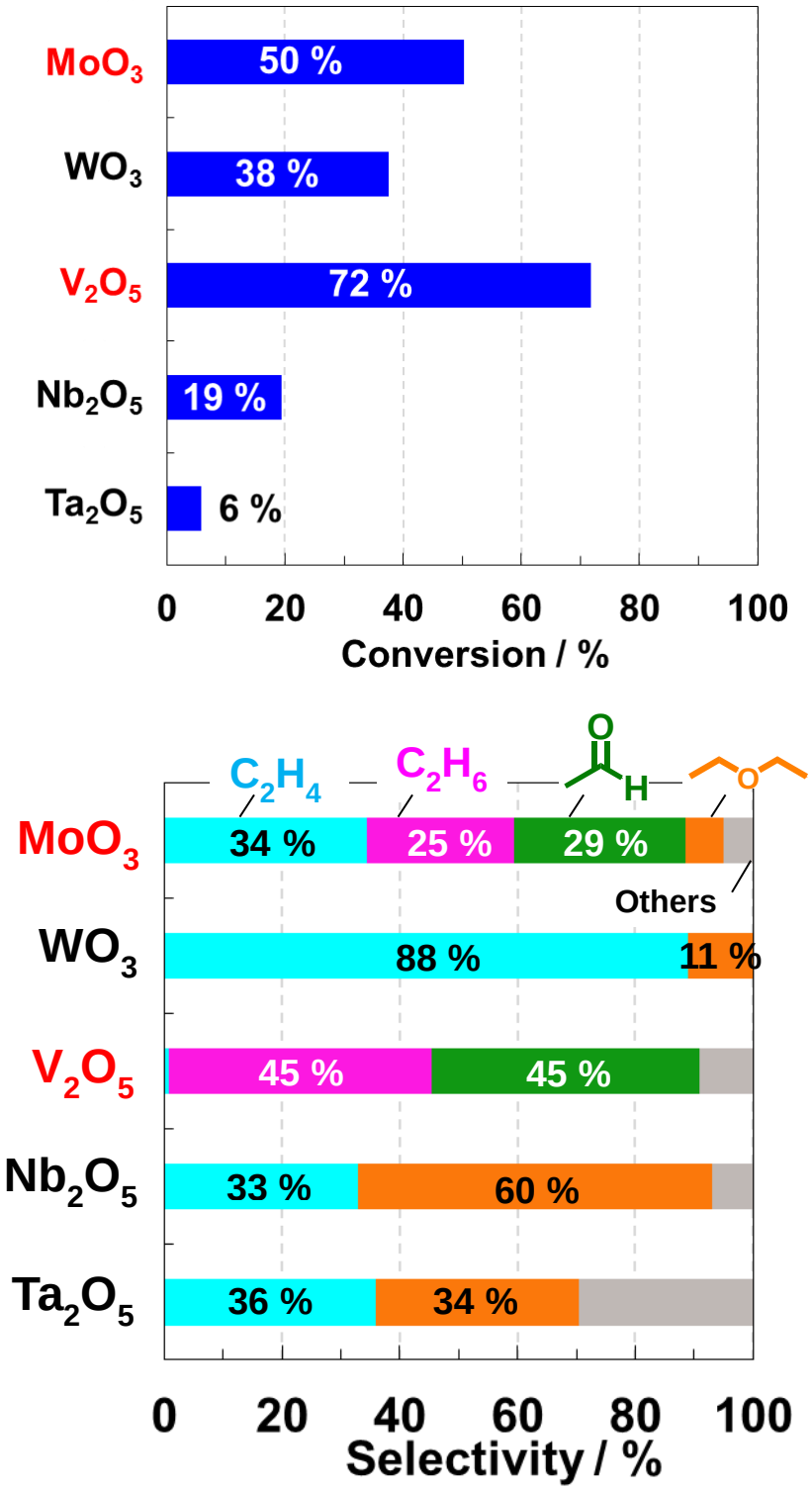

Fig. 3-1 Catalytic performance over 5 and 6 group metal oxides at 573 K. Cat. 0.15g, SiO_2 2.5g, 6 h time on stream, 573 K, flow rate: N_2 21 ml/min, ethanol 0.39 ml/min.

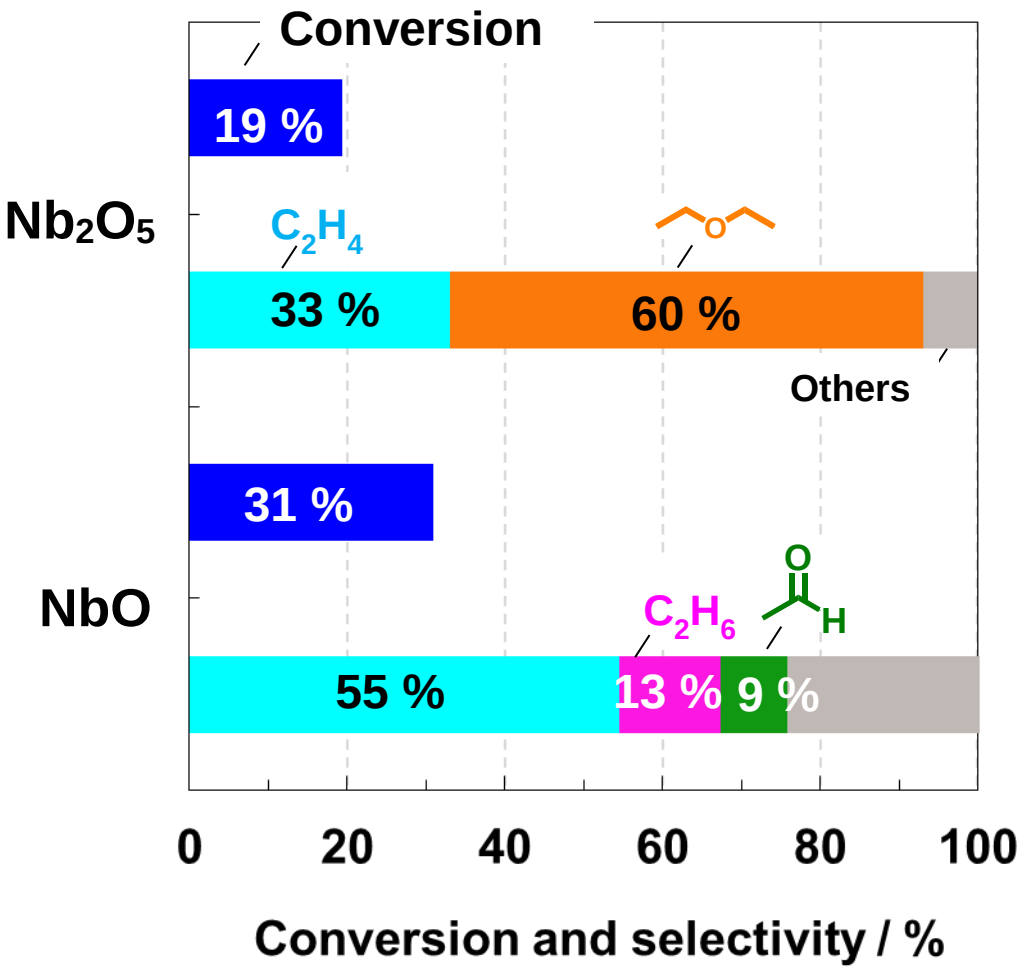

Fig.3-2 Catalytic performance of Nb_2O_5 and NbO catalyst in ethanol reaction at 573 K under N_2. Cat. 0.15g, SiO_2 2.5g, 3h time on stream, flow rate: N_2 21 ml/min, ethanol 0.39 ml/min.

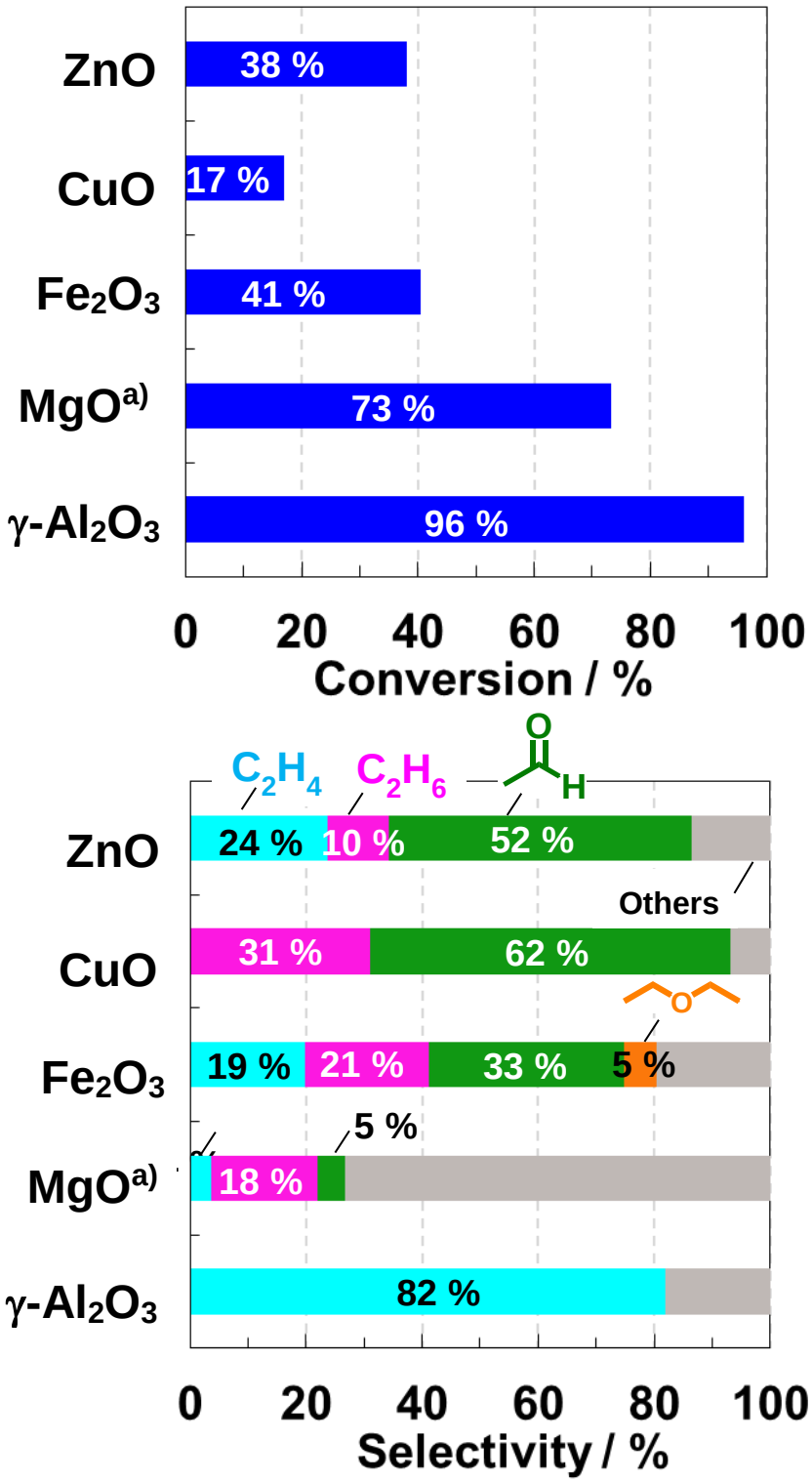

Fig.3-3 Catalytic performance for the ethanol conversion on some base catalysts. Cat. 0.15 g, SiO_2 2.5 g, reaction temperature 623 K, 3 h time on stream flow rate: C_2H_5OH 0.24 ml/min, N_2 21.4 ml/min, 0.1 h[a)] time on stream

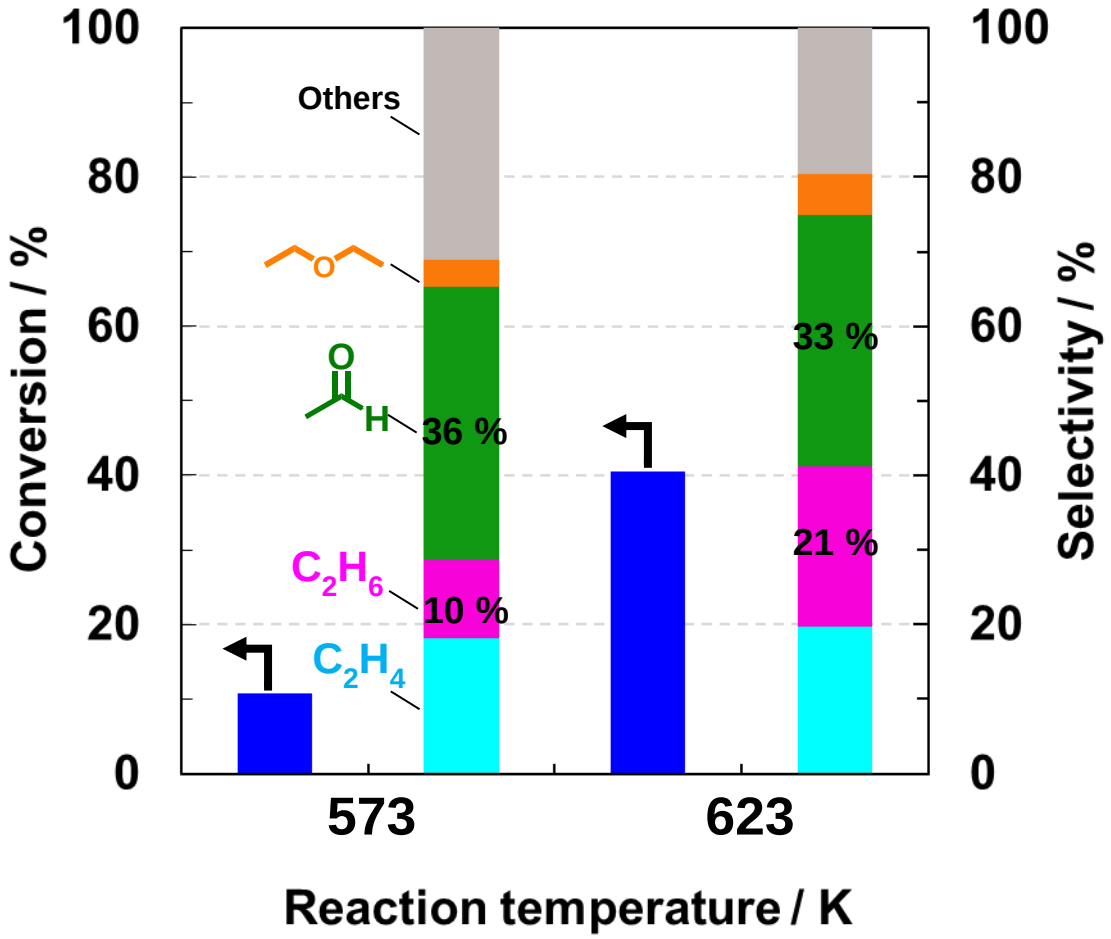

Fig. 3-4 Effect of reaction temperature for the product distributions in the reaction of ethanol over Fe_2O_3 catalyst under N_2. Fe_2O_3 0.15g, SiO_2 2.6 g, 3 h time on stream, flow rates: N_2 21 ml/min, ethanol 0.39 ml/min

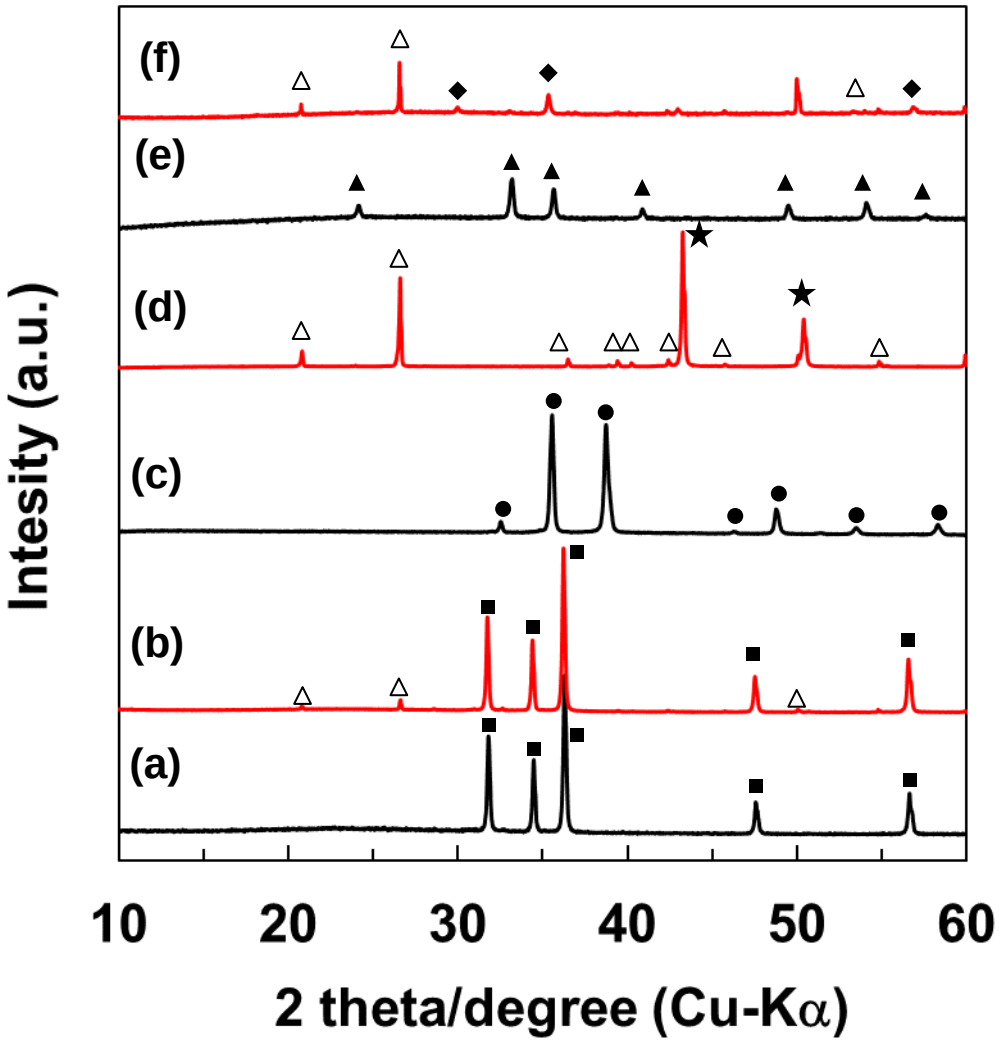

Fig.3-5 Comparison of XRD patterns of the Fe_2O_3, CuO and ZnO. Reaction condition: cat. 0.15g, reaction temperature 623 K, flow rate: N_2 21 ml/min, ethanol 0.24 ml/min. (a) ZnO before reaction, (b) ZnO after reaction, (c) CuO before reaction, (d) CuO after reaction, (e) Fe_2O_3 before reaction and (f) Fe_2O_3 after reaction, (▲)Fe_2O_3, (◆) Fe_3O_4, (●)CuO, (★)Cu metal, (■)ZnO, (□)NiO, (○)Ni metal, (△) SiO_2.

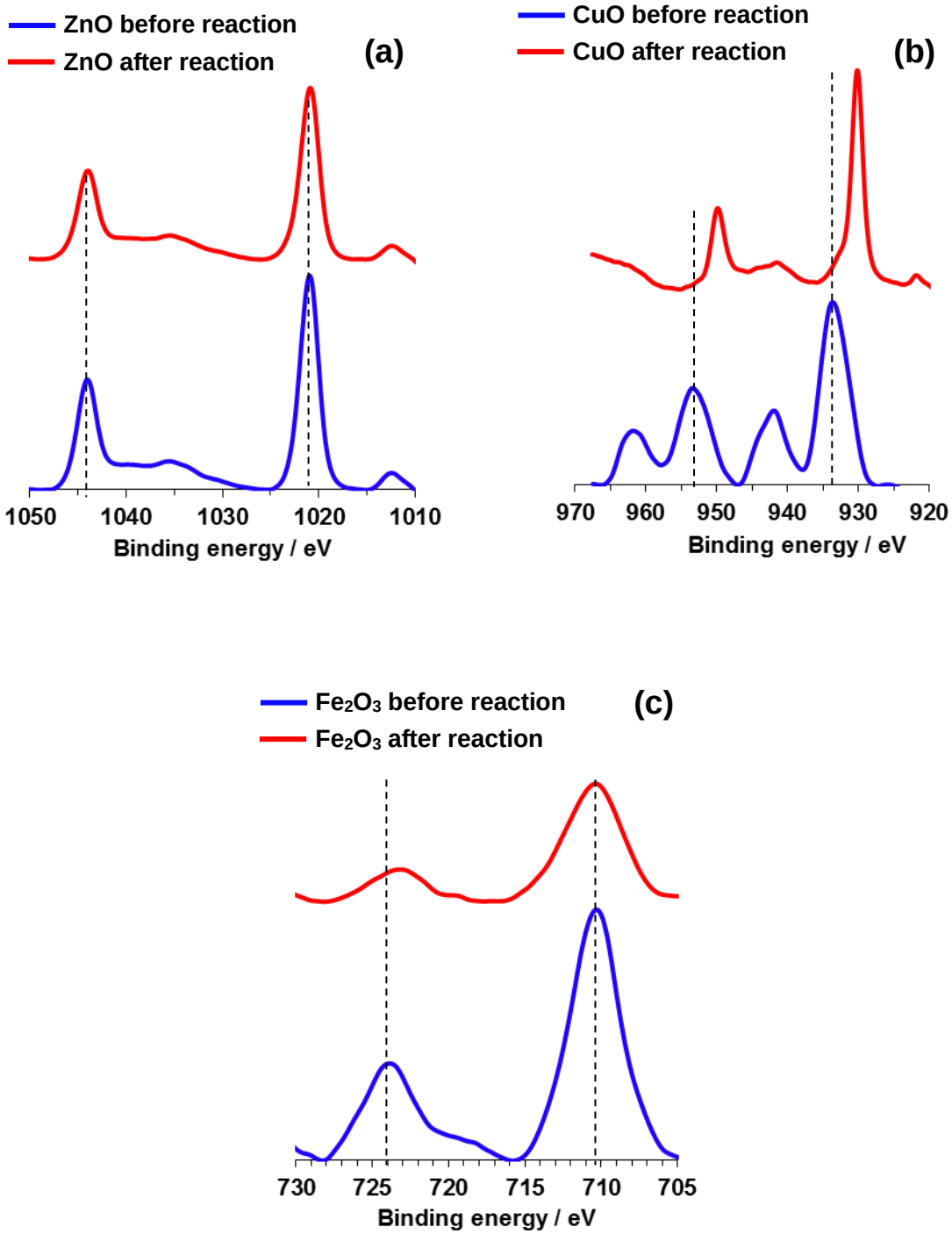

Fig.3-6 XPS spectra for Zn, Cu, Ni and Fe binding energy on ZnO, CuO, NiO and Fe_2O_3, respectively after ethanol reaction. Cat. 0.15g, SiO_2 2.5 g, 623 K, 5 h time on stream, flow rate: C_2H_5OH 0.24ml/min, N_2 21 ml/min.

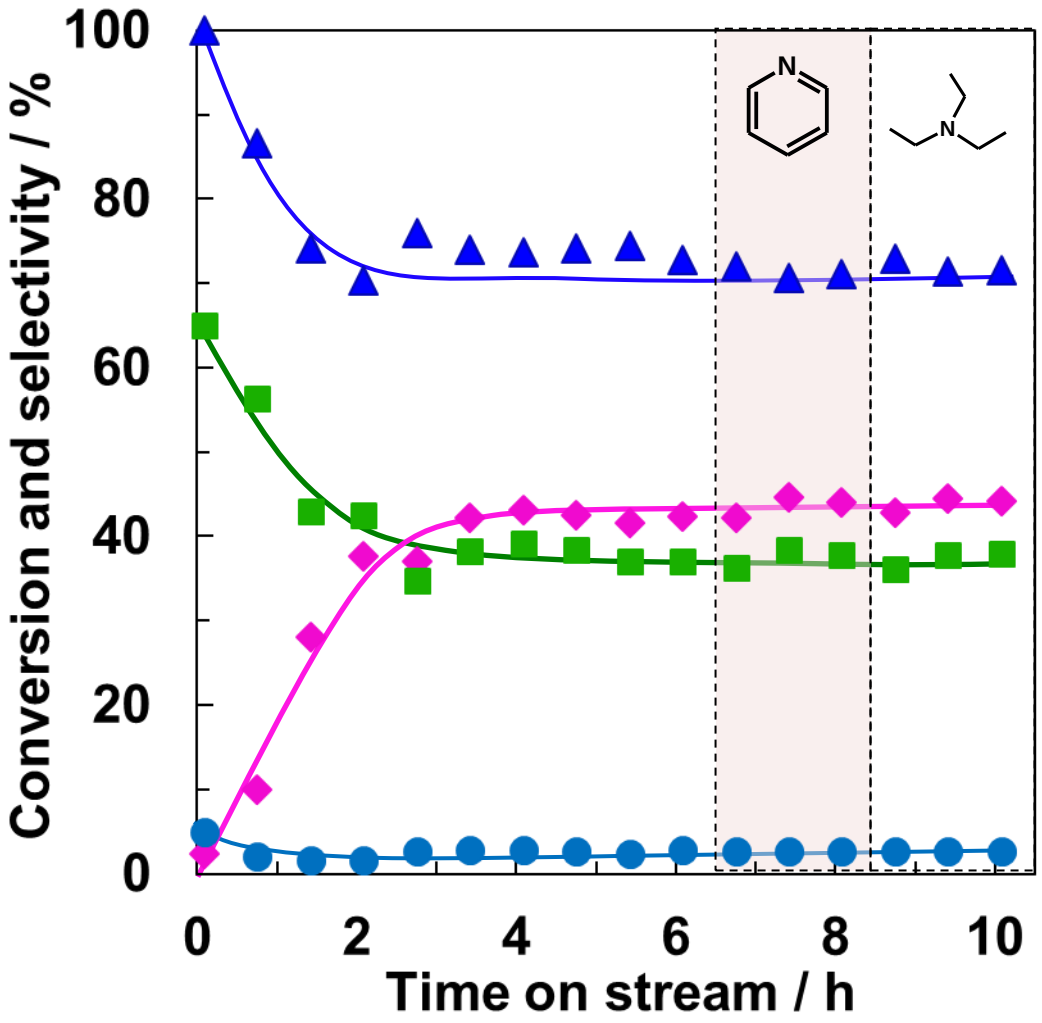

Fig.3-7 Effect of addition of pyridine and tri-ethylamine into reaction stream over MoO_3 catalyst. The amount of introduction of base compounds were 5 μl. Reaction condition: V_2O_5 0.15g, reaction temperature 573 K, flow rate: N_2 21 ml/min, ethanol 0.24 ml/min. (▲) conversion of ethanol, selectivity to (◆) ethane, (●) ethylene, (■) acetaldehyde

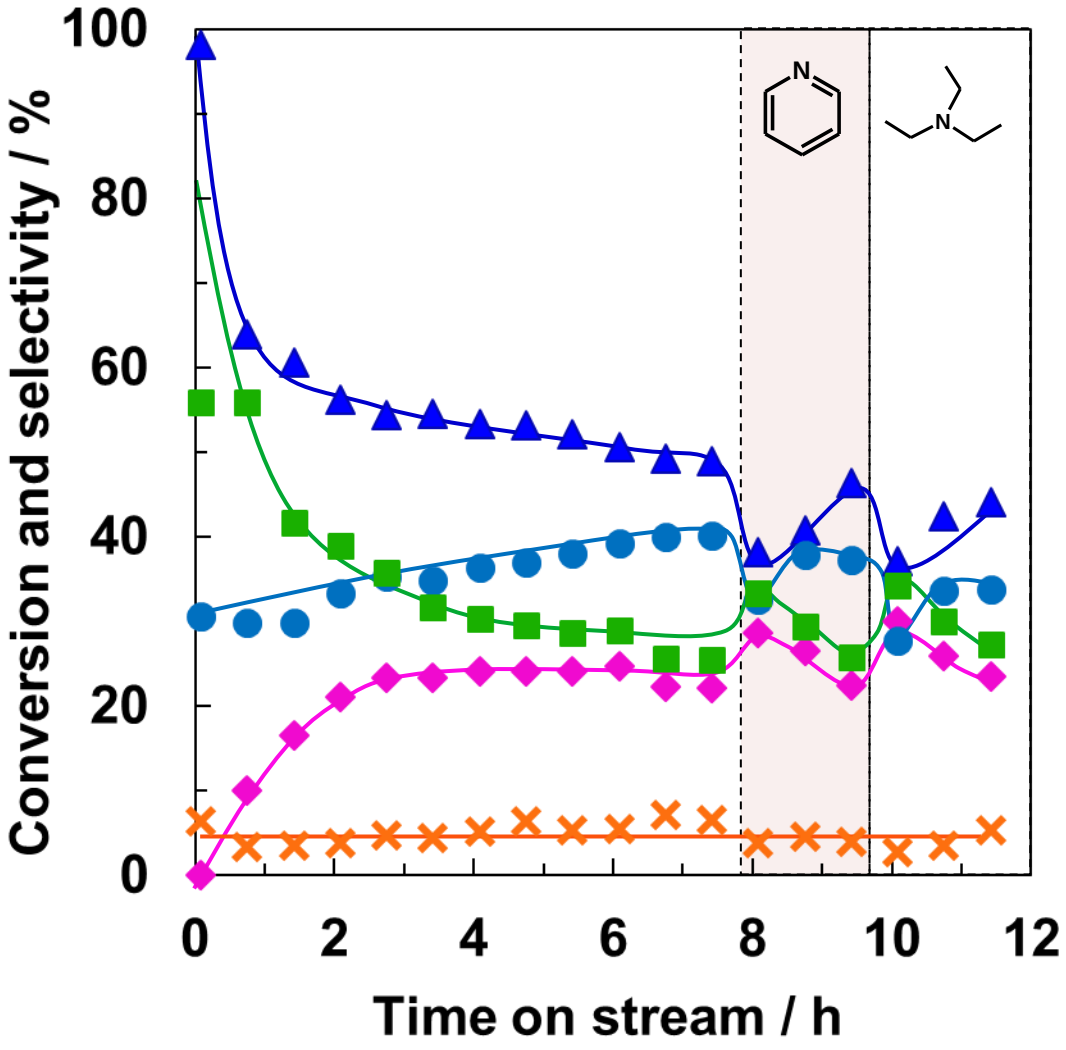

Fig. 3-8 Effect of addition of pyridine and tri-ethylamine into reaction stream over MoO_3 catalyst. The amount of introduction of base compounds were 5 μl. Reaction condition: MoO_3 0.15g, reaction temperature 573 K, flow rate: N_2 21 ml/min, ethanol 0.24 ml/min. (▲) conversion of ethanol, selectivity to (◆) ethane, (●) ethylene, (■) acetaldehyde, (×) diethyl ether

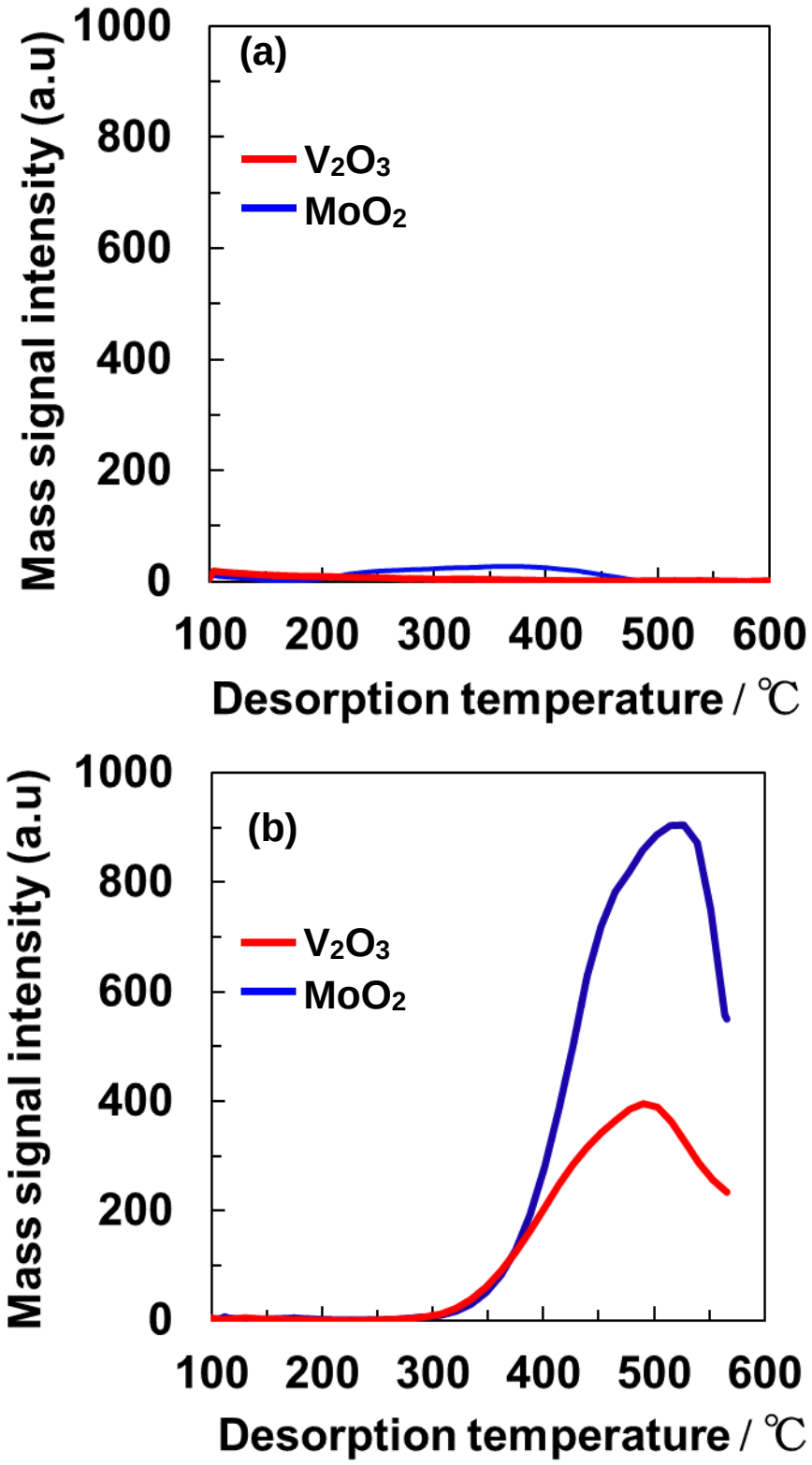

Fig. 3-9 NH_3-TPD profiles (m/z = 16) (a) and CO_2-TPD profiles (m/z = 44) (b) of V_2O_3 and MoO_2. V_2O_3 and MoO_2 50 mg

Table 3-1

Ethanol reaction in the presence of H_2 and C_2H_4 over V_2O_3 and MoO_2 catalysts.

Catalysts	S_{BET} (m^2/g_{cat})[a]	Condition	Conversion (%)	Selectivity (%)			
				C_2H_4	C_2H_6	CH_3CHO	Others[e]
V_2O_3	17	N_2 [a]	13.4	2.0	42.7	43.6	11.7
		with H_2 [b]	16.5	1.1	45.7	42.4	10.8
		with C_2H_4 [c]	16.8	1.3 [d]	45.8	41.5	11.4
MoO_2	6	N_2 [a]	41.0	1.2	47.4	47.6	3.8
		with H_2 [b]	38.0	1.1	44.4	45.9	8.6
		with C_2H_4 [c]	36.8	4.3[d]	43.4	45.5	6.8

Reaction condition: reaction temperature 573 K, catalyst 0.15 g, 5 h time on stream

[a] N_2 21 ml/min, ethanol 0.39 ml/min.

[b] N_2 20 ml/min, C_2H_5OH 0.39 ml/min, H_2 1.0 ml/min.

[c] N_2 20 ml/min, C_2H_5OH 0.39 ml/min, C_2H_4 1.0 ml/min.

[d] Obtained by subtraction of the concentration of ethylene introduced into the feed from the concentration of ethylene in the products.

[e] Others are attributed to C4 compounds mainly.

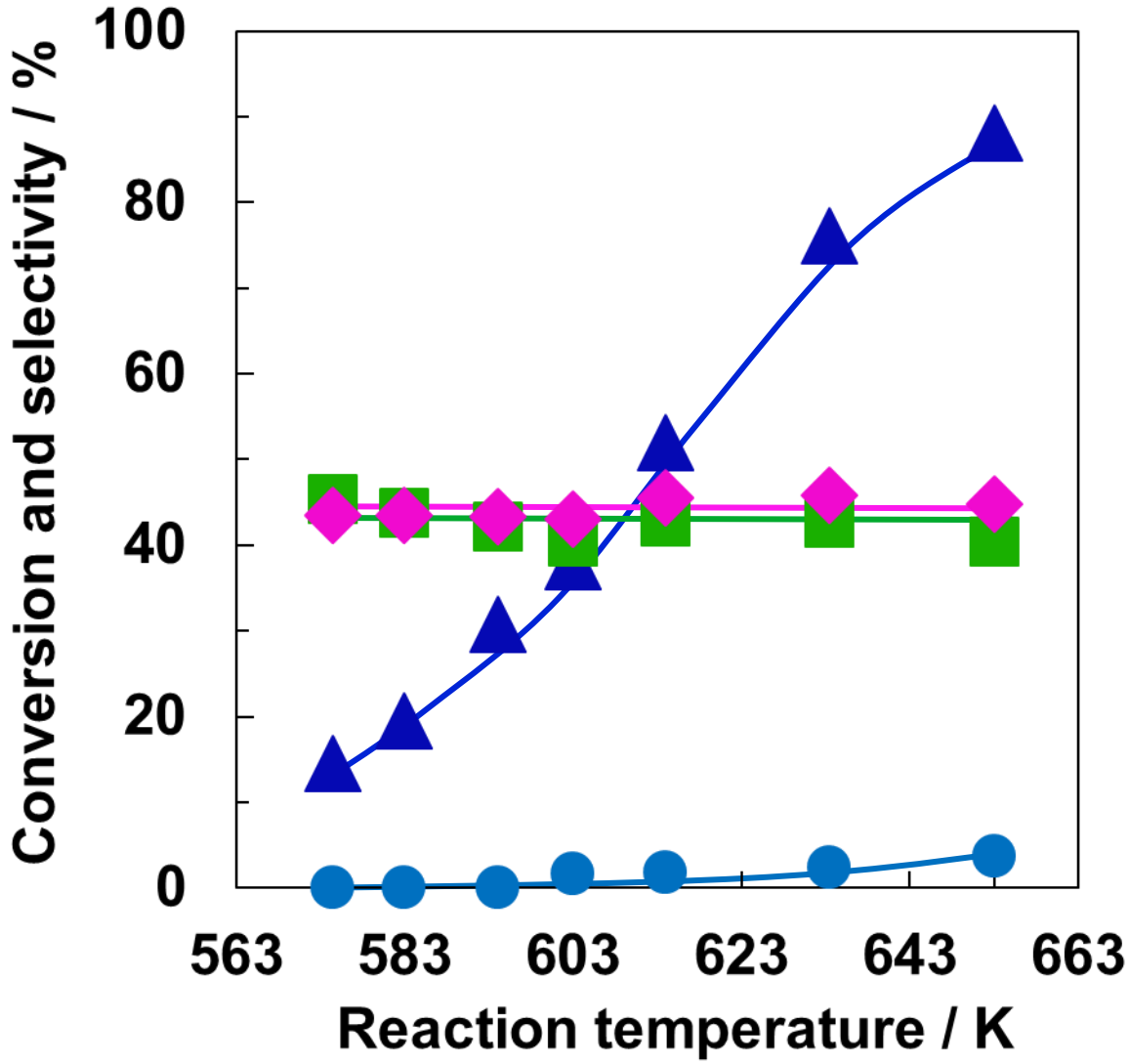

Fig. 3-10 Ethanol reaction at different reaction temperature form 563 K to 653 K over V_2O_3 under N_2. V_2O_3 0.15g, SiO_2 2.6 g, 5 h time on stream, flow rate : N_2 21 ml/min, ethanol 0.39 ml/min, (▲) conversion of ethanol, selectivity to (◆) ethane, (●) ethylene, (■) acetaldehyde

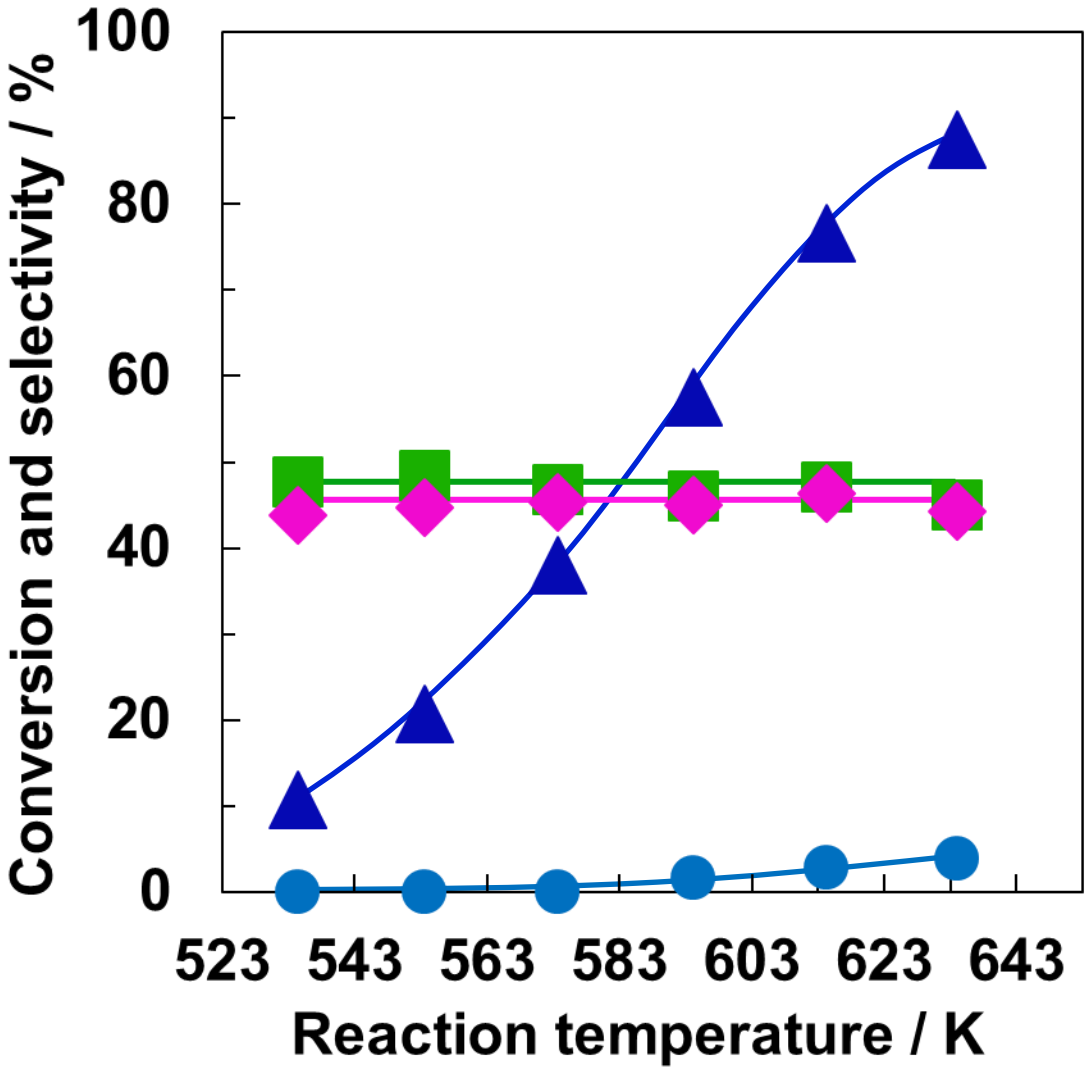

Fig. 3-11 Ethanol reaction at different reaction temperature form 563 K to 653 K over MoO_2 under N_2. V_2O_3 0.15g, SiO_2 2.6 g, 5 h time on stream, flow rate : N_2 21 ml/min, ethanol 0.39 ml/min, (▲) conversion of ethanol, selectivity to (◆) ethane, (●) ethylene, (■) acetaldehyde

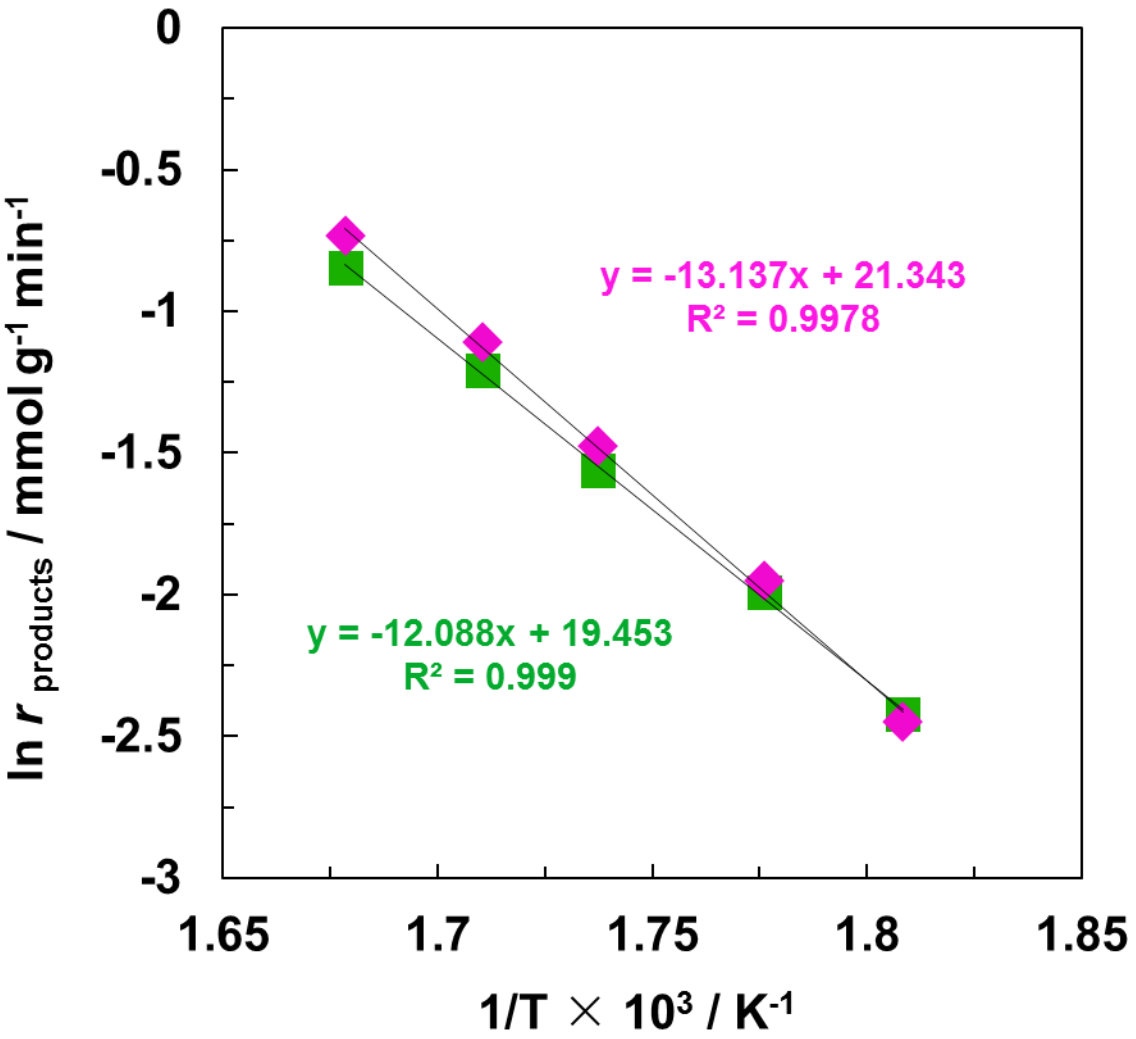

Fig. 3-12 Arrhenius plots for the formation of ethane and acetaldehyde over V_2O_3. V_2O_3 0.15 g, SiO_2 2.6 g, 5 h time on stream, flow rate : N_2 21 ml/min, ethanol 1.67 ml/min, (◆) ethane, (■) acetaldehyde

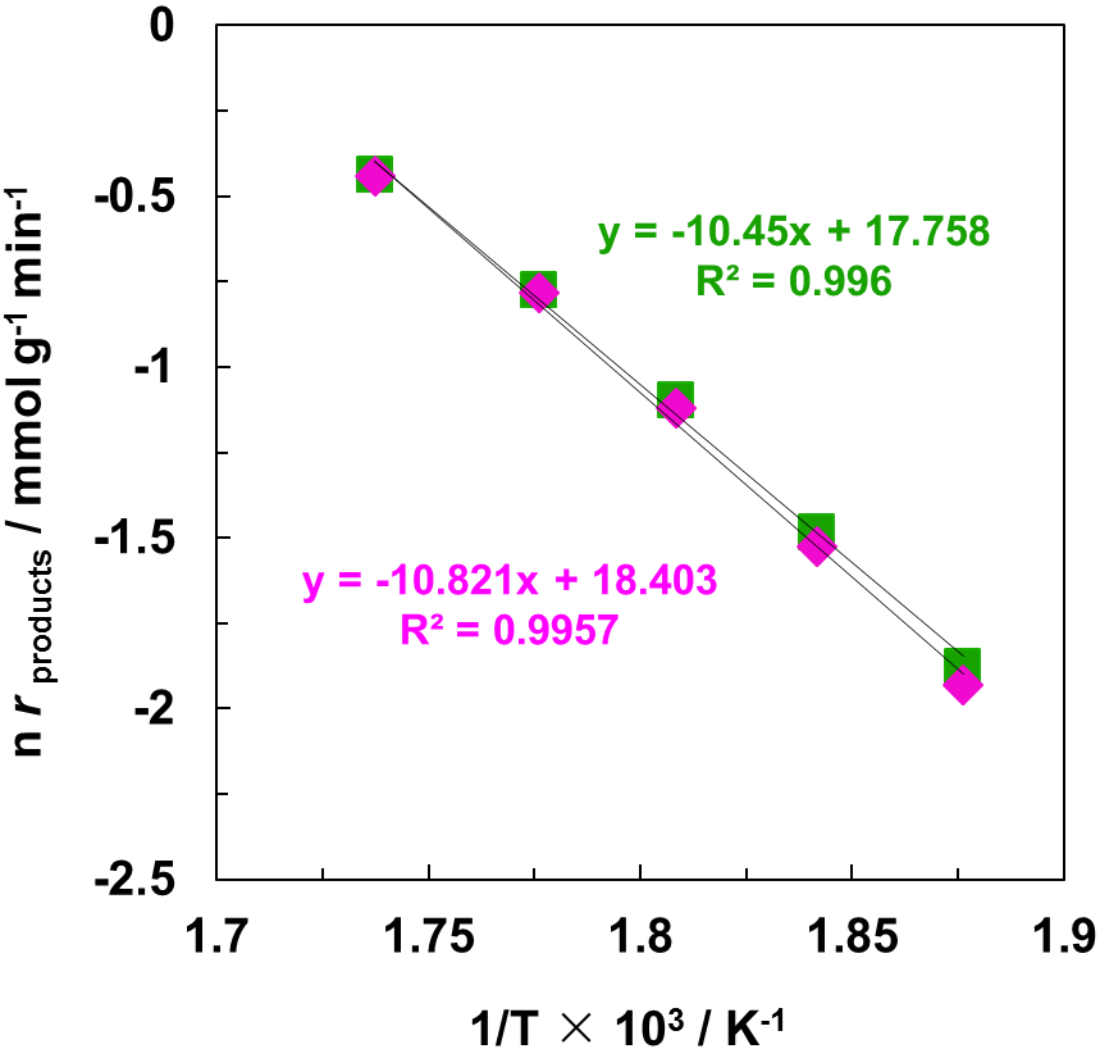

Fig. 3-13 Arrhenius plots for the formation of ethane and acetaldehyde over MoO_2. MoO_2 0.15 g, SiO_2 2.6 g, 5 h time on stream, flow rate : N_2 21 ml/min, ethanol 1.67 ml/min, (◆) ethane, (■) acetaldehyde

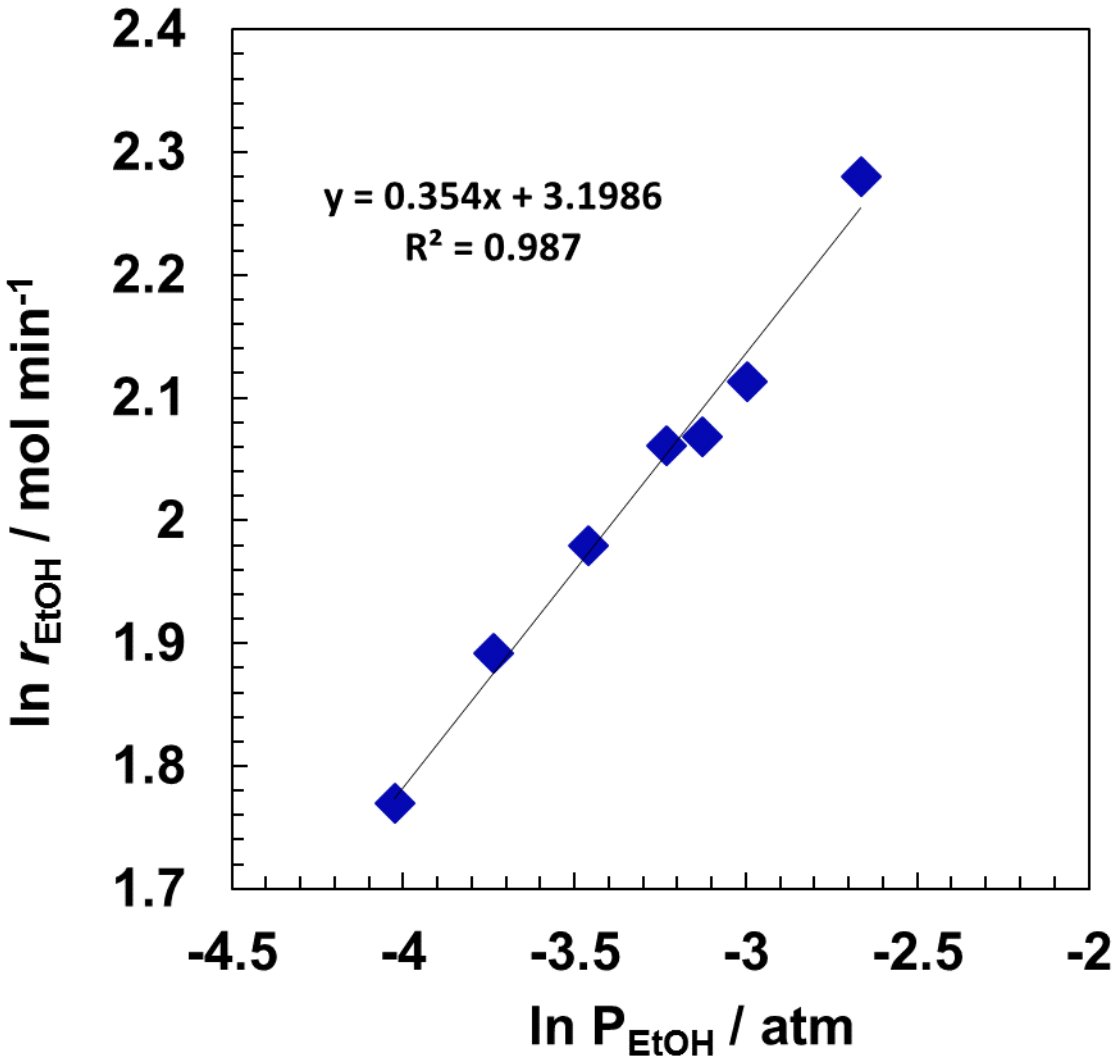

Fig. 3-14The correlation between the partial pressure of ethanol and the reaction rate of ethanol over V_2O_3.

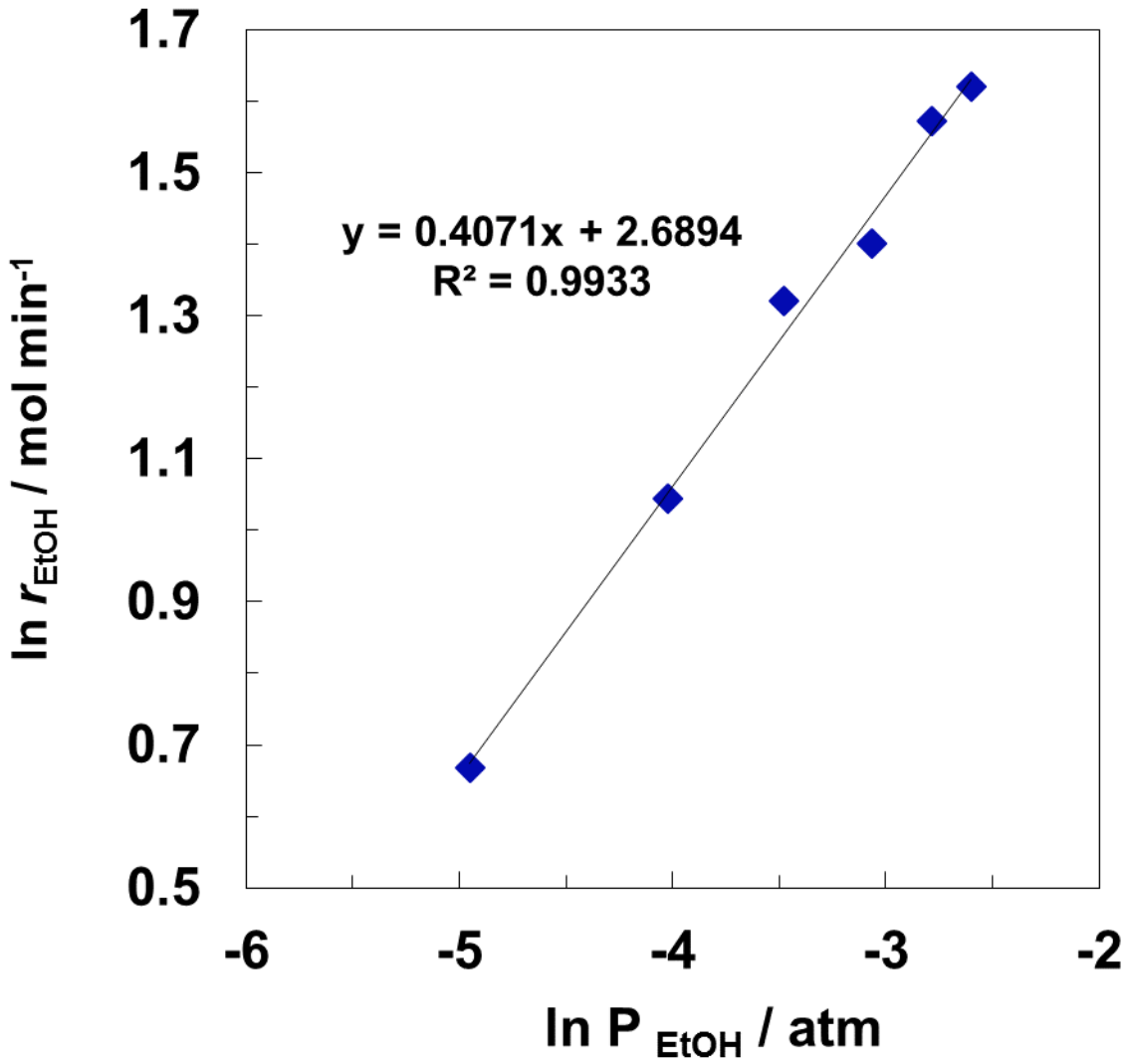

Fig. 3-15 The correlation between the partial pressure of ethanol and the reaction rate of ethanol MoO_2.

Table.3-2 The comparison of apparent activation energy for the formation of acetaldehyde from ethanol over V_2O_3, MoO_2 catalysts and several catalysts.

Catalysts	Reaction condition	E_{app} / kJ mol^{-1}		Ref.
		C_2H_6	CH_3CHO	
V_2O_3	N_2	100	106	This work
MoO_2	N_2	90	86	This work
Activated Carbon	He		48 ~67	[4]
MgO	N_2		123	[5]
V-Cu-Zn oxide	N_2		109	[6]
$VO_x/TiO_2/SiO_2$	O_2		46	[7]
VO_x/MO_2 (M = Ti,Zr,Ce)	O_2		82 ~ 117	[8]
MO_x/Al_2O_3 (M = V, Mo, W)	O_2		17 ~ 23	[9]

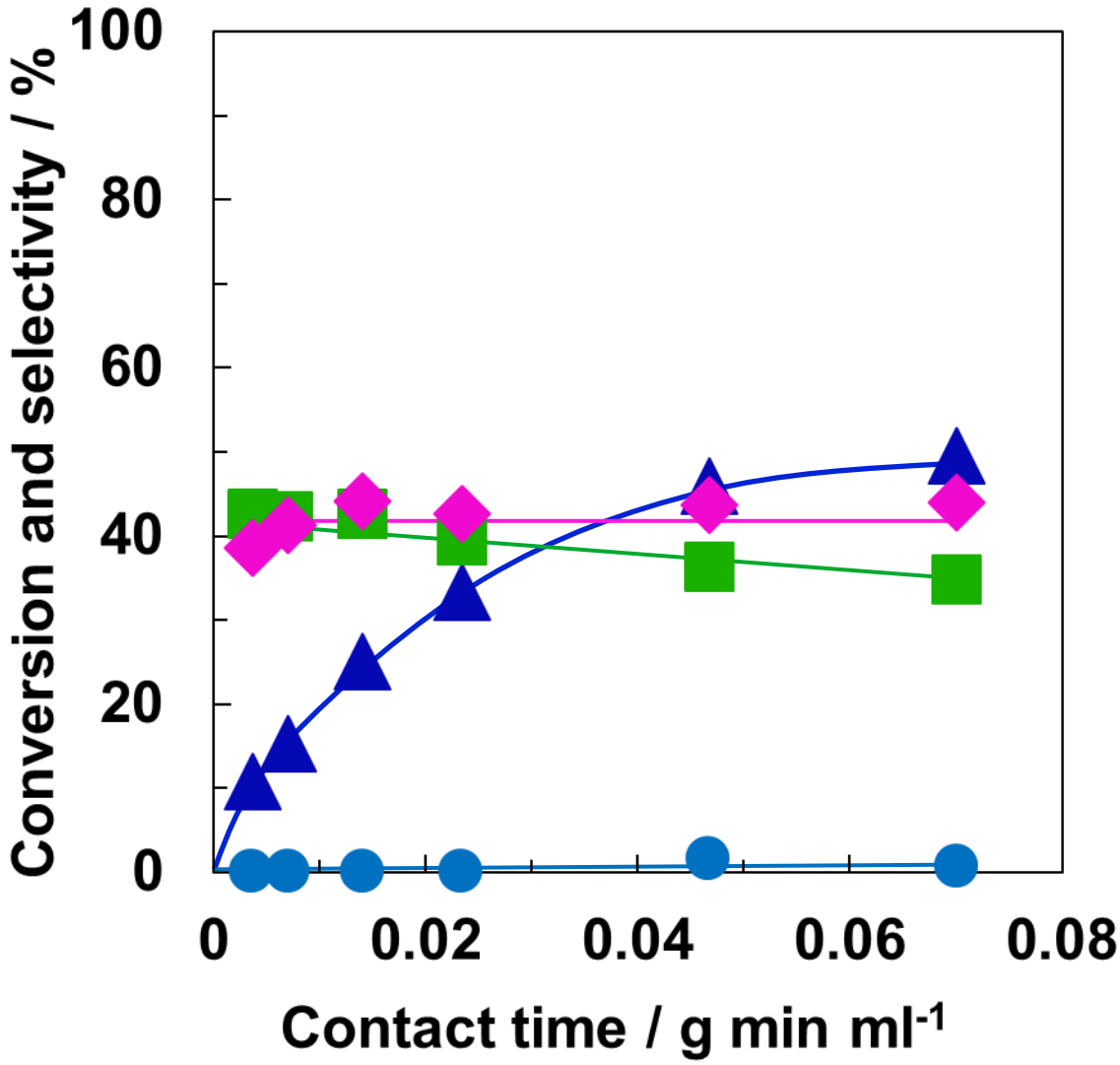

Fig. 3-16 Effect of different contact time from 0.0005 to 0.035 g min/ml at 573 K under N_2. V_2O_3 0.001 ~ 0.75g, SiO_2 1.9 ~ 2.6 g, 5 h time on stream, flow rate : N_2 21 ml/min, ethanol 0.39 ml/min, (▲) conversion of ethanol, selectivity to (◆) ethane, (●) ethylene, (■) acetaldehyde

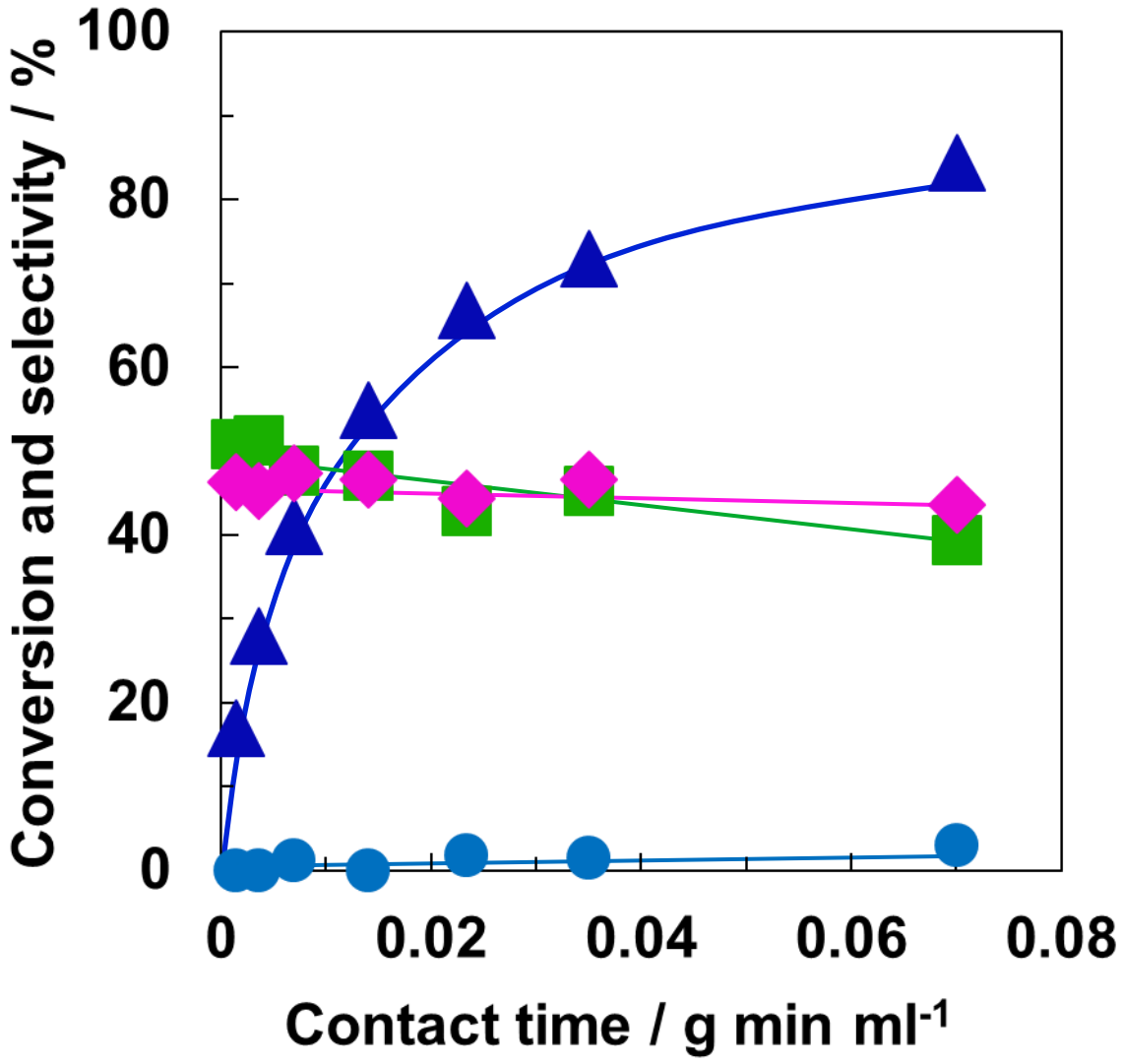

Fig. 3-17 Effect of different contact time from 0.0005 to 0.035 g min ml^{-1} at 573 K under N_2. MoO_2 0.001 ~ 0.75g, SiO_2 1.9 ~ 2.6 g, 5 h time on stream, flow rate : N_2 21 ml/min, ethanol 0.39 ml/min, (▲) conversion of ethanol, selectivity to (◆) ethane, (●) ethylene, (■) acetaldehyde

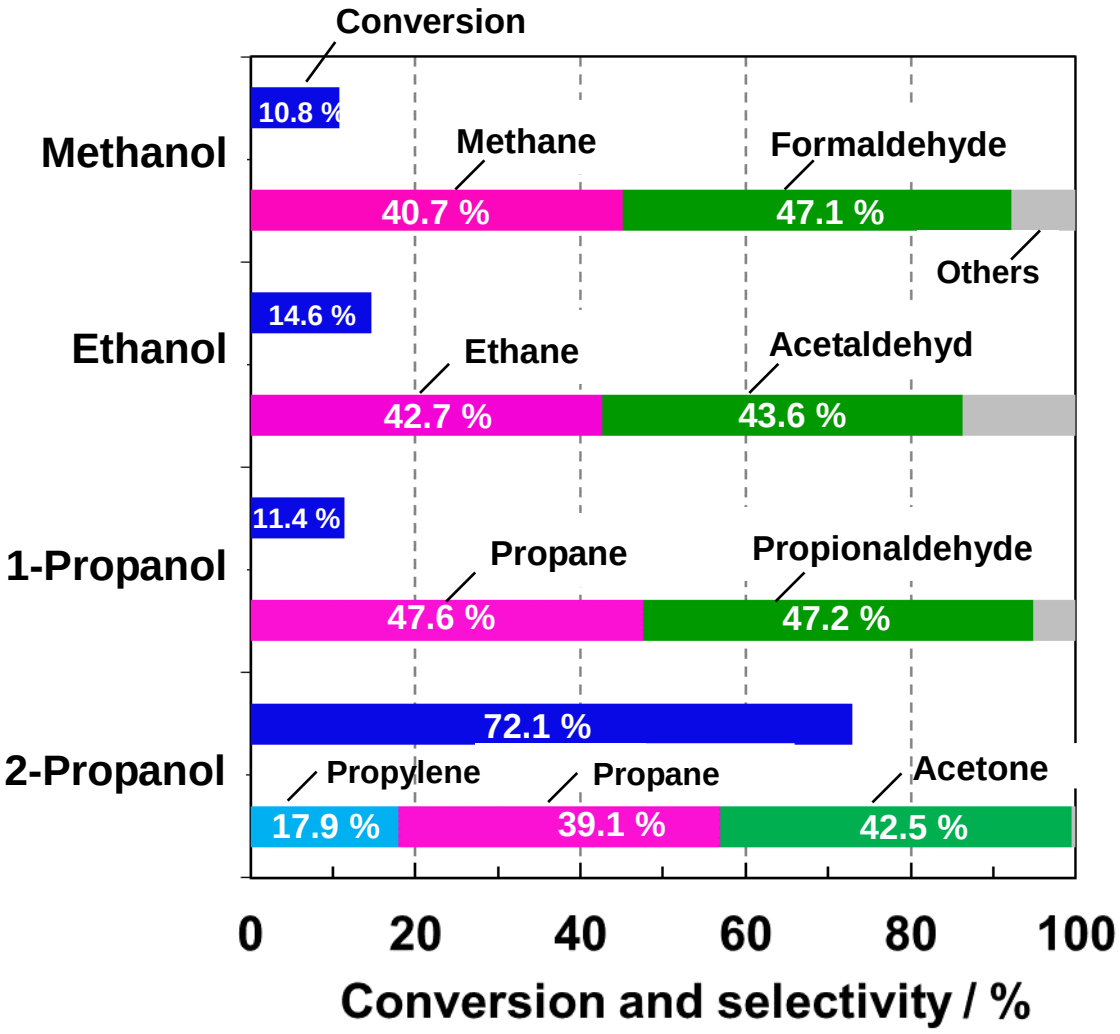

Fig. 3-18 Reaction of various alcohols over V_2O_3 catalysts at 573 K. Reaction condition: cat. 0.15g, 5 h time on stream, flow rate: N_2 21 ml/min, CH_3OH 0.59 ml/min, C_2H_5OH 0.39 ml/min, C_3H_7OH 0.36 ml/min, $CH_3CH(OH)CH_3$ 0.93 ml/min.

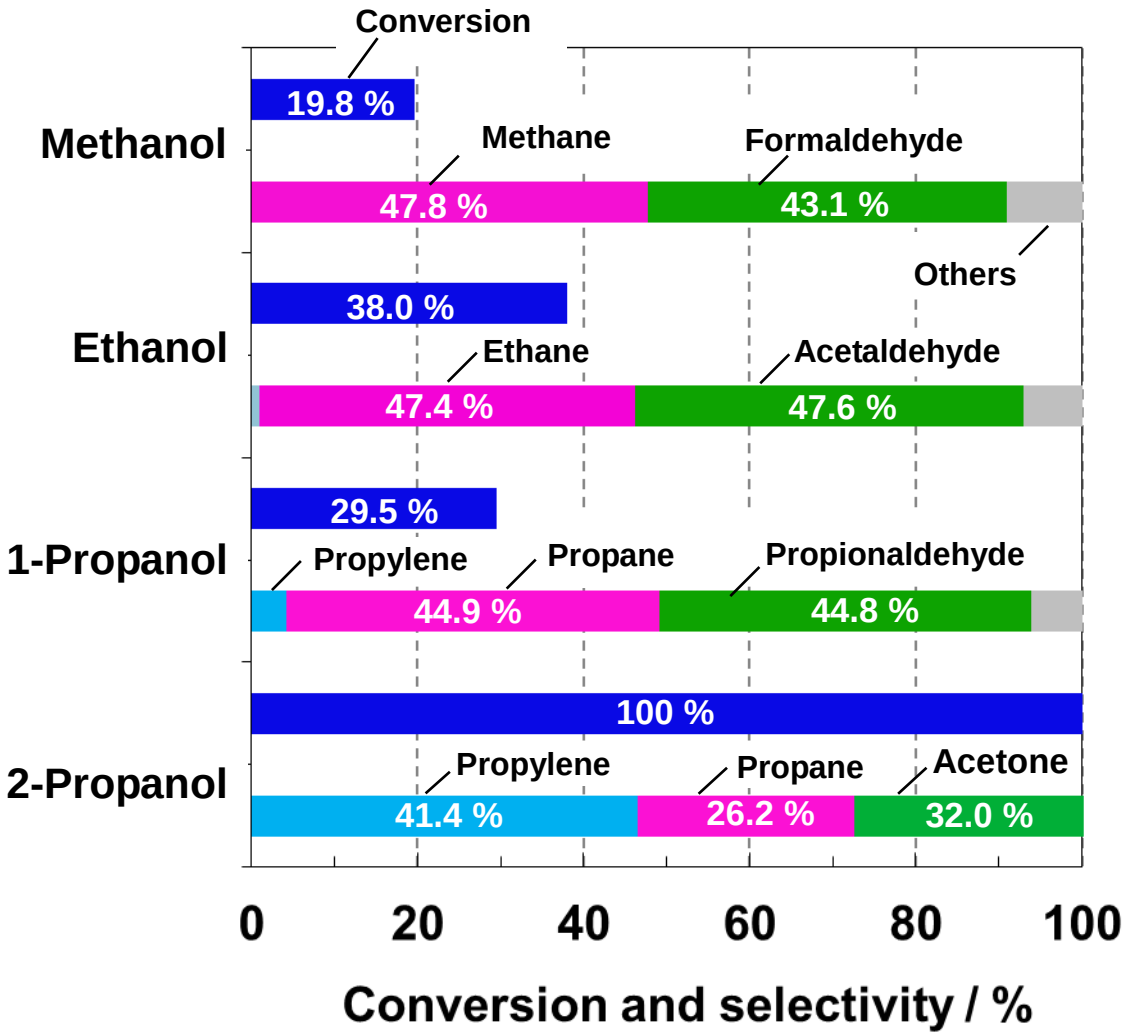

Fig. 3-19 Reaction of various alcohols over MoO_2 catalysts at 573 K. Reaction condition: cat. 0.15g, 5 h time on stream, flow rate: N_2 21 ml/min, CH_3OH 0.59 ml/min, C_2H_5OH 0.39 ml/min, C_3H_7OH 0.36 ml/min, $CH_3CH(OH)CH_3$ 0.93 ml/min.

Table 3-3

Rates of products formation in the various alcohol reactions on V_2O_3 and MoO_2 catalysts.

Catalysts	Reactant	Rate of product formation / μmol g^{-1} min^{-1}		
		Alkene	Alkane	Aldehyde
V_2O_3	CH_3OH	—	7.6	8.4
	C_2H_5OH	0.6	6.9	7.4
	C_3H_7OH	0.2	5.3	5.2
	$CH_3CH(OH)CH_3$	33.2	74.6	80.4
MoO_2	CH_3OH	—	12.9	11.6
	C_2H_5OH	0.6	23.8	24.1
	C_3H_7OH	1.5	14.7	14.5
	$CH_3CH(OH)CH_3$	106.9	62.3	70.4

[a] Reaction condition: cat. 0.15 g, reaction temperature 573 K, 5 h time on stream, flow rate N_2 21 ml/min, CH_3OH 0.59 ml/min, C_2H_5OH 0.39 ml/min, C_3H_7OH 0.36 ml/min, $CH_3CH(OH)CH_3$ 0.93 ml/min.

Table 3-4
Kinetic isotope effect (KIE) in alcohol reactions over several catalytic systems.

Entry	Catalysts	Reactions	Temp. (K)	KIE values $v_{-OH/-OD}$ ( )[a]	KIE values $v_{-CH/-CD}$ ( )[a]	Ref.
1	V_2O_3	C_2H_5OD, C_2D_5OD → ethane, acetaldehyde, H_2O	573	1.09 (3.1)	0.84 (2.8)	This work
2	MoO_2	C_2H_5OD, C_2D_5OD → ethane, acetaldehyde, H_2O	573	1.12 (3.1)	1.32 (2.8)	This work
3	VO_x/Al_2O_3	C_2H_5OD, C_2D_5OD → acetaldehyde, H_2O	473	1.02 (3.9)	4.90 (5.0)	[10]
4	Ru/carbon	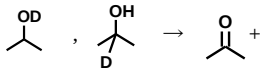	373	1.57 (5.6)	1.69 (4.6)	[11]
5	Hydroxyapatite	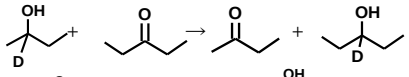	573		1.80 (2.8)	[12]
6	Al-complex[b]	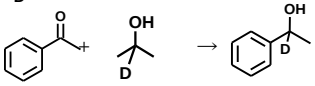	310		2.33 (6.5)	[13]
7	Zr-complex[c]	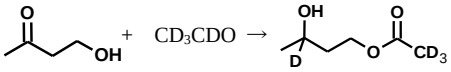	353		1.80 (4.1)	[14]

[a] Estimated values for KIE as primary isotope effect are shown in parenthesis.

[b] BINOLate/Al/^{i}PrOH system, BINOL (2,2'-dihydroxy-1,1'-binaphthyl).

[c] Zirconocene complex, Cp_2ZrH_2.

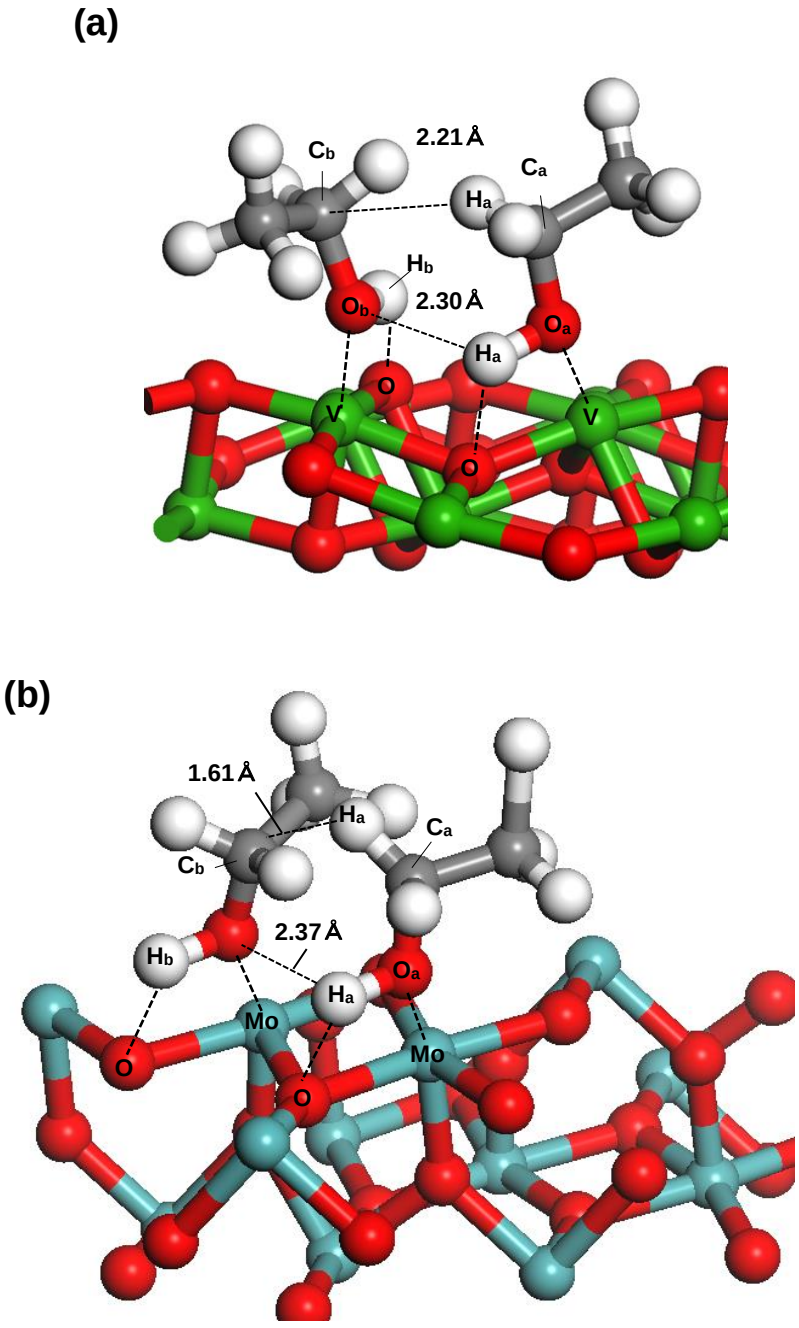

Fig. 3-20 Model of adsorbed ethanol on (0 1 2) planes of V_2O_3 (a) and (-1 1 1) plane of MoO_2 (b) surface. Green, blue, red, grey and white balls correspond to V, Mo, O, C and H, respectively.

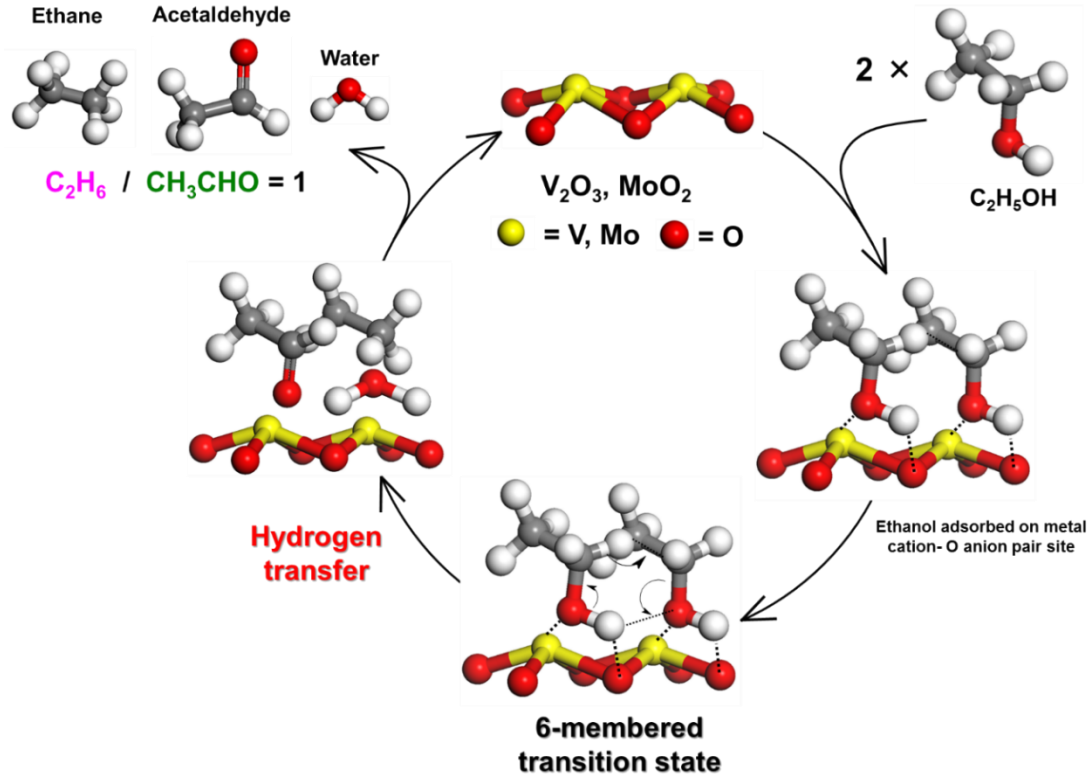

Scheme 3-1. Reaction scheme for the co-formation of ethane and acetaldehyde from ethanol via hydrogen transfer reaction between two ethanol molecules adsorbed on the adjacent metal cation-oxygen anion pair sites.

Chapter 4
Intramolecular hydrogen-transfer dehydration over V_2O_3 and MoO_2 catalysts in vicinal diol reactions

4. 1 Introduction

In Chapters 2 and 3, I discussed co-formation of alkanes and aldehydes or ketones from corresponding alcohols. I concluded that the formation of alkanes and aldehydes or ketones in a 1:1 ratio took place over V_2O_3 and MoO_2 catalysts through the intermolecular hydrogen-transfer reaction between two molecules of the primary alcohol adsorbed on metal cation – oxygen anion pair sites. It is interesting to examine how the reaction take place if the reactant is changed from mono-alcohols to diols such as ethylene glycol, propylene glycol and 1,3-propane diol, over V_2O_3 and MoO_2 catalysts.

The reactions of vicinal diols over several catalysts to produce corresponding aldehydes via dehydration of alcohols were reported [1-5]. In the reaction of ethylene glycol, acetaldehyde was formed as a main product. The major product was reported for propionaldehyde formed through dehydration of propylene glycol [4, 5]. On the other hand, selective conversion of vicinal alcohols to corresponding olefins over V, Mo and Re complexes were reported [6-8]. However, the reaction mechanism for the formation of aldehydes from vicinal diols has not been studied extensively. Therefore, we studied the reaction of vicinal diols over V_2O_3 and MoO_2 catalysts in order to elucidate the reaction mechanism of the dehydration of diols, focusing on the point whether the reaction involves intramolecular hydrogen-transfer reaction or not. If the regioselectivity of hydrogen-transfer reaction is involved, we can expect to apply our results to biomass conversion.

This study shows that intramolecular hydrogen-transfer reaction take place between primary and secondary hydroxyl groups in vicinal dios. The reaction of ethylene glycol led to the formation of acetaldehyde as a major products. In the reaction of propylene glycol, acetone was observed as a main product over both V_2O_3 and MoO_2 catalysts. These results are in contrasts to the results observed for various solid acid catalysts (zeolite, heteropoly acid, W-based and Amberlyst-70 catalyst) that propanal was a main product. For both the reaction of ethylene glycol and propylene

glycol, relatively low amount of corresponding olefins were formed. To the best of our knowledge, this is the first time to show the heterogeneous catalysts for the formation of corresponding olefins in the reactions of vicinal diols without addition of reductants.

4. 2 Experimental

4. 2.1 Catalyst preparation

Preparation of catalysts (V_2O_3 and MoO_2) was described in Chapter 2. V_2O_3 was prepared by the reduction of the prepared V_2O_5 (0.3 g) in a tubular furnace under H_2 stream (30 ml/min) at 773 K for 2 h. The reduced sample were then exposed to air when they cooled to room temperature before use as catalysts. MoO_2 was prepared by the reduction of the obtained MoO_3 (0.3 g) in a tubular furnace under H_2 stream (30 ml/min) at 773 K for 2 h. The reduced molybdenum oxide sample was exposed to air once after they cooled to room temperature and then treated again in a tubular furnace under 5 % H_2/Ar stream (30 ml/min) at 773 K for 2 h. Finally, the reduced sample was cooled to room temperature, followed by exposure to air. Thus obtained MoO_2 was used for the reactions.

4. 2. 2 Catalytic tests

Catalytic test procedures in diol reaction are almost the same as those of ethanol reaction. Catalytic reactions were carried out in a continuous flow fixed bed reactor (Pyrex). A mixture of the catalyst (0.3 g) and SiO_2 sands (2.0 g) as a diluent was placed in the reactor and heated to a desired reaction temperature (523~573 K) under a N_2 flow (20.0 ml/min). Then, the catalytic reaction was started by the introduction of 5 M substrate solutions (0.03 mmol/min) using microfeeder with N_2 carrier into the reactor as shown in Fig. 4-1. The total flow rate of the reactant gas (N_2+substrates) was kept constant (1.23 mmol/min) for all the reactions. The reaction products were analyzed by gas

chromatography. The products in the gas phase were analyzed with on-line two gas chromatographs. Liquid products trapped by ice water bath were analyzed by gas chromatography with ZB-1 column, n-butyl acetate (2 mmol) being used as an internal standard material and products. The calculation of the conversion of substrates and the selectivities to products are the same as described in Chapter 2.

4. 3 Results and discussion

4. 3. 1 Ethylene glycol reaction over V_2O_3 and MoO_2 catalysts

The conversion and selectivities in the ethylene glycol reaction as a function of time on stream are shown in Fig.4-2 for V_2O_3 and Fig.4-3 for MoO_2.

Over V_2O_3 catalyst, the conversion of ethylene glycol was extremely high with 96.7 % at a time on stream of 0.5 h. Then, the conversion of ethylene glycol slightly decreased to 93.1 % at 5.1 h time on stream. Ethylene glycol converted to acetaldehyde with 72.7 % selectivity and to ethylene with 15.5 % selectivity were observed at a time on stream of 0.5 h time on stream. Both conversion and selectivity were kept unchanged until 5.1 h. The selectivities to CO_2 and ethanol were less than 1 %.

Over MoO_2 catalyst, ethylene glycol was completely converted to acetaldehyde, ethylene, ethanol and CO_2 at a time on stream of 0.5 h. The selectivities to acetaldehyde and ethylene were 76.4% and 17.1 %, respectively. The conversion decreased with time on stream, and reached to 76 % at a time on stream of 7 h. In the steady states, the conversion of ethylene glycol was lower over MoO_2 than over V_2O_3 catalysts. The conversion order of MoO_2 and V_2O_3 for ethylene glycol was opposite to that for ethanol. The decrease of conversion over MoO_2 catalyst is considered to be due to low surface area compared with V_2O_3 catalyst. This result indicates that MoO_2 catalyst was strongly affected by water. The selectivity to acetaldehyde also slightly decreased with time on stream to

67.8 % and kept unchanged for the time on stream from 1.5 h to 7 h. On the other hand, the selectivities to ethanol and CO_2 were less than 1.5 % at 0.5 h and kept unchanged until 7 h.

The rates of the consumption of substrate and the formation of products over V_2O_3 and MoO_2 catalysts in ethylene glycol reaction are shown in Table 4-1. The rates of the consumption of ethylene glycol over V_2O_3 and MoO_2 catalysts were 96.5 μmol g^{-1} min^{-1} and 74.8 μmol g^{-1} min^{-1}, respectively, and the rates of the formation of acetaldehyde over V_2O_3 and MoO_2 catalysts were 70.3 μmol g^{-1} min^{-1} and 50.0 μmol g^{-1} min^{-1}, respectively. Compared to the ethanol reaction, the rates of the consumption of substrate and the products formation over V_2O_3 and MoO_2 catalysts in ethylene glycol reaction were much higher than those in the ethanol reaction (shown in Table 3-3) for both V_2O_3 and MoO_2 catalysts under similar conditions. This result showed that the reaction mechanism for the formation of acetaldehyde in the ethylene glycol reaction differs from that of ethanol reaction. Moreover, ethylene would not be formed via dehydration of ethanol formed by intermolecular hydrogen-transfer dehydration between two ethylene glycol molecules. If ethylene was formed by dehydration of ethanol, we could have observed much more amount of ethane because the selectivity to ethane was much higher than that of ethylene in the ethanol reaction over V_2O_3 and MoO_2 catalysts as discussed in the Chapter 2.

These results showed that the formation of acetaldehyde from ethylene glycol takes place through the intramolecular hydrogen-transfer reaction of ethylene glycol, while reaction of ethanol takes place via intermolecular hydrogen-transfer reaction between two adsorbed ethanol molecules. Although it was reported that acetaldehyde was also formed through dehydration of ethylene glycol over acid sites on catalysts, the formation of acetaldehyde over V_2O_3 and MoO_2 catalysts in the ethylene glycol reaction is considered to occur via intramolecular hydrogen-transfer reaction of ethylene glycol, because these catalysts have only weak acid sites, which could not promote dehydration of alcohols (in Chapter 2). Moreover, if intermolecular hydrogen-transfer reaction

occurred between two ethylene glycol molecules, ethane di-al, hydroxyethanal, ethane and much more amount of ethanol would have been observed (as shown in Scheme 4-1(b)). However, we could not observe the formation of ethane and ethane di-al, suggesting that intermolecular hydrogen-transfer reaction of ethylene glycol did not occur.

In order to study the effect of water on the Lewis acid sites of V_2O_3 and MoO_2 catalysts, ethanol reaction was carried out under similar conditions with the reaction of ethylene glycol. The catalytic performance of V_2O_3 in the presence of water is shown in Fig. 4-4. The selectivities to ethane and acetaldehyde were % and %, respectively, suggesting that the ethane and acetaldehyde were formed in 1:1 ratio. Moreover, the conversion of ethanol was almost same with that carried out in the absence of water. Therefore, the presence of water in the reaction stream had no remarkable effect on Lewis acid sites of V_2O_3 catalyst. This result indicates that transformation of Brönsted acid sites to Lewis acid sites by adsorption of water on Lewis acid sites did not occur. Moreover, Lewis acid sites on V_2O_3 and MoO_2 catalysts would show soft acidity, which could not interact with hard base compounds such as water, amines and NH_3.

4. 3. 2 Effect of the reaction temperature on the reaction of ethylene glycol over V_2O_3 and MoO_2 catalysts

In order to study of the ethylene glycol reaction, the effect of reaction temperature on this reaction was investigated. The conversion of ethylene glycol and the selectivities for products at different reaction temperatures over V_2O_3 catalysts are shown in Fig.4-5. The reaction represented in Fig.4-5 was carried out in the following sequence. The first reaction was carried out at 573 K for 5 h, and the second reaction was carried out at 523 K. Thereafter, the reaction temperature was increased stepwise by an increment of 50 K. The conversion of ethylene glycol increased with the reaction temperature as expected. The selectivities to ethanol and CO_2 were less than 1.5 % in all reaction

temperature range. It is interesting that the selectivity for acetaldehyde was increased with reaction temperature, while the selectivities to ethylene and CO_2 were unchanged in all reaction temperature range. On the other hand, the selectivity to acetaldehyde increased with increase of reaction temperature, and showed 68-72 % selectivity in the range of 553-573 K.

This result indicates that the active sites on V_2O_3 catalyst to form acetaldehyde is different from those to form ethylene. MoO_2 also possess the similar active sites with V_2O_3 catalyst, because similar results were obtained between V_2O_3 and MoO_2 catalysts in the reaction of ethylene glycol as a function of time on stream. Mo metal sites on Mo based oxides were reported to be active sites for deoxygenation [9-12]. Therefore, ethylene would be formed via deoxygenation of ethylene oxide formed on V_2O_3 and MoO_2 catalysts as discussed in detail later.

4. 3. 3 Propylene glycol reaction over V_2O_3 and MoO_2 catalysts

Variations in the conversion and selectivities in the reaction of propylene glycol over V_2O_3 and MoO_2 catalysts are shown in Fig.4-6 and Fig.4-7, respectively. In the reaction of propylene glycol over V_2O_3 (Fig.4-6) catalyst, propylene glycol was completely converted in all range of time on stream 0.5-8 h. This was the same as those observed in the reaction of ethylene glycol. The selectivities for all products were unchanged with increase of time on stream. Acetone was predominantly formed with 56.4 % selectivity. In addition to acetone, propionaldehyde with 15.6 % selectivity, propylene with 14.5 % selectivity and a small amount of CO_2 (less than 1.5 % selectivity) were also observed at 0.5 h time on stream. The formation of 1-, or 2-propanol may be produced in this reaction, but it could not be detected because the amount of these products were quite low. This point is different between the reaction of propylene glycol and that of ethylene glycol in which ethanol was formed.

MoO_2 catalyst showed similar results with V_2O_3 catalyst. The conversion of propylene glycol over MoO_2 catalysts were 100 % in all range of time on stream, 0.5-8 h. On the other hand, the selectivity to acetone was lower than those over V_2O_3 catalysts while the selectivities to propionaldehyde, propylene and CO_2 were slightly higher than those over V_2O_3 catalysts. The products distribution was unchanged from the initial reaction period to 8 h time on stream.

Compared to ethylene glycol reaction, propylene glycol reaction gave a high conversion over both V_2O_3 and MoO_2 catalysts. For both V_2O_3 and MoO_2 catalysts, the formation of propane was not observed. Considering that the reaction of propanol yielded propane and not yielded propylene as described in Chapter 3, the result indicates that the propylene was not formed through simple dehydration of propanol.

4. 3. 4 Effect of the reaction temperature on the propylene glycol reaction over V_2O_3 and MoO_2 catalysts

The results of the reaction of propylene glycol over V_2O_3 and MoO_2 catalysts at different reaction temperatures are shown in Fig.4-8 and 4-9, respectively.

Conversion of propylene glycol increased with the reaction temperature. V_2O_3 showed moderate amount of propylene (with 32.9 % selectivity) and acetone (with 46.8 % selectivity) at 523 K. The selectivity to acetone increased to 58 % while the selectivity to propylene decreased to 18.3 % as the reaction temperature was increased to 573 K. On the other hand, selectivity to propionaldehyde was kept unchanged (16.7-19.5 %) in all reaction temperature range.

MoO_2 catalyst showed similar catalytic performance to V_2O_3. However, the selectivity to acetone did not change much with increase in reaction temperature as that observed with V_2O_3 catalyst. The conversion of propylene glycol was higher over MoO_2 than over V_2O_3 catalyst in the all reaction temperature range. The reaction temperature had no remarkable effect on the selectivity to

propionaldehyde as observed with V_2O_3 catalyst. On the other hand, the selectivity to propylene slightly decreased while the selectivity to acetone slightly increased with an increase of reaction temperature. The selectivity to acetone was lower over MoO_2 catalyst than that over V_2O_3 catalyst above 543 K, while the selectivity to propionaldehyde was slightly higher over MoO_2 catalyst than over V_2O_3 catalyst in all reaction temperature range. These result good correlate with the results of 2-propanol reaction over V_2O_3 and MoO_2 catalysts which higher selectivity to acetone and lower selectivity to propylene were observed on V_2O_3 catalyst compared with MoO_2 catalyst in the reaction of 2- propanol. Therefore, the active sites relevant to the formation of propionaldehyde and acetonesis in the reaction of propylene glycol are same with the formation of propylene and acetone in the reaction of 2-propanol. For the formation of propylene, almost the same selectivity was observed for V_2O_3 and MoO_2 catalyst. This is in contrast to the selectivity to propylene in the reaction of 2-propanol in which MoO_2 catalysts showed higher selectivity than V_2O_3 catalyst due to a higher acidity of MoO_2 as compare to V_2O_3 as discussed in chapter 3.

These results indicate that the mechanism for the formation of acetone was different from that of propionaldehyde. In the reaction of ethylene glycol, it can conclude that the reaction mechanism for the formation of ethylene (olefin) are different from that for the formation of acetaldehyde. Therefore, V_2O_3 and MoO_2 possess three types of active sites to form acetone, propionaldehyde and propylene.

4. 3. 5 The reaction of propylene glycol over various solid acid and base catalysts

In order to elucidate the relation between acid-base properties of catalysts and the product selectivity in the reaction of propylene glycol, various kinds of solid acid and base catalysts were used. The catalysts selected and results are summarized in Table 4-2. Zeolite, $Cs_{2.5}H_{0.5}PW_{12}O_{40}$,

W-Nb-O and Amberlyst-70 were used as solid acid catalysts. γ-Al_2O_3 is representative dehydration catalyst and possesses amphoteric property.

For all acid catalysts, the propionaldehyde was predominantly formed (76.8 - 81.6 % selectivity). Similar result was reported by Zhang et al. They studied that the dehydration of propylene glycol over various zeolite catalysts and reported that propionaldehyde was formed as a major product and acetone selectivity increased with the temperature but did not exceed 10 % over all kinds of zeolites [4]. Partially Cs^+ ion-exchanged dodecatungstophosphoric acid ($Cs_{2.5}H_{0.5}PW_{12}O_{40}$), which acted as heterogeneous catalysts and showed the highest catalytic acidity compared with other Cs contents catalysts in dehydration reaction, showed predominant formation of propionaldehyde with 81.5 % selectivity. We also investigated the W-Nb-O complex oxide catalyst, which also possesses strong acid sites and exhibits a high performance for conversion of glycerin to acrolein [13]. This catalyst led to a high selectivity to propionaldehyde of 80.0 %. Amberlyst-70 was reported to be active for the dehydration, and yield mainly acetol by dehydration of terminal hydroxyl group [14, 15]. Propylene glycol was selectively converted to propionaldehyde over Amberlyst-70. If terminate hydroxyl group of propylene glycol were dehydrated, acetone would have been formed as a main product. Although the formation of acetone was also observed for all the acid catalysts mentioned above, the selectivity was quite low (less than 7 %) compared with those observed for V_2O_3 and MoO_2 catalysts.

In general, secondary alcohols undergo dehydration more easily than primary alcohols by E1 elimination mechanism, because secondary carbocations are more stable than primary carbocations formed from primary alcohols. Therefore, the formation of propionaldehyde took place via dehydration of propylene glycol by E1 mechanism on acid catalysts. On the other hand, acetone was mainly formed (with 90.4 % selectivity) over γ-Al_2O_3 catalyst. The dehydration of alcohols over γ-Al_2O_3 is known to proceed by E2 mechanism, which occurs by the concerted interaction between

acid-base sites of catalyst and substrates [16]. The hydroxyl group acted as acid site on the surface of catalysts to interact with hydroxyl group of alcohols. Then β-hydrogen of alcohols is abstracted by the lattice oxygen acting as base sites. Therefore, dehydration of alcohols over γ-Al_2O_3 catalyst takes place through E2 elimination mechanism. The methyl hydrogen in propylene glycol is more easily abstracted by the lattice oxygen as a proton than methylene hydrogen in the E2 elimination mechanism, because the primary carbanion is more stable than the secondary carbanion. Therefore, the formation of acetone over γ-Al_2O_3 catalyst takes place via E2 mechanism.

There are a few papers reporting that dehydration of diol and triol as E2 mechanism. The dehydration of terminal hydroxyl group of glycerol to produce acetol occurred over Amberlyst-15 [14, 15], Cu-based and Ni based catalysts [17]. Because this reaction was carried out under H_2, acetol was observed in a quite low amount as an intermediate leading to the formation of propylene glycol. Miyazawa et al. reported that protons on Amberlyst-15 react the with terminal hydroxyl group of glycerol to produce propylene glycol However, the reasons why the protons do not attack the hydroxyl group on the center carbon were not explained [14, 15].

4. 3. 6 The reaction scheme for the formation of acetone and propionaldehyde in the propylene glycol reaction

For V_2O_3 and MoO_2 catalysts, the major product in the reaction of propylene glycol was acetone. In addition to acetone, propionaldehyde and propylene were formed to a considerable extent. The formation of propionaldehyde is suggested to take place on the weak acid sites of V_2O_3 and MoO_2 catalysts through E1 mechanism as described on the acid catalysts. Although the formation of acetone was observed as described on γ-Al_2O_3 catalyst, the reaction mechanism of acetone formation from propylene glycol over V_2O_3 and MoO_2 catalysts would be different from that on γ-Al_2O_3 catalyst. In the reaction of ethanol discussed in Chapter 3, γ-Al_2O_3 catalyst could not produce ethane

and acetaldehyde, but produced ethylene predominantly. On the other hand, V_2O_3 and MoO_2 catalysts could not produce much amount of ethylene, less than 3 % selectivity being observed for both catalysts. This result indicates that the active sites over V_2O_3 and MoO_2 catalysts differ from those on γ-Al_2O_3 catalyst. Therefore, the formation of acetone over V_2O_3 and MoO_2 catalysts is suggested not to take place via E2 mechanism. If the active sites on V_2O_3 and MoO_2 catalysts for the synthesis of acetone in the reaction of propylene glycol were the same as those on γ-Al_2O_3 catalyst, I could have observed the much amount of ethylene in the reaction of ethanol on V_2O_3 and MoO_2 catalysts. Therefore, it is speculated that acetone is formed through the intramolecular hydrogen-transfer dehydration of propylene glycol as shown in Scheme 4-2(a). Based on these results, dehydration of primary hydroxyl group is favorable in intramolecular hydrogen-dehydration of vicinal diols to form corresponding ketones.

4. 3. 7 The reaction scheme for the formation of olefins from vicinal diols

Moreover, corresponding of olefins were also formed in the reaction of vicinal alcohols (both ethylene glycol and propylene glycol) over V_2O_3 and MoO_2 catalysts. Recently, conversions of vicinal diols to corresponding olefins have attracted much attention because deoxygenation of oxygen-rich biomass derived compounds such as glycol and sugars into platform chemicals is one of the important issues in biomass chemistry. Re, V and Mo complexes as homogenous catalysts were reported to produce corresponding olefins in the conversion of vicinal alcohols via deoxydehydration [6-8]. This reaction was carried out in the presence of reductants, such as triphenylphosphine and sodium sulfite. These reports showed the reaction pathways for the formation of corresponding olefins. In the first and second steps, oxo-metal species in metal complexes (-M=O, M=Re, V) were reduced by reductatnt or interact with glycol to form glycolate. Finally, catalysts were reoxygenated via deoxygenation of glycolate. As a result, olefins and water were formed.

For the V_2O_3 and MoO_2 catalysts, the reaction pathway is shown in Scheme 4-3. The formation of olefins from vicinal alcohols involved the oxygenation of V_2O_3 and MoO_2 to produce VO_2 and MoO_3. The oxygen produced by deoxygenation of substrates is utilized for the oxygenation. For the regeneration of V_2O_3 and MoO_2, substrates or products act as reductants.

4. 4 Conclusion

The catalytic properties of V_2O_3 and MoO_2 in the reaction of vicinal diols are different from those of acidic catalysts. In the reaction of ethylene glycol, the products consisted of acetaldehyde and ethylene. In addition to acetaldehyde as a main product, ethylene was alsho produced to a considerable extent. The formation of ethylene has not been reported for the reaction over solid acidic catalysts. In the reaction of propylene glycol, considerable amounts of propylene and propionaldehyde in nearly 1 to 1 ratio were formed in addition to the main product acetone. The formation of considerable amounts of propylene and propionaldehyde has been reported neither for acidic catalysts not for the dehydration catalysts of γ-Al_2O_3.

The reaction mechanism are proposed for the formation of acetaldehyde in the reaction of ethylene glycol and the formation of acetone in the reaction of propylene glycol over V_2O_3 and MoO_2 catalysts. Intramolecular hydrogen-transfer dehydration is involved in the formation of both acetaldehyde from ethylene glycol and acetone from propylene glycol. Moreover, it is suggested that the mechanism for the formation of corresponding olefins from vicinal diols is involved in deoxydehydration of vicinal diols and redox of V_2O_3 and MoO_2 catalysts.

4. 5 References

[1] A. Yamaguchi, N. Hiyoshi, O. Sato, C. V. Rode, M. Shirai, *Chem. Lett*. 37 (2008) 926-927.

[2] M. Balaraju, V. Rekha, P. S. S. Prasad, B. L.A. P. Devi, R.B.N. Prasad, N. Lingaiah, *Appl. Catal. A* 354 (2009) 82-87.

[3] M. A. Dasari, P. P. Kiatsimkul, W. R. Sutterlin, G. J. Suppes, *Appl. Catal. A* 281 (2005) 225-231

[4] D. Zhang, S. A. I. Barri, D. Chadwick, *Appl. Catal. A* 400 (2011) 148-155.

[5] T. D. Courtney, V. Nikolakis, G. Mpoirmpakis, J. G. Chen, D. G. Vlachos, *Appl. Catal. A* 449 (2012) 59-68.

[6] G. Chapman Jr. K. M. Nichola, *Chem. Commun*, 49 (2013) 8199-8201.

[7] J. R. Dethlefsen, D. Lupp, B. C. Oh, P. Fristrup, *ChemSusChem*, 7 (2014) 425-428.

[8] S. Vkuturi, G. Chapman, I. Ahmad, K. M. Nicholas, *Inorg.Chem*. 49 (2010) 4744-4746.

[9] J. G. Serafin, C. M. Friend, *J. Am. Chem. Soc*, 111 (1989) 6019-6926.

[10] D. G. Lee, S. Helliwell, V. S. Chang, *J. Org. Chem*. 41 (1976) 3647-3648.

[11] (a) F. Dury, V. Misplon, E. M. Gaigneaux, *Catal. Today*. 111-116 (2004) 91-92, (b) F. Dury, E. M. Gaigneaux, *Catal. Today*. 117 (2006) 46-52.

[12] K. G. Moloy, *Inorg. Chem*. 27 (1988) 677-681.

[13] K. Omata, S. Izumi, T. Murayama, W. Ueda, *Catal. Today* 201 (2013) 7– 11.

[14] (a) T. Miyazawa, S. Koso, K. Kunimori and K. Tomishige, *Appl. Catal., A*, 329 (2007) 30–35, (b) Y. Nakagawa, K. Tomishige, *Catal. Sci. Technol.* 1 (2011) 179–190.

[15] (a) T. Miyazawa, Y. Kusunoki, K. Kunimori, K. Tomishige, *J. Catal.* 240 (2006) 213-221, (b) T. Miyazawa, S. Koso, K. Kunimori, K. Tomishige, *Appl. Cata .A* 329 (2007) 30-35.

[16] S. Roy, G. Mpourmpakis, D. Y. Hong, D. G. Vlachos, A. Bhan, R. J. Gorte, ACS Catal. 2 (2012) 1846-1853.

[17] S. Wang, H. Liu, Catal. Lett. 117 (2007) 62-67.

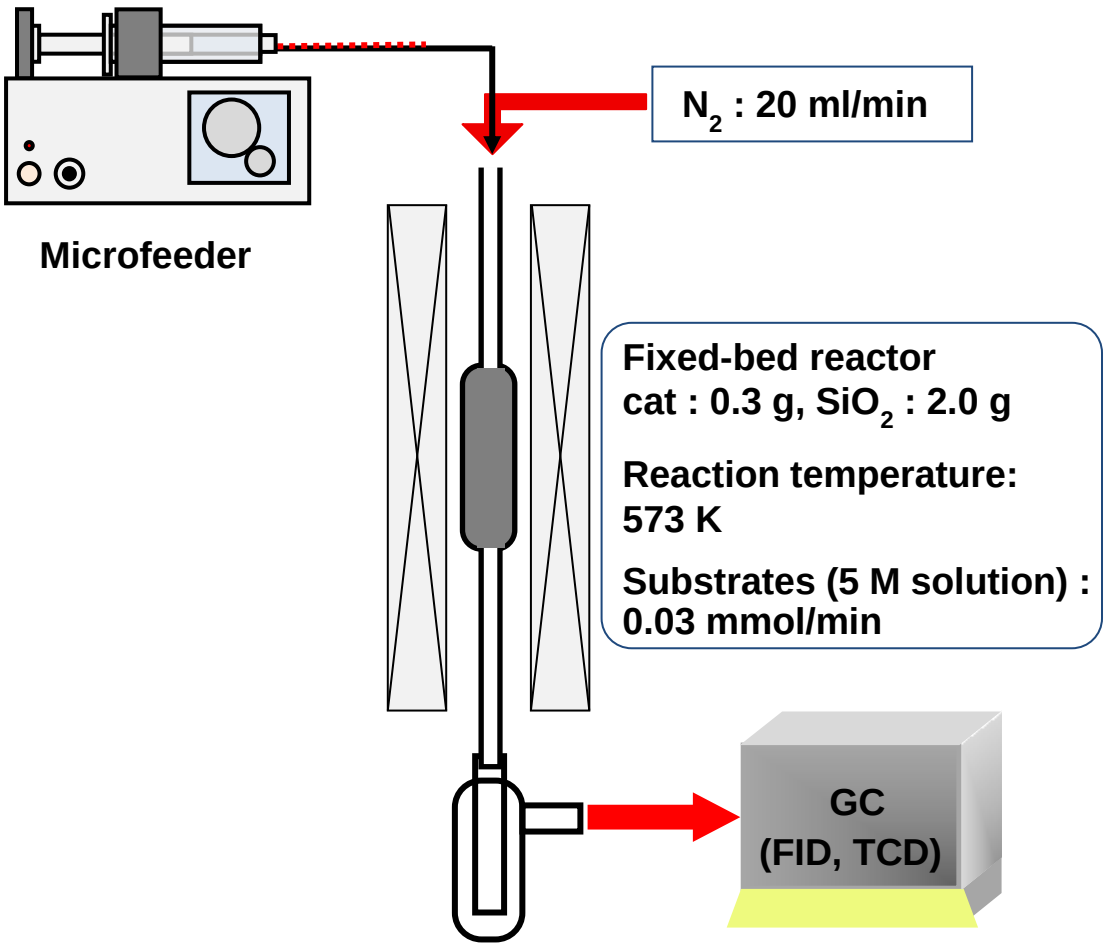

Fig. 4-1 Catalytic reaction system for the reaction of vicinal diols.

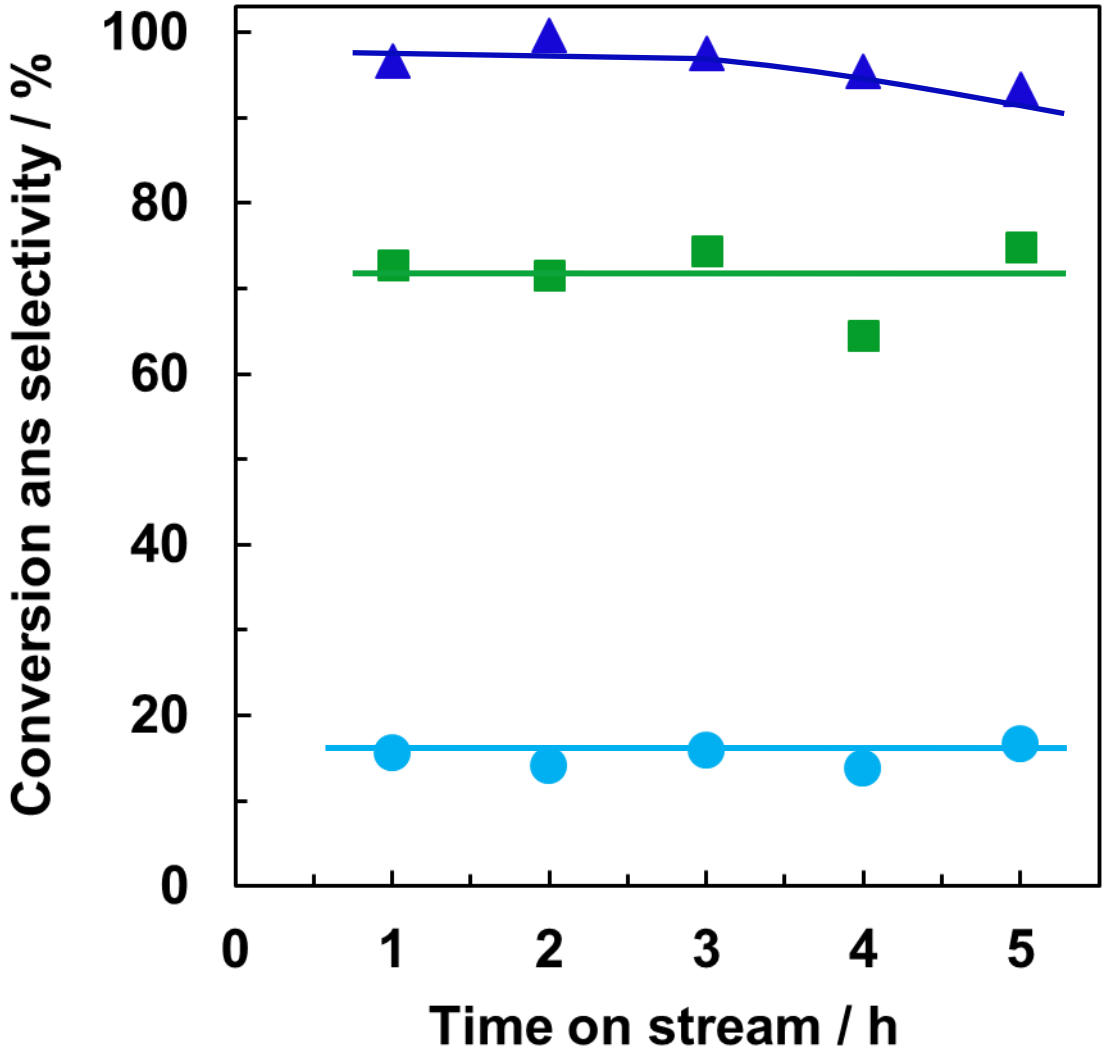

Fig. 4-2 Ethylene glycol reaction over V_2O_3 under N_2. V_2O_3 0.30g, SiO_2 2.0 g, 573 K, flow rate : N_2 20 ml/min (0.89 mmol/min), ethylene glycol 0.03 mmol/min, (▲) conversion of ethylene glycol, selectivity to (●) ethylene, (■) acetaldehyde

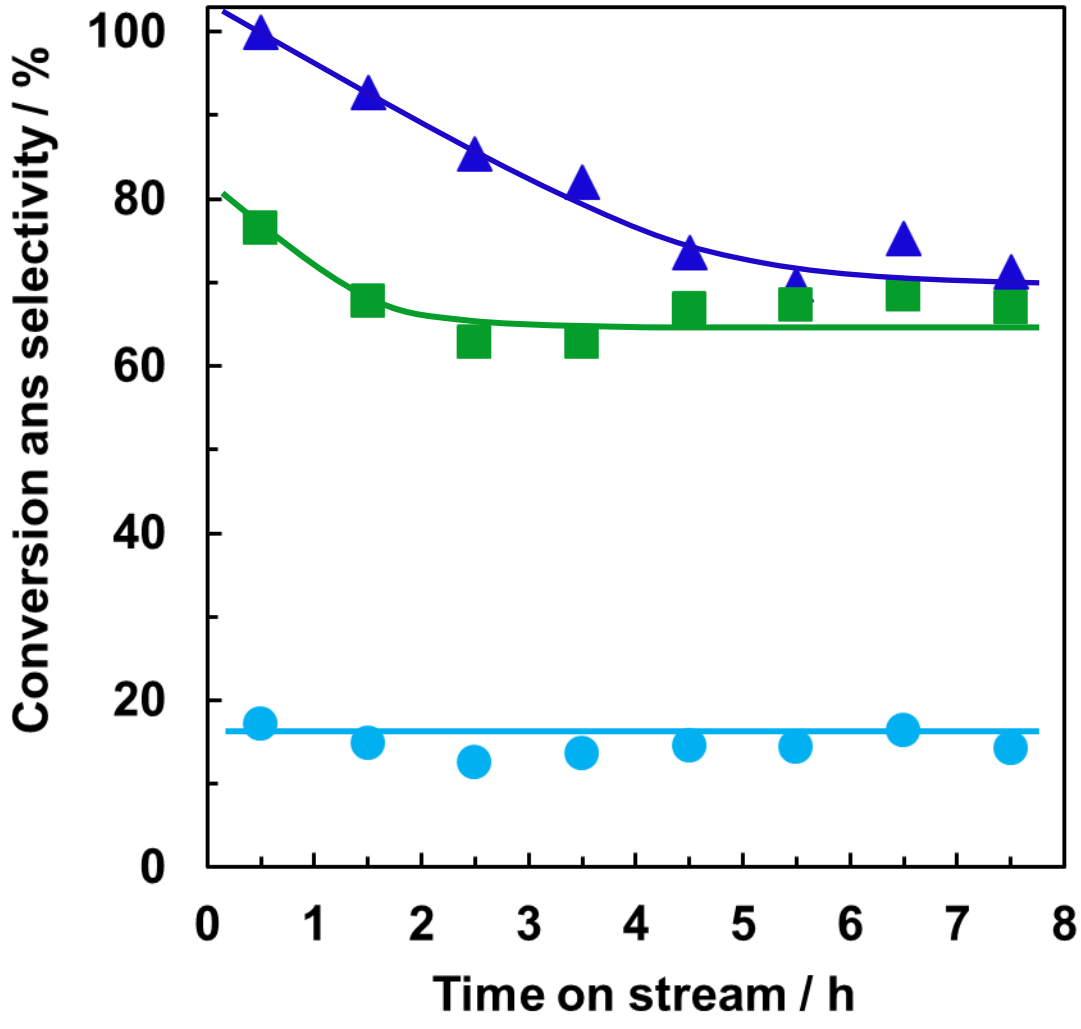

Fig. 4-3 Ethylene glycol reaction over MoO_3 under N_2. MoO_2 0.30g, SiO_2 2.0 g, 573 K, flow rate : N_2 20 ml/min (0.89 mmol/min), ethylene glycol 0.03 mmol/min, (▲) conversion of ethylene glycol, selectivity to (●) ethylene, (■) acetaldehyde

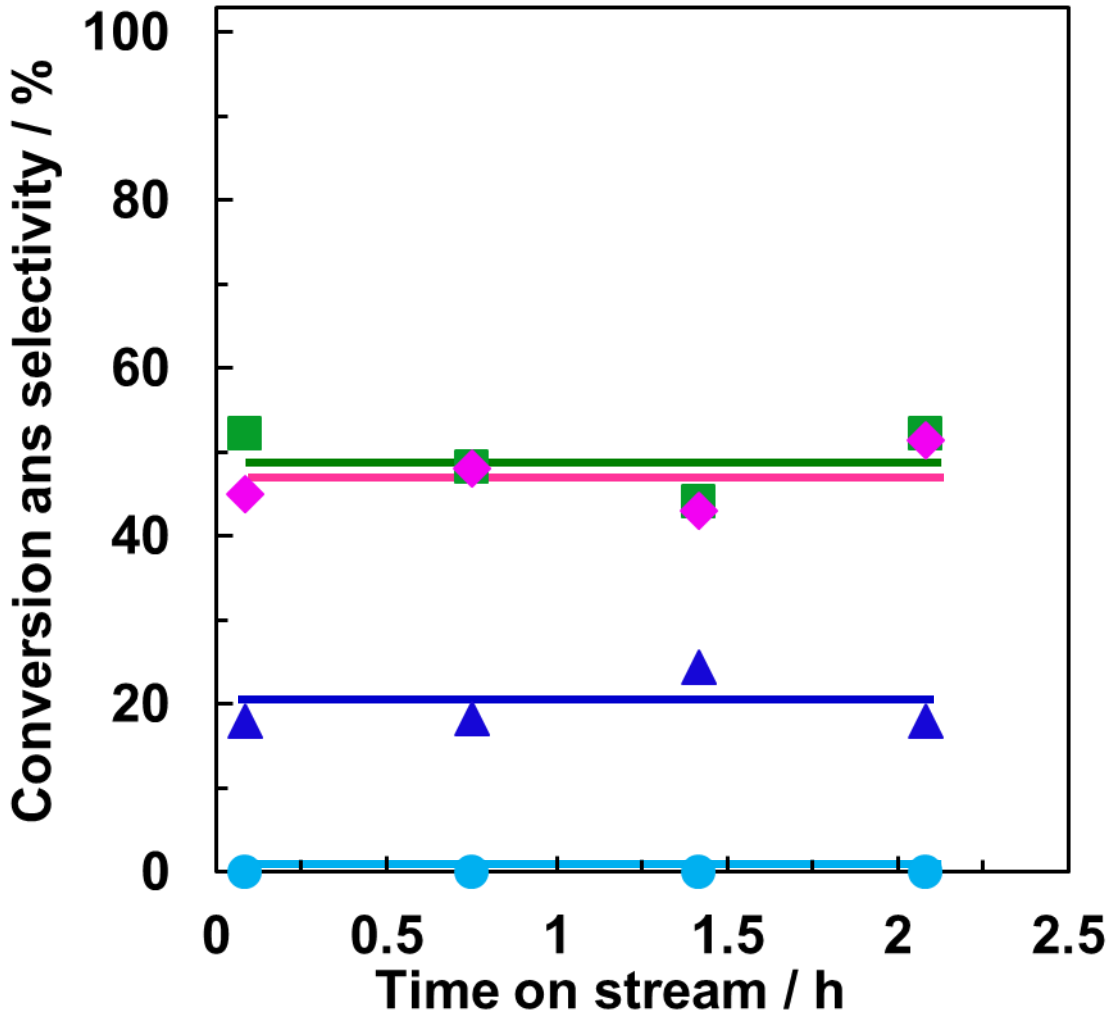

Fig. 4-4 Ethylene glycol reaction over MoO_3 under N_2. MoO_2 0.30g, SiO_2 2.0 g, 573 K, flow rate : N_2 20 ml/min (0.89 mmol/min), ethylene glycol 0.03 mmol/min, (▲) conversion of ethylene glycol, selectivity to (●) ethylene, (■) acetaldehyde

Table 4-1

Rates for the formation of products and the consumption of substrate in ethylene glycol reaction over V_2O_3 and MoO_2 catalysts.

Catalysts	Reaction temp. (K)	Rate of substrate consumption (μmol g^{-1} min^{-1})	Rate of products formation (μmol g^{-1} min^{-1})	
			C_2H_4	
V_2O_3	573	96.5	14.2	70.3
MoO_2	573	74.8	12.3	50.0

Cat. 0.3g, SiO_2 2.0g, time on stream of 4.5 h N_2 20 ml/min (0.89 mmol/min), propylene glycol 0.03 mmol/min

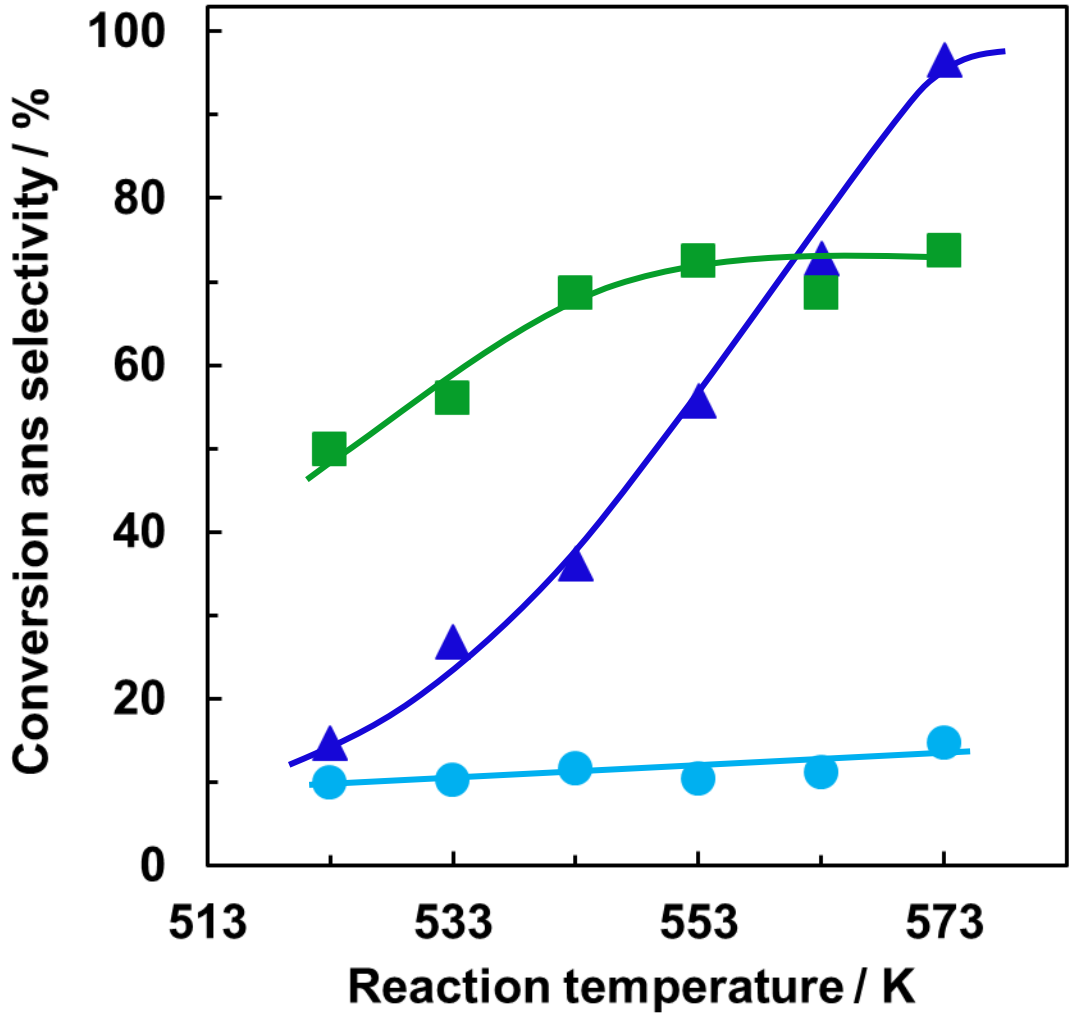

Fig. 4-5 Effect of the reaction temperature on ethylene glycol reaction over V_2O_3 under N_2. V_2O_3 0.30g, SiO_2 2.0 g, 3 h time on stream, flow rate : N_2 20 ml/min (0.89 mmol/min), ethylene glycol 0.03 mmol/min, (▲) conversion of ethylene glycol, selectivity to (●) ethylene, (■) acetaldehyde

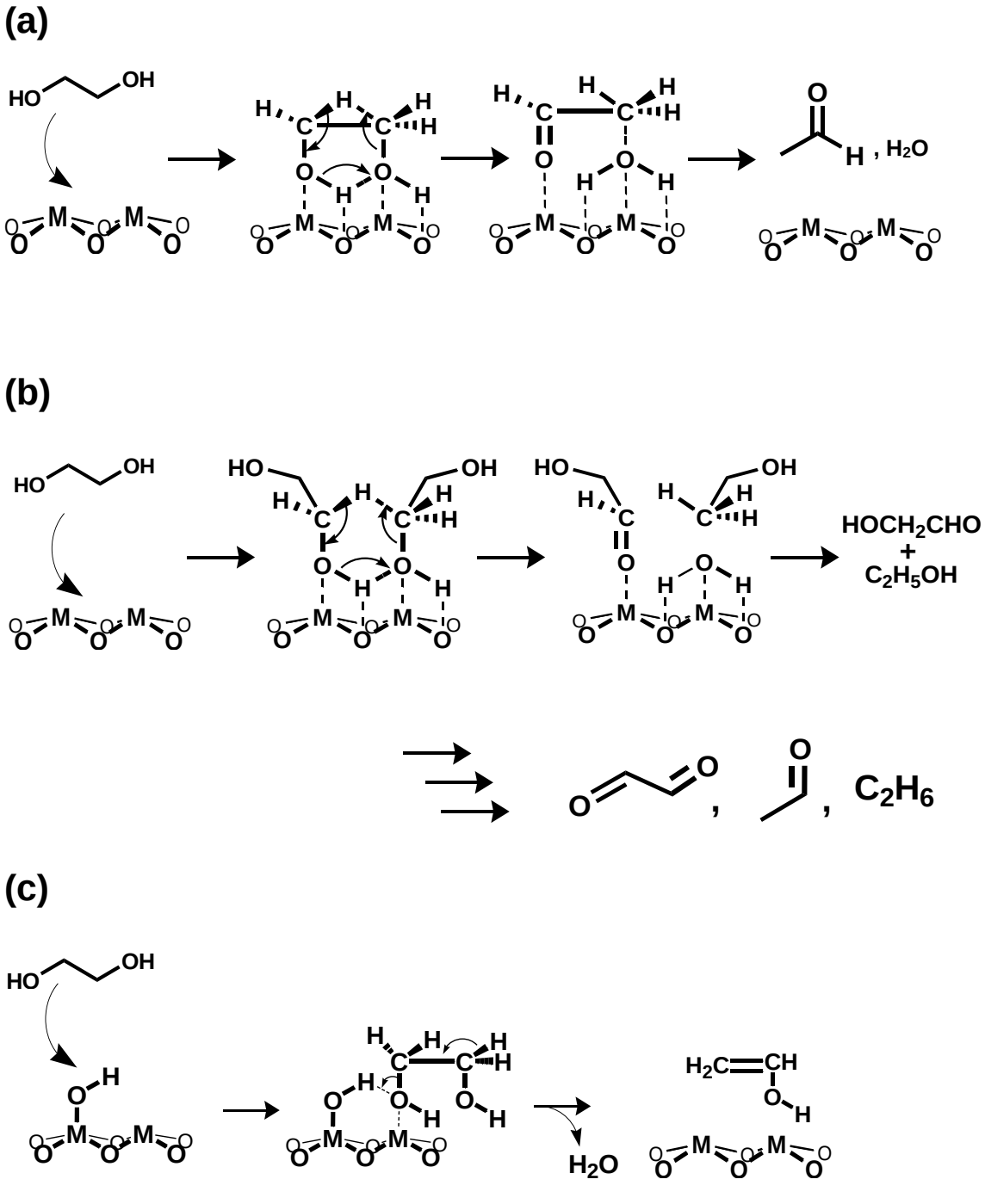

Scheme 4-1 Reaction scheme for the formation of acetaldehyde from ethylene glycol. (a) Intramolecular hydrogen-transfer reaction, (b) intermolecular hydrogen-transfer reaction, (c) dehydration of ethylene glycol.

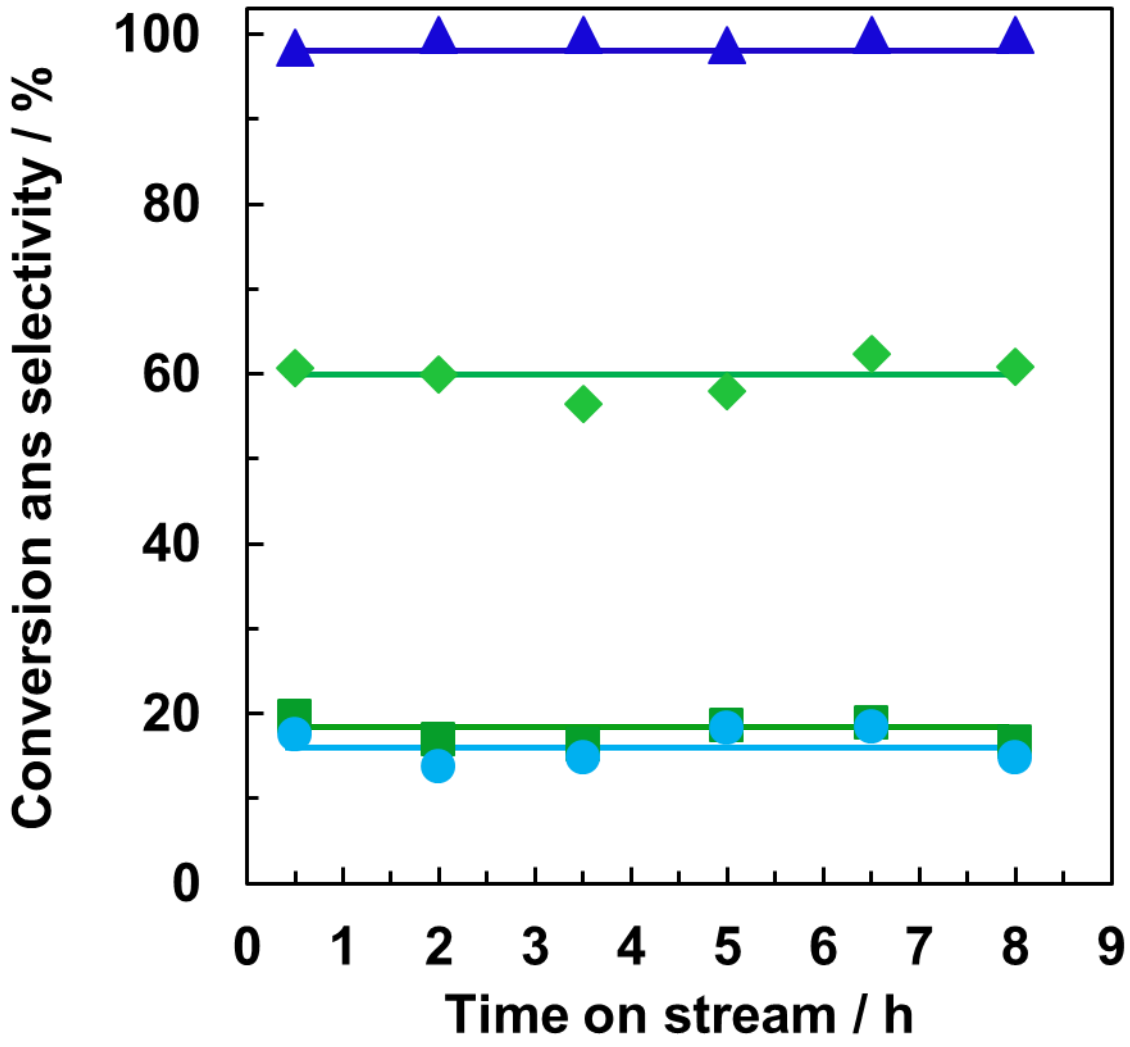

Fig. 4-6 Propylene glycol reaction at 573 K over V_2O_3 under N_2. V_2O_3 0.30g, SiO_2 2.0 g, flow rate : N_2 20 ml/min (0.89 mmol/min), propylene glycol 0.03 mmol/min, (▲) conversion of propylene glycol, selectivity to (●) propylene, (◆) acetone, (■) propionaldehyde

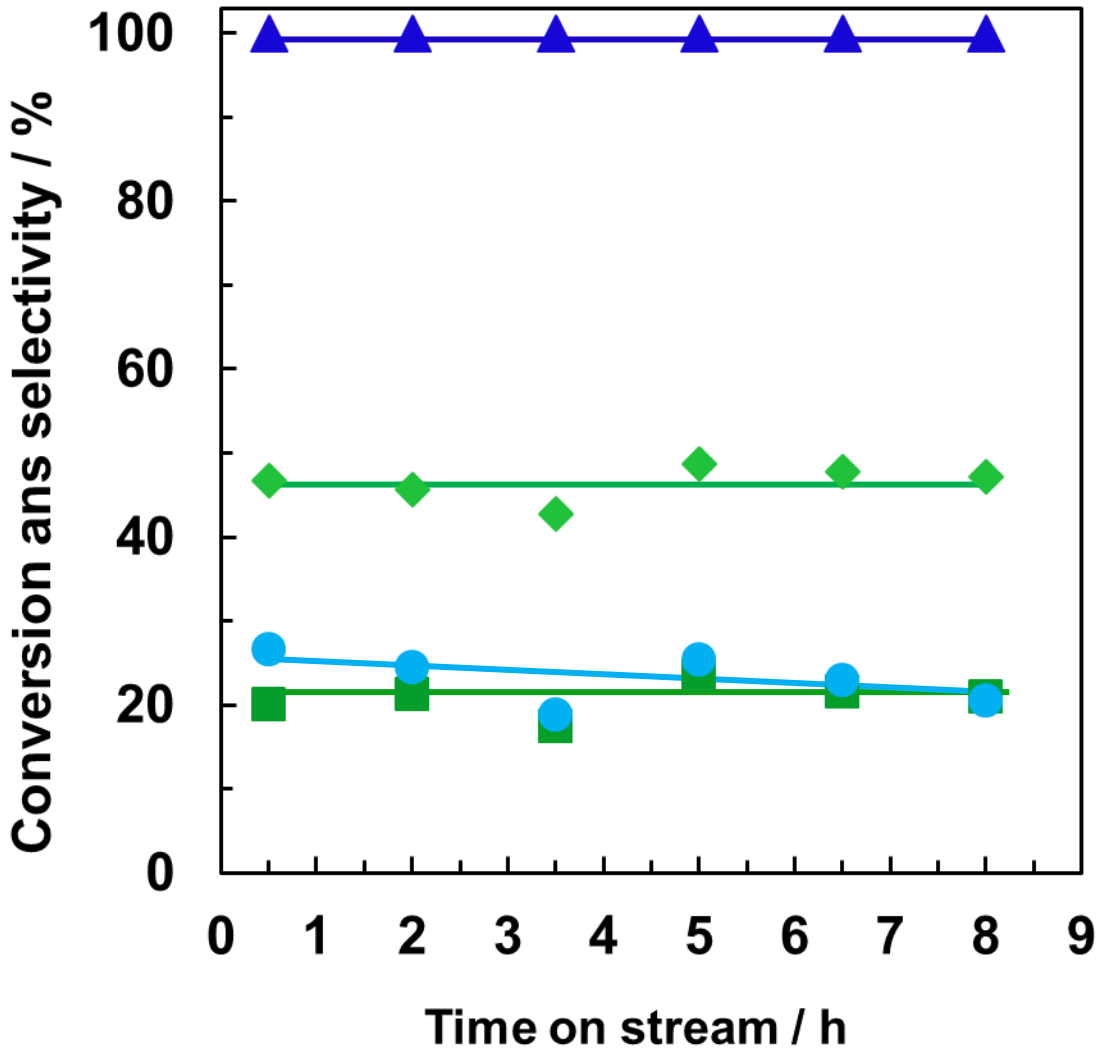

Fig. 4-7 Propylene glycol reaction at 573 K over MoO_2 under N_2. MoO_2 0.30g, SiO_2 2.0 g, flow rate : N_2 20 ml/min (0.89 mmol/min), propylene glycol 0.03 mmol/min, (▲) conversion of propylene glycol, selectivity to (●) propylene, (◆) acetone, (■) propionaldehyde

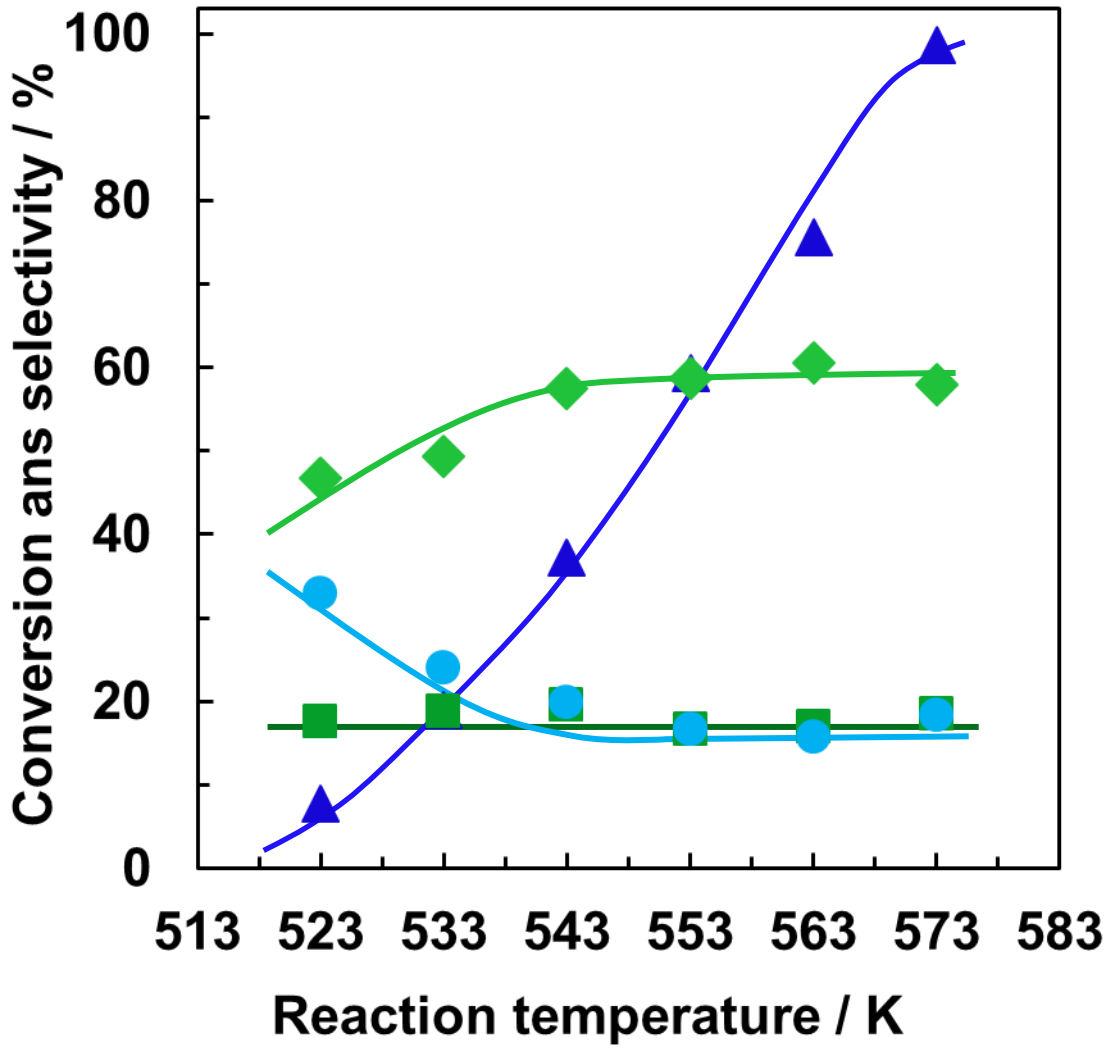

Fig. 4-8 Propylene glycol reaction over V_2O_3 under N_2. V_2O_3 0.30g, SiO_2 2.0 g, flow rate : N_2 20 ml/min (0.89 mmol/min), time on stream of 3 h, propylene glycol 0.03 mmol/min, (▲) conversion of propylene glycol, selectivity to (●) propylene, (◆) acetone, (■) propionaldehyde

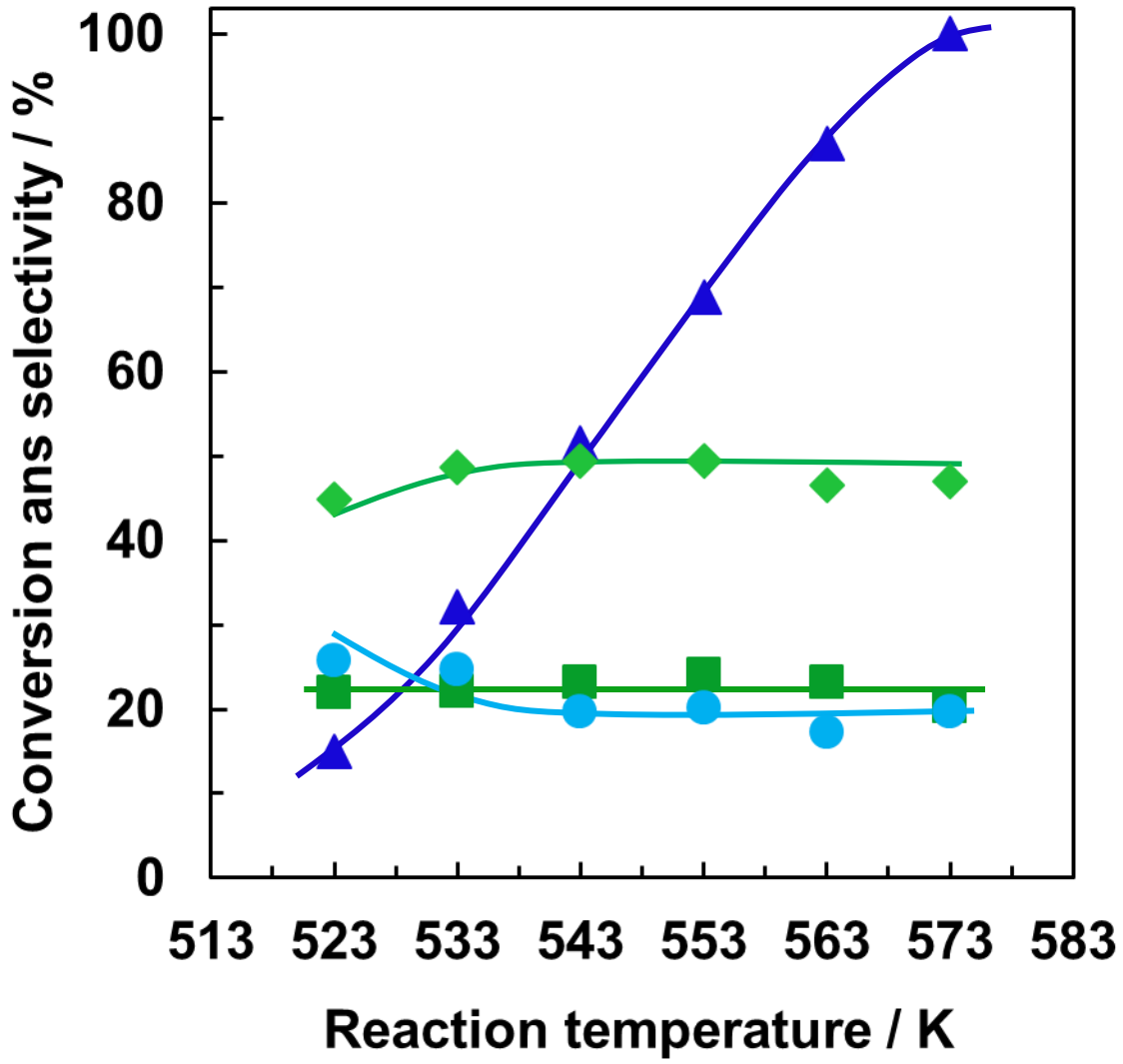

Fig. 4-9 Propylene glycol reaction over MoO_2 under N_2. MoO_2 0.30g, SiO_2 2.0 g, flow rate : N_2 20 ml/min (0.89 mmol/min), time on stream of 3 h, propylene glycol 0.03 mmol/min, (▲) conversion of propylene glycol, selectivity to (●) propylene, (◆) acetone, (■) propionaldehyde

Table 4-2

The comparison of the product distribution in propylene glycol reaction over V_2O_3, MoO_2 and other acid catalysts.

Catalysts	Reaction temp. / K	Conv. / %	Selectivity / %				
			CO_2	C_3H_6			Others
V_2O_3	563	76	< 1	16.6	17.7	58.7	0.5
MoO_2	563	87	< 1	20.1	24.1	49.5	12.2
V_2O_5[1)]	523	82	3.3	< 1	80.7	4.0	11.8
MoO_3[1)]	523	100	< 1	18.3	72.0	5.1	4.6
JRC-5Z-90H (Zeolite) [2)]	473	87	< 1	< 1	76.8	1.9	21.3
$Cs_{2.5}H_{0.5}PW_{12}O_{40}$ [3)]	523	100	< 1	< 1	81.5	< 1	18.0
W-Nb-O[2)]	573	100	< 1	1.5	80.0	6.5	< 12
Amberlyst-70[3)]	473	96	< 1	< 1	81.6	< 1	< 19
γ-Al_2O_3	473	51	< 1	—	4.9	90.4	< 5

Cat. 0.3g, SiO_2 2.0g, time on stream of 4.5 h N_2 20 ml/min (0.89 mmol/min), propylene glycol 0.03 mmol/min

[1)] time stream of 0.5 h

[2)] Cat. 0.15 g

[3)] Cat. 0.05 g

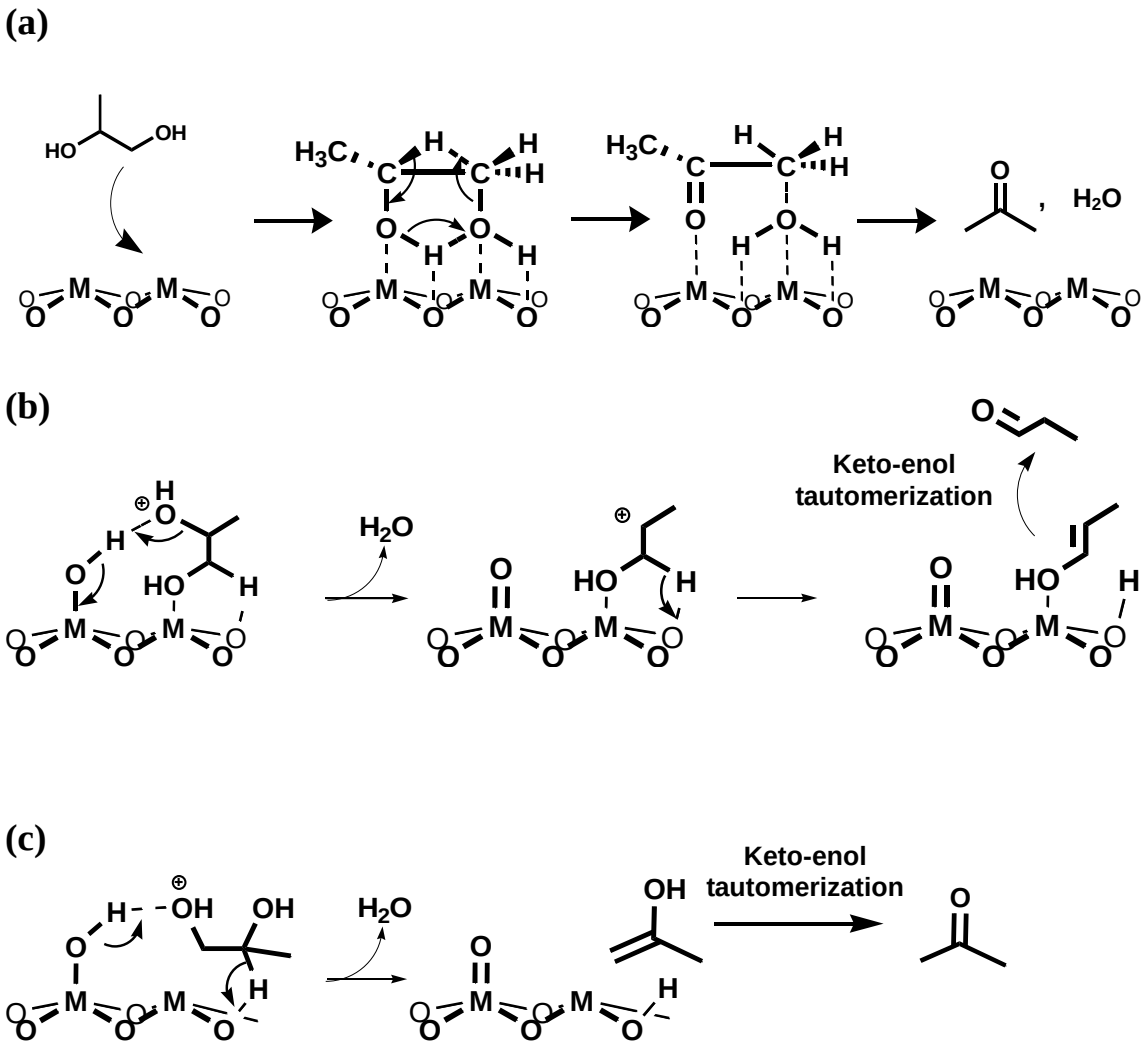

Scheme 4-2. Reaction mechanism of propylene glycol reaction over solid acid-base catalysts. (a) Intramolecular hydrogen-transfer reaction, (b) E1 mechanism, (c) E2 mechanism

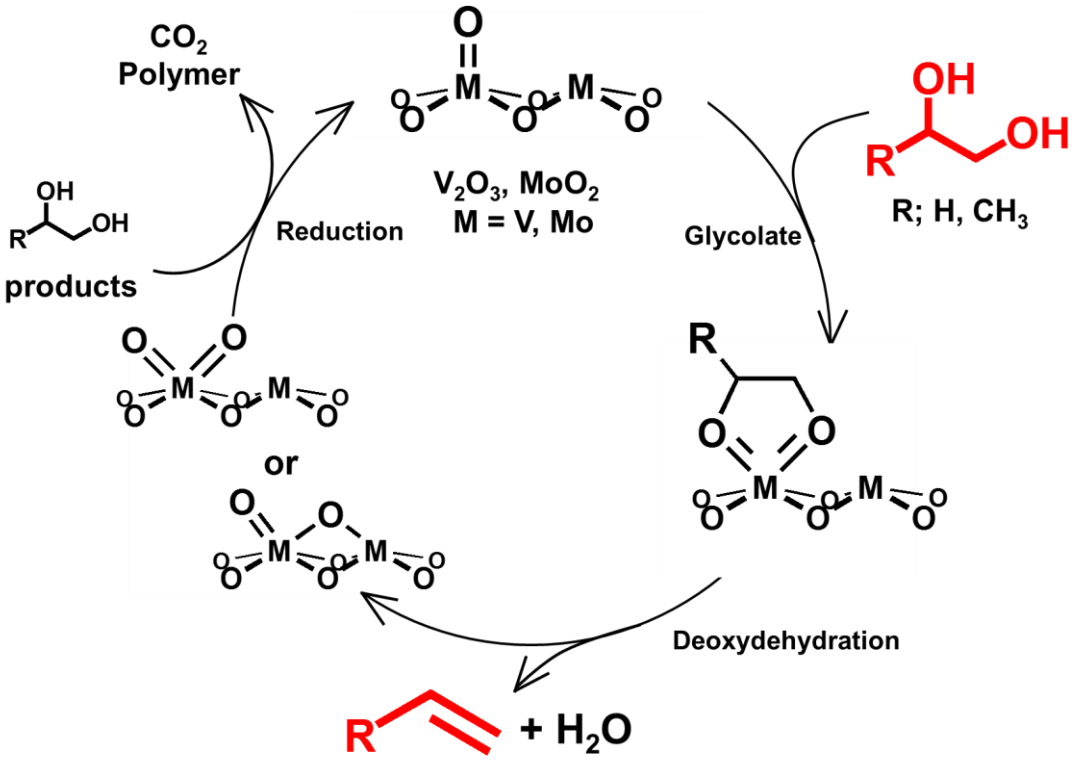

Scheme 4-3. Proposed reaction scheme for formation of corresponding olefins in the reactions of vicinal alcohols over V_2O_3 and MoO_2 catalysts.

Chapter 5
Selective synthesis of primary amines by reductive amination of ketones with ammonia over MoO_2/TiO_2 supported Pt catalyst

5. 1 Introduction

Amination of aldehydes and ketones is common way to produce primary, secondary and tertiary amines, and has been widely investigated [1] because alkyl amines are very important intermediates in the fine- and bulk- chemical industries as fundamental building blocks for production of polymers [2]. The reductive amination of carbonyl compounds is one of the most practical methods of C-N bond formation from carbonyl compounds [2-6].

The reductive amination of alcohols and carbonyl compounds with amines to produce secondary and tertiary amines has been widely studied over various catalysts. However, there are a few reports for synthesis of primary amines over heterogeneous catalysts. Potentially, aliphatic primary amines can be synthesized by the reductive amination of carbonyl compounds with NH_3 and H_2, even though the controlling the selectivity for primary amines are very difficult because primary amines are more reactive than ammonia, resulting in the conversion of primary amines to secondary and tertiary amines [7-11].

Many different transition metal complexes as homogenous catalysts were reported for synthesis of primary amines by amination with NH_3 under mild conditions [12-20]. Fukuzumi showed reductive amination of carbonyl compounds with NH_3 over iridium complex catalysts for the first time to. Ir complex as homogeneous catalysts can produce secondary and tertiary amines in the amination of various alcohols with aqueous ammonia, however, the formation of primary amines has not been reported [12]. Gunanathan et al. [13] and Ye et al. [14] reported for the first time that Ru PNP pincer complex exhibited high yields for primary amines in the amination of alcohols with ammonia, although this catalysts were inactive for secondary alcohols. Beller's group also showed that Rh-catalysts in water-soluble phosphine and ammonia acetate system exhibited high yield for benzyl amines [15], and Ru complex with phosphine ligands could produce relatively high yields of the primary amines in amination of secondary alcohols with ammonia [16]. However, these complexes

act as homogenous catalysts and possess several disadvantages such as the separation of catalyst from reactant solution and low reusability. Recently reported homogeneous methods for the selective synthesis of primary amines from ketones with NH_3 did not use H_2 but used less atom-efficient reductants such as HCO_2NH_4 [12], the Hantzsch ester [17], silnae [18] and $NaBH_4$ [19].

Ni-supported catalysts showed high yields for primary amines in amination of alcohols with ammonia and Lewis acidity of support affected the formation of primary amines [20]. For amination of aldehydes with NH_3 using H_2 as a reductant, most of the methods with heterogeneous catalysts produce secondary amines. Raney Ni was used for the synthesis of primary and secondary amines through amination of aldehydes with ammonia, and primary amines were mainly produced in the amination of aldehydes with equimolar ammonia [21].

Nobel metal supported materials were widely used as heterogeneous catalysts for the amination of aldehydes with ammonia [22-25]. Pt nanowire showed the highest selectivity to dibenzyl amine as compared with Pt nanorods and nanoparticles, but all of the Pt catalysts exhibited low selectivity to benzyl amines less than 21 % [22]. Peter's group reported Pd/C and Ru/C catalysts for the reductive amination of benzaldehyde with ammonia solutions [23-25]. In this report, Pd/C exhibited a low selectivity for benzyl amines (35 %) under a high ammonia concentration (molar ratio NH_3/benzaldehyde = 16), while Ru/C showed the predominant formation of benzyl amine (over 77 % selectivity) regardless of NH_3 concentration [25]. However, these catalysts have drawbacks such as limited substrate scope (no example for aliphatic aldehydes) and requirement of high hydrogen pressure (20 – 100 bar) for the reductive amination. Therefore, the selective synthesis of primary amines by reductive amination of ketones is more challenging.

Cu- and zeolite-based heterogeneous catalysts were reported to show a low selectivity for primary amines in amination of ketones with NH_3 and H_2 [26, 27]. In the amination of carbonyl compounds over Hβ and HY zeolites exhibited more than 90 % selectivity for dicyclohexylamine while the

selectivity to cyclohexyl amine was less than 20 % through amination of cyclohexanone with ammonia in the presence of hexanol [28].

To the best of our knowledge, there are no reports for the effective heterogeneous catalysts to produce primary amines as main products in the reductive amination of ketones with NH_3. Pt-MoO_x/TiO_2 catalyst showed high catalytic activity for reductive amination of levulinic acid with amines, which was attributed to Lewis acidity on transition metal acted as effective promoters for the reduction of C = O bonds [29].

In the present study, we report the reductive amination of various ketones with ammonia over Pt-MoO_x/TiO_2. Pt-MoO_x/TiO_2 exhibited a good yield for the corresponding primary amines under relatively mild condition. The role of MoO_x/TiO_2 was investigated by IR analysis in the reductive amination of ketones with ammonia. This is the first time to report that primary amines are mainly formed in the reductive amination of ketones with ammonia over heterogeneous catalysts under mild condition.

5. 2 Experimental

5. 2.1 Catalyst preparation

Commercially available organic and inorganic compounds (from Tokyo Chemical Industry, Wako Pure Chemical Industries, Kishida Chemical, or Mitsuwa Chemicals) were used without further purification.

The procedures for the preparation of catalysts were followed by the report in [29, 30]. Pt(5)-MoO_3(7)/TiO_2 was prepared by sequential impregnation method. The preparation of MoO_3-loaded TiO_2 as precursor material in the first step was follows; TiO_2 (5g), $(NH_4)_6Mo_7O_{24}$·$4H_2O$ (0.88 mmol) and citric acid (0.88 mmol) were added to 50 ml H_2O, then evaporated at 50 °C.

After drying the precursor sample at 90℃ for overnight, precursor samples was calcinated in air at 350 ℃ for 2 h. MoO_3-loaded TiO_2 was immersed in an aqueous HNO_3 solution of $(Pt(NH_3)_2(NO_3)_2$ with desired amount, subsequently the sample was evaporated at 50 ℃ and dried at 90℃ for overnight.

5. 2. 2 Catalytic tests

Typically, 5 wt% Pt-7wt%MoO_3/TiO_2 (Pt(5)-MoO_3(7)/TiO_2) was put into the test tube and closed with septum inlet, then air in the glass tube was replaced by nitrogen (10 ml/min) for 5min and hydrogen (20 ml/min) for 5min. Catalyst was reduced at 300 ℃ under hydrogen (20 ml/min) for 30 min. After reduction of catalysts, catalysts was cooled to room temperature under hydrogen, followed by injection of the mixtures of substrates (1.0 mmol), dodecane (0.5 mmol) as internal standard and *o*-xylene (3.0 ml) to the reduced catalysts inside the glass tube through the septum inlet as shown in Fig. 5-1. The septum inlet was removed then magnetic stir was put into the glass tube under air. Glass tube puts into the stainless steel autoclave with a dead space of 33 cm^3. Subsequently, gas in stainless steel autoclave was purged by flushing of NH_3, then 4 bar NH_3 and 2 bar H_2 were filled into the stainless steel autoclave. The reactor was heated at 80-150 ℃ under stirring (300 rpm). The amount of NH_3 and H_2 present in the reactor before heating was 4.0 mmol and 2 mmol (4.0 equiv. and 2.0 equiv. with respect to the ketones).

Conversion and yields of products were determined by GC using n-dodecane as an internal standard. The products were identified by GC-MS equipped with the same column as GC and by comparison with commercially pure products.

5. 2. 3 Characterization (In situ IR)

In situ IR measurement was carried out at 40 ℃ with a JASCO FT/IR-4200 with an

MCT detector. The sample was pressed into a 30 mg self-supporting wafer (ϕ = 2 cm) and mounted into the quartz IR cell (CaF_2 windows) connected to a conventional flow reaction system. For a wafer of Pt/carbon, 15 mg of Pt/carbon mixed with 15 mg of KBr was used. Spectra were measured accumulating 15 scans at a resolution of 4 cm^{-1}. A reference spectrum of the catalyst wafer in He taken at 40 °C was subtracted from each spectrum. Prior to the experiment, the catalyst wafer was heated in H_2 flow (20 ml/ min) at 300 °C for 0.5 h, followed by cooling to 40 °C and purging with He. Then, 1 μL of acetone was injected to He flow preheated at 150 °C, which was fed to the IR cell. Then, the IR disk was purged with He for 500 s, and IR measurement was carried out.

5. 3 Results and discussion

5. 3. 1 Reductive amination of 2-adamantanone with ammonia over various supported Pt catalysts

The effect of support was investigated for the reductive amination of 2-adamantanone with NH_3. The products distribution for the corresponding primary amine (2a), alcohol (3a) and secondary amine (4a) in the amination of 2-adamantanone over various Pt supported catalysts (Pt(5)/M, M = MoO_3(7)/TiO_2, TiO_2, Nb_2O_5, θ-Al_2O_3, ZrO_2, SiO_2, MgO, CeO_2, ZSM-5 and Carbone) is summarized in Table 5-1. All of these catalytic system were carried out under the same conditions (Pt = 0.5 mol % respect to 2-adamantanone T = 373 K, 20 h). Catalytic reaction was carried out under 0.3 MPa NH_3 and 0.1 MPa H_2 using o-xylene as solvent because o-xylene showed the highest yield for benzyl amine in the reductive amination of benzladehyde with 25 % aqueous ammonia solution among other solvents (methanol, ethanol, water, n-heptane, toluene, dioxane, m- and p-xylene) [22]. Touchy et al. discussed the structure of Pt(5)-MoO_x(7)/TiO_2 catalyst [30]. MoO_x in Pt(5)-MoO_x(7)/TiO_2 were reduced to MoO_2 based on the XPS measurement. Moreover, the

dominant Pt species in Pt(5)-MoO_x(7)/TiO_2 were shown to be Pt metal nanoparticles with average size of 4.1 nm based on the results of temperature-programmed reduction in H_2, X-ray adsorption spectroscopy, and CO adsorption. Pt(5)-MoO_x(7)/TiO_2 exhibited the highest catalytic activity for the formation of 5-methyl-1-octyl-purrolidine-2-one in the amination of levulinic acid with ammonia amoung Pt-M^1O_x/M^2O_x catalysts (M^1 = Mo, V, W, Re, Cr, M^2O_x = Ti, Al, Zr, Si). Pt supported catalysts as shown in Table 5-1, MoO_3(7)/TiO_2 as support showed the highest yield for 2-adamantlyamine (75 %), while other Pt supported catalysts exhibited moderate yield for 2-adamantlyamine (40-60 %). Tertiary amines may be formed in this reaction, but they could not be detected by GC with Ultra ALLOY capillary column UA^+-5. As for the catalysts which produced relatively high yield of 2-adamantylamine (over 50 % yield), support materials (TiO_2, ZrO_2, θ-Al_2O_3 and Nb_2O_5) were reported to act as Lewis acid catalyst. Therefore, Lewis acid sites would play an important role for the formation of primary amines in the reductive amination of ketones with ammonia.

5. 3. 2 IR measurement for the acetone adsorbed on catalysts

In order to evaluate the active site on catalysts, we measured IR of adsorbed acetone as model compound of ketone. Fig.5-2 showed that the C=O stretching band region of the acetone adsorbed on catalysts. For acetone adsorbed on Pt-MoO_x/TiO_2, Pt-/Nb_2O_5, Pt-/θ-Al_2O_3, Pt/ZrO_2 and Pt/TiO_2 which showed relatively high yield for primary amine, the C=O stretching band of acetone adsorbed on catalysts were centered at lower wavenumber region. This result indicates that ketones are strongly interacted with Lewis acid sites on the active catalysts. C=O stretching band of the acetone adsorbed on Pt(5)-MoO_3(7)/TiO_2 and Pt(5)/Nb_2O_5 were centered at lower wavenumber (ν = 1691 cm^{-1}) than that on Pt/Carbon (ν = 1740 cm^{-1}, 1710 cm^{-1}) and other Pt supported catalysts (ν =

1696-1710 cm^{-1}), suggesting that carbonyl are more activated on Lewis acid sites of Pt(5)-MoO_3(7)/TiO_2 and Pt(5)/Nb_2O_5 catalysts compared with other Pt supported catalysts.

The tendency of catalytic activity for the formation of primary amine in the reductive amination of 2-adamantanone with ammonia was correlated with Lewis acidity of catalysts. The yield of 2-adamantyl amine as a function of the wavenumber of C=O adsorbed on catalysts is shown in Fig.5-3. The linearly correlation between yield for 2-adamantyl amine and wavenumber of acetone adsorbed on catalysts was observed. The yield for 2-adamantyl amine increased with a decrease of the wavenumber for C=O stretching band of the acetone adsorbed on catalysts, suggesting that strong interaction of ketones and Lewis acid sites led to the high yield for the formation of primary amines. Therefore, this reaction is required Lewis acid sites of the support material to active C=O bond to produce amines as main products.

The formation of imines is known as intermediate to produce amines in the amination of alcohols, aldehydes and ketones. Then, imines are hydrogenated to produce the corresponding amines (Shceme 1). Assuming this pathway, we can propose two possible role of the Lewis acid; it can promote the formation of the imines and/or the reduction of the imine via Lewis acid activation of C=O or C=N group.

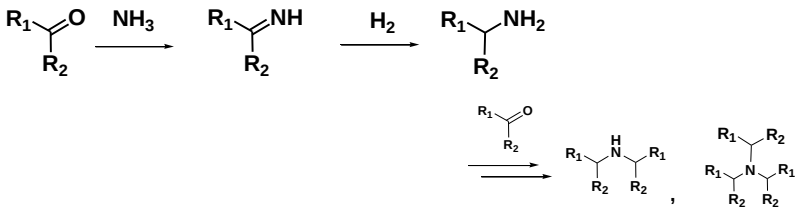

Scheme 1. Reaction pathway for the formation of primary amines in the reductive amination of ketones with ammonia.

However, the formation of imine was not detected in the reductive amination of 2-adamantanone over Pt supported catalysts. This result indicates that the rate of imines formation from ketones with ammonia is much slower than hydrogenation of imines. Therefore, the rate controlling step in the formation of primary amines reaction is the formation of imines and Lewis acid sites affect this step.

In spite of the same wavenumber of the C=O stretching of acetone adsorbed on Pt(5)-MoO_x(7)/TiO_2 and Pt(5)/Nb_2O_5, the catalytic activity for the formation of primary amine over Pt(5)-MoO_x(7)/TiO_2 was higher than that over Pt(5)/Nb_2O_5. In order to investigate the role of support material, the hydrogenation of benzylideneaniline which is intermediate for the formation of phenylbenzylamine in the amination of benzaldehyde with aniline was studied as a model reaction. The hydrogenation of benzylideneaniline over Pt supported catalysts is summarized in Table 5-2. Pt(5)-MoO_x(7)/TiO_2 showed higher yield of the corresponding primary amine than Pt(5)/Nb_2O_x, suggesting that MoO_x(7)/TiO_2 enhanced the hydrogenation of imine as intermediates to produce primary amines compared with Nb_2O_5. Reduced molybdenum oxide was reported as catalyst for hydrogen-transfer reaction between two alcohol molecules adsorbed on metal cation-oxygen anion pair sites discussed in Chapter 3 [32]. Therefore, MoO_x(7)/TiO_2 could exhibit the high hydrogen accessibility. From these results, it is indicates that Pt(5)-MoO_x(7)/TiO_2 is a candidate for a good catalyst for the amination of ketones with ammonia to produce primary amines.

5. 3. 3 Reductive amination of various ketones with ammonia over Pt-MoO_x/TiO_2

Table 5-3 showed that the reductive amination of other ketones and aldehydes with ammonia over Pt(5)-MoO_3(7)/TiO_2 catalyst at 80-150 ℃ under 4 bar NH_3 and 2 bar H_2. All substrates showed significantly high conversions under the mild reaction conditions. Aliphatic and aromatic ketones selectively converted to corresponding primary amines with high yield (59-75 %), whereas relatively low amount of secondary amines, alcohols and quite a small amount of alkanes formed by

hydrogenation of ketones were also obtained. It is interesting that primary amines were selectively produced in the high conversion range (over 90 %). In general, more sterically-hindered substrates produce higher selectivity to primary amines and cyclic ketones more easily produce secondary amines than corresponding linear ketones [25]. 3-Octanone converted to 3-octyl amines in a higher yield of 76.6 % (primary amine) than 2-octanone, because 3-octanone possesses high steric hindrance compared with 2-octanone. However, the high yield of primary amines was observed regardless of linear or cyclic ketones. Unfortunately, quit a small amount of primary amine (only 9% yield) was observed in the amination of benzaldehyde under same condition, while the secondary amine was mainly formed (yield 70 %).

5. 4 Conclusion

It is concluded that Pt and MoO_x co-loaded TiO_2 (Pt-MoO_x/TiO_2) catalyst is an effective catalyst for the synthesis of primary amines in the reductive amination of ketones with ammonia. The relationship between the catalytic activity and Lewis acid nature of support was observed from IR measurement of acetone adsorbed on support material. The strong Lewis acidity of MoO_3(7)/TiO_2 catalyst improved the formation of imines from corresponding ketones with ammonia, then corresponding amines are formed via hydrogenation of the imines by hydrogenation over Pt metal. As a result, primary amines are obtained as a major product in the reductive amination of keones with ammonia over Pt(5)- MoO_3(7)/TiO_2 catalyst.

5. 5 References

[1] S. Bahn, S. Imm, L. Neubert, M. Zhang, H. Neumman, M. Beller, *ChemCatChem. 3* (2011) 1853-1864.

[2] A. Baiker, J. Kijenski, *Catal. Rev. Sci. Eng.* 27 (1985) 653 –697.

[3] K. S. Hayes, Appl. Catal. *A*, 221 (2001) 187-195.

[4] S. Gomez, J. A. Peters, T. Maschmeyer, *Adv. Synth. Catal.* 344 (2002) 1037-1057.

[5] S. Werkmeister, K. Junge, M. Beller, *Green Chem*. 14 (2012) 2371–2374.

[6] S. Ichikawa, T. Seki , T. Ikariya, *Chem. Lett*. 41 (2012) 1628–1629.

[7] K. V.R. Chary, K. K. Seela, D. Naresh, P. Ramakanth, Catal. Commun. 104 (2005) 23–28.

[8] S. R. Kirumakki, M. Papadaki, K. V. R. Chary, N. Nagaraju, *J. Mol. Catal. A.* 321 (*2010)* 15-21.

[9] F. Qiu, L. Hu, S. Lu, X. Cao, H, Gu, *Chem. Commun.* 48 (2012) 9631-9633.

[10] A. W. Heinen, J. A. Peters, H. van Bakkum, *Eur. J. Org. Chem.* (2000) 2501-2506.

[11] J. Bódis, L. Lefferts, T.E. Müller, R. Pestman, J.A. Lercher, *Catal. Lett*. 9 (2008) 75–81.

[12] S. Ogo, K. Uehara, T. Abura, S. Fukuzumi, *J. Am. Chem. Soc*. 126 (2004) 3020–3021..

[13] C. Gunanathan, D. Milstein, *Angew. Chem. Int. Ed*. 47 (2008) 8861-8664.

[14] X. Ye, P. N. Plessow, M. K. Brimks, M. Schelwies, T. Schaub, F. Rominger, R. Paciello, M. Limbach, P. Hofman, *J. Am. Chem. Soc*. 136 (201) 5923-5929.

[15] S. Imm, S. Bajn, L. Neubert, H. Neumann, M. Beller, *Angew. Chem. Int. Ed.* 49 (2010) 8126-8129.

[16] T. Gross, A. M. Seayad, M. Ahmad, M. Beller, *Org. Lett*. 4 (2002) 2055–2058.

[17] D. Menche, J. Hassfeld, J. Li, G. Menche, A. Ritter, S. Rudolph, *Org. Lett*. 8 (2006) 741–744.

[18] (a) D. Menche, F. Arikan, J. Li, S. Rudolph, *Org. Lett*. 9 (2007) 267–270, (b) J. Zheng, T. Roisnel, C. Darcel, J. B. Sortais, *ChemCatChem*. 5 (2013) 2861-2864.

[19] B. Miriyala, S. Bhattacharyya, J. S. Williamson, *Tetrahedron*. 60 (2004) 1463–1471.

[20] K. Shimizu, K. Kon, W. Onodera, H. Yamazaki, J. N. Kondo, *ACS catal.* 13 (2013) 112-117.

[22] F. Qiu, L. Hu, S. Lu, X. Cao, H, Gu, *Chem. Commun.* 48 (2012) 9631-9633.

[23] A. W. Heinen, J. A. Peters, H. van Bakkum, *Eur. J. Org. Chem.* (2000) 2501-2506.

[24] S. Gomez, J. A. Peters, J. C. van der Waal,W. Zhou, T. Maschmeyer, *Catal. Lett.* (2002) 84, 1-5,

[25] S. Gomez, J. A. Peters, J. C. Vanderwaal, T. Maschmeyer, *Appl. Catal. A* 254 (2003) 77–84.

[26] K. V. R. Chary, K. K. Sheela, D. Naresh, P. Ramakanth, *Catal. Commun.* 9 (2008) 75-81.

[27] L. Brabec, J. Novaova, L. Kubelkovh, J. Mol. Catal. 94 (1994) 243-253

[28] S. R. Kirumakki, M. Papadaki, K. V. R. Chary, N. Nagaraju, *J. Mol. Catal. A* 321 (2010) 15-21.

[29] K. Kon, S. M. A. H. Siddiki, W. Onodera, K. Shimizu, *Chem. Eur. J. 20* (2014) 6264–6267.

[30] A. S. Touchy, S. M. A. H. Siddiki, K. Kon, K. Shimizu, *ACS catal.* 4, (2014) 3045–3050.

[31] M. Tamura, K. Shimizu, A. Satsuma, *Appl. Catal. A 433–434* (2012) 135–145.

[32] (a) Y. Nakamura, T. Murayama, W. Ueda, *ChemCatChem*, 6 (2014) 741-744, (b) Y. Nakamura, T. Murayama, W. Ueda, *J. Mol. Catal. A*, 394 (2014) 137-144.

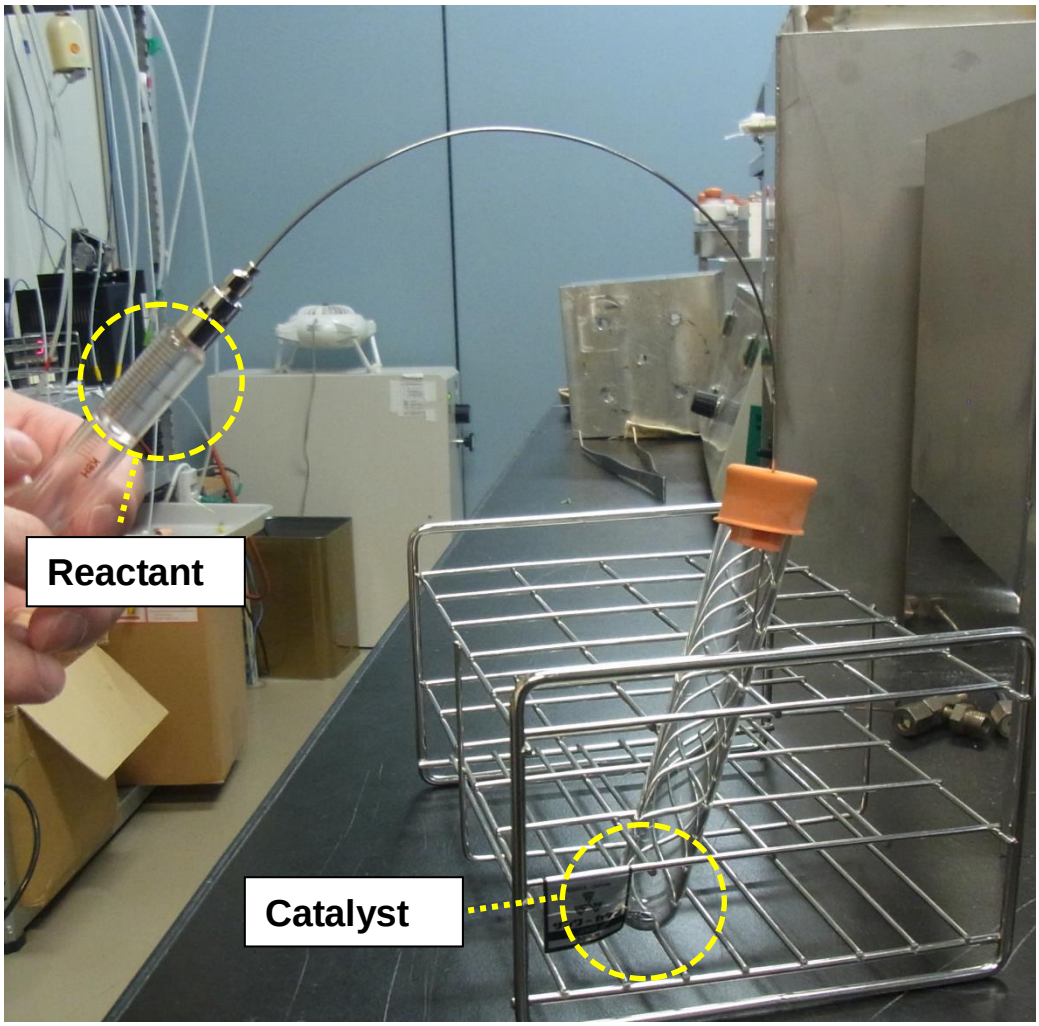

Fig.5-1 Direct injection of reactant into catalyst.

Table 5-1. Amination of 2-adamantanone over various catalysts [a].

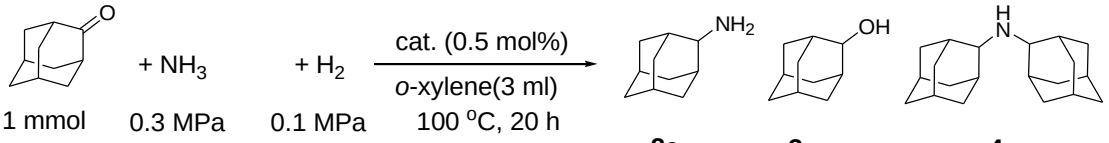

1 mmol **1a** | 0.3 MPa | 0.1 MPa | **2a** | **3a** | **4a**

Catalysts	Conversion (%)	Yield (%)		
		2a	3a	4a
Pt-MoO_x(7)/TiO_2	100	75	4	10
Pt/Nb_2O_5	100	64	6	14
Pt/θ-Al_2O_3	100	62	13	9
Pt/ZrO_2	100	56	13	15
Pt/TiO_2	100	54	6	10
Pt/MgO	100	45	43	<1
Pt/SiO_x	100	44	6	32
Pt/ZSM-5	100	41	24	10
Pt/C	100	38	6	39
Pt/ CeO_2	100	16	58	<1

[a] Conversion of **1a** and yields of **2a, 3a** and **4a** were determined by GC based on **1a**. [b] T = 100 °C, Pt = 0.5 mol%, [e] Pre-reduced under H_2 stream at 300 °C for 0.5 h.

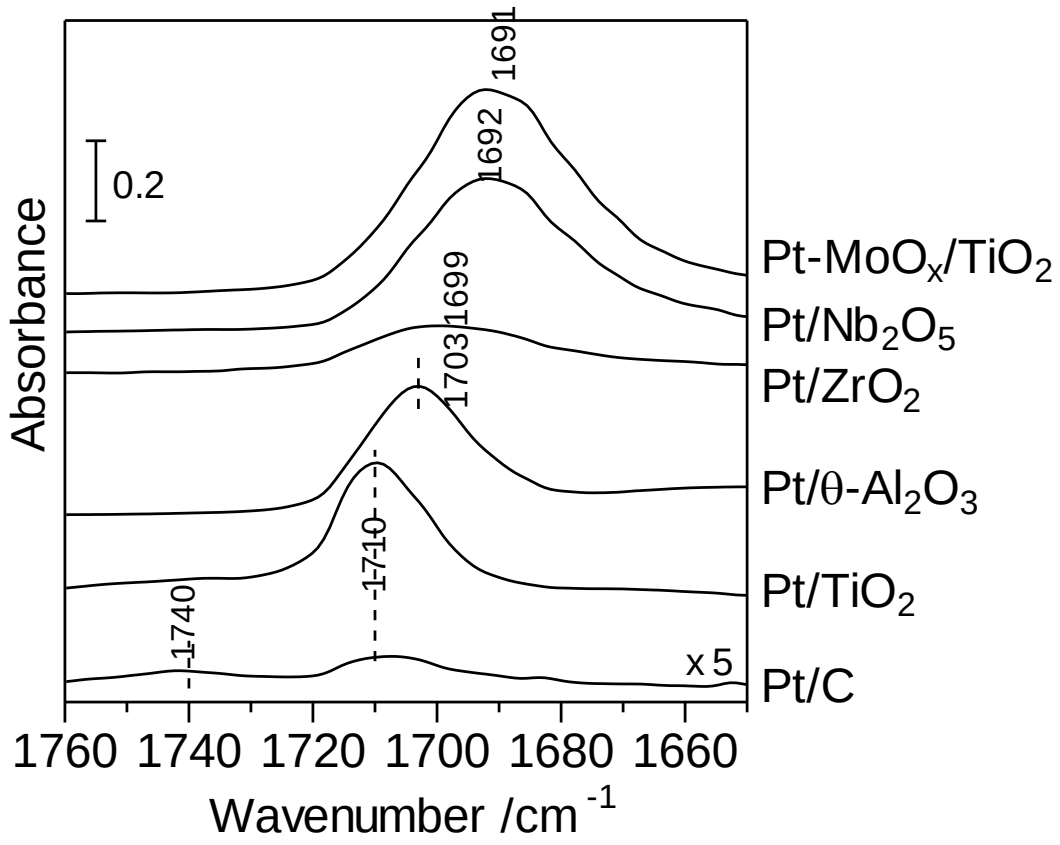

Fig.5-2 IR spectra of acetone adsorbed on the catalysts at 40 ºC.

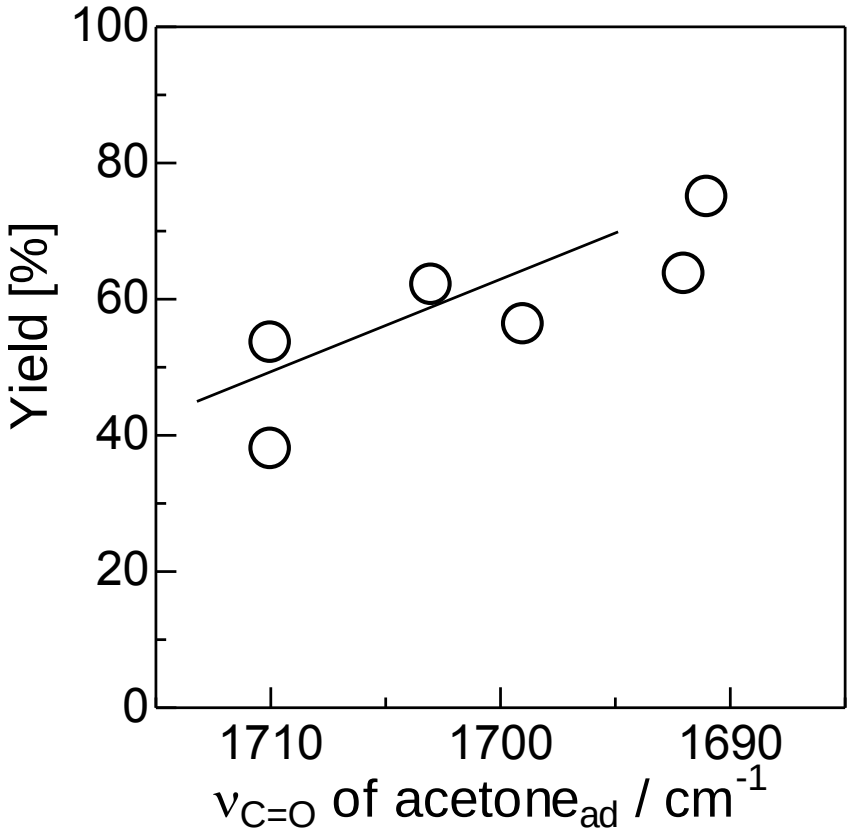

Fig.5-3 Relationship between the wavenumber of acetone adsorbed on the catalyst and yield of 2-adamantyl amine.

Table 5-2. Hydrogenation of benzylideneaniline over Pt-supported catalysts [a].

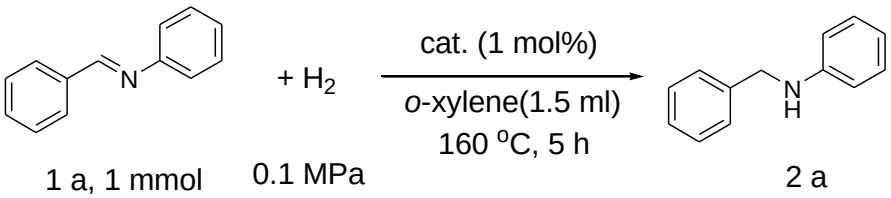

Catalysts	Conversion (%)	Yield (%) 2 a
Pt(5)-MoO_x(7)/TiO_2	**70**	**40**
Pt/TiO_x	**85**	**24**
Pt/Nb_2O_x	**83**	**20**
Pt/θ-Al_2O_x	**88**	**47**
Pt/ZrO_x	**89**	**40**
Pt/C	**82**	**49**

[a] Conversion of 1a and yields of 2a, were determined by GC based on 1a. *T* = 160 °C, Pt = 1.0 mol%, Pre-reduced under H_2 stream at 300 °C.

Table 5-3. Reductive amination of various ketones and aldehydes with ammonia over Pt(5)-MoO_x(7)/TiO_2 catalyst [a]

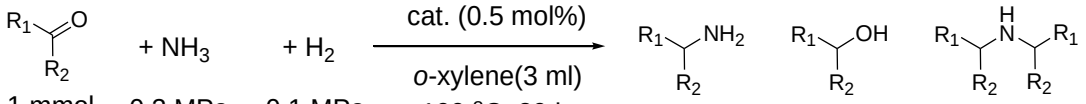

1 mmol **1** | 0.3 MPa | 0.1 MPa | **2** | **3** | **4**

Entry	Reactants	Conversion (%)	Yield (%)		
			2	**3**	**4**
1	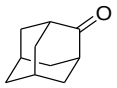	**100**	**75 (71)[b]**	**7**	**11**
2[c]	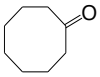	**98**	**70**	**13**	**10**
3		**97**	**68**	**4**	**7**
4	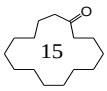	**95**	**64**	**3**	**< 1**
5	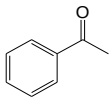	**96**	**74**	**< 1**	**6**
6	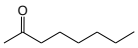	**100**	**71**	**10**	**10**
7	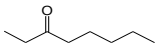	**95**	**77**	**3**	**3**
8[d]		**98**	**60**	**8**	**14**
9	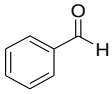	**92**	**9**	—	**70**

[a] Conversion and yields were determined by GC based on alcohol. T_{H2} = 300 °C. T = 100 °C. in *n*-dodecane (0.34 g). catalyst = 0.5 mol%.

[b] Isolated yield

[c] T = 80 °C.

[d] T = 150 °C.

Chapter 6
Summary of thesis

In this doctoral thesis, I studied the catalytic properties of reduced V, Mo oxide catalysts in the reactions of alcohols and extended their application to the synthesis of primary amines by the reductive amination of ketones with NH_3 and H_2. The thesis consists of six chapters. Each chapter is summarized as follows.

In Chapter 1, several catalytic reactions using reduced vanadium and molybdenum oxide based catalysts are summarized, and objectives of the thesis are presented.

In Chapter 2, the catalytic activities of vanadium and molybdenum oxide catalysts are investigated in the ethanol reaction under N_2. In the reaction of ethanol over vanadium and molybdenum oxide, the formation of ethane and acetaldehyde in an equal amount is observed. Among the vanadium and molybdenum oxide catalysts with different oxidation states, V_2O_3 and MoO_2 catalysts exhibit the formation of ethane and acetaldehyde in a ratio 1:1 from the beginning of the time on stream and catalytic states of these oxides did not change during the ethanol reaction. Based on these results, the active sites for the formation of ethane and acetaldehyde in a 1:1 ratio are determined to be V_2O_3 and MoO_2.

In Chapter 3, the reaction scheme is elucidated for the formation of ethane and acetaldehyde from ethanol over the V_2O_3 and MoO_2 catalysts. The reaction conditions (reaction temperature and contact time) have no remarkable effect on the selectivity to products. The reactions of methanol, 1-propanol and 2-propanol also produced corresponding alkanes and aldehydes in an 1:1 ratio. Smaller kinetic isotope effects compared to those expected for primary isotope effects observed when C_2H_5OD and C_2D_5OD are used with respect to C_2H_5OH indicate that the reaction take place by hydrogen-transfer reaction. The reaction model that two ethanol molecules adsorbed on the adjacent metal cation-oxygen anion pair sites of V_2O_3 and MoO_2 oxides undergo intermolecular hydrogen-transfer

and dehydration accounts for the observed kinetic isotope effects.

In Chapter 4, the catalytic activities of V_2O_3 and MoO_2 catalysts are studied for the reaction of ethylene glycol and propylene glycol. In the reaction of propylene glycol, both V_2O_3 and MoO_2 catalysts showed predominant formation of acetone, and small amounts of propionaldehyde and propylene. It is concluded that the formation of propionaldehyde and acetone over V_2O_3 and MoO_2 catalysts results from simple dehydration mechanism (E1 and E2 mechanism) as those observed on solid acid-base catalysts, such as zeolite, Amberlyst, $Cs_{2.5}H_{0.5}PW_{12}O_{40}$, W-Nb-O and γ-Al_2O_3 catalysts. Referring to the results of alcohol conversions discussed in chapter 3, the active sites on V_2O_3 and MoO_2 catalysts are different from those on solid acid-base catalysts because these solid acid-base catalysts do not produce ethane in ethanol reaction. On the other hand, V_2O_3 and MoO_2 catalysts possess weak acid sites to produce propylene in the reaction of iso-propanol. Therefore, it is concluded that propionaldehyde is formed via dehydration of secondary alcohols in propylene glycol, while the formation of acetone takes place through intramolecular hydrogen-transfer dehydration of propylene glycol which is different from those taking place on solid acid-base catalysts. In contrast to mono-alcohols reaction, corresponding olefins are formed in the vicinal diols reaction over V_2O_3 and MoO_2 catalysts. The formation of olefins would takes place via deoxydehydration of vicinal diols and re-reduction of catalysts occurs by oxidation of vicinal diols to form CO_2 or polymer compounds.

In Chapter 5, the application of reduced molybdenum oxide as support material to the reductive amination of ketones with ammonia. Pt supported on MoO_x co-loaded TiO_2 catalysts (Pt-MoO_x/TiO_2) showed good yields for the formation of primary amines as main products in the reductive amination of ketones with ammonia. The relationship between the catalytic activity and

Lewis acid nature of support material is observed; and strong interaction of C=O on Lewis acid sites of MoO_x/TiO_2 lead to a high catalytic activity for the formation of primary amines.

Through all the studies in this thesis, the following conclusions are drawn.

V_2O_3 and MoO_2 catalysts show the characteristic catalytic properties in conversions of alcohols. The reactions of alcohols over V_2O_3 and MoO_2 catalysts produce corresponding alkanes and aldehyde or ketones in an equal amount through hydrogen-transfer reaction between two alcohol molecules adsorbed on metal cation (Lewis acid site) and oxygen anion pair sites. This hydrogen-transfer reaction takes place as in an intramolecular fashion in diol reactions. Reduced molybdenum oxide is effective support material for the reductive amination of ketones with ammonia to produce corresponding primary amines. It becomes clear that these characteristic catalytic activities of reduced vanadium and molybdenum oxides are attributed to Lewis acid sites on their surface.

List of publications

Papers included in this thesis

Chapter 2 **"**Reduced Vanadium and Molybdenum Oxides Catalyze the Equivalent Formation of Ethane and Acetaldehyde from Ethanol", Yoichi Nakamura, Toru Murayama, and Wataru Ueda, *ChemCatChem*, **6** (2014) 741-744.

Chapter 3 **"**Reduced Vanadium and Molybdenum Oxides Catalyze the Equivalent Formation of Ethane and Acetaldehyde from Ethanol", Yoichi Nakamura, Toru Murayama, and Wataru Ueda, *ChemCatChem*, **6** (2014) 741-744.

"Hydrogen-transfer dehydration between alcohols over V_2O_3 and MoO_2 catalysts for the formation of corresponding alkanesand aldehydes", Yoichi Nakamura, Toru Murayama, and Wataru Ueda, *J. Mol. Catal. A*, **394** (2014) 137-144.

Chapter 4 **"**Intramolecular hydrogen-transfer dehydration in the conversion of diols over V_2O_3 and MoO_2 catalysts", Yoichi Nakamura, Toru Murayama, and Wataru Ueda, in preparation.

Chapter 5 **"**Selective Synthesis of Primary Amines by Reductive Amination of Ketones with Ammonia over Supported Pt catalysts", Yoichi Nakamura, Kenichi Kon, Abeda Sultana Touchy, Ken-ichi Shimizu, and Wataru Ueda, *ChemCatChem*, in press

Acknowledge

This research work was performed under the supervisors Prof. Wataru Ueda during 2011-2015 at Catalysts Research Center, Hokkaido University.

The author would like to express his deepest gratitude to Prof. Dr. Wataru Ueda for is supervision of his, continuous guidance, support and simulating discussion, also for this reliance on his encouragement to complete this work.

The author also would like to express his sincere gratitude to Prof. Dr. Hideshi Hattori for his valuable comments, invaluable suggestion and encouragement throughout the course of this work. He would like to sincere thanks to Prof. Dr. Ken-ichi Shimizu for his consistent guidance and fruitful suggestions throughout this study until accomplishment. He also would like to express his great thanks to Assistant Prof. Toru Murayama for his guidance and support throughout the experimental techniques.

He would like to be thankful Prof. Dr. Takao Masuda, Prof. Dr. Shin Mukai and Prof. Dr. Atsushi Fukuoka for their kindness in assisting this thesis.

He also would like to thank all other members of Prof. Dr. Ueda's laboratory, especially to Assistant Prof. Hiroki Takahashi in Akita University for their kindness and help throughout accomplishment this works.

Finally, the author acknowledges his parents for their continuous understanding and encouragement.

Yoichi Nakamura

March 2015